Proceedings of the Twentieth Annual Pacific Climate Workshop

Asilomar Conference Grounds
Pacific Grove, California
April 6-9, 2003

Edited by
Scott W. Starratt and Nikki L. Blomquist

Technical Report 72
of the
Interagency Ecological Program for the
San Francisco Estuary

March 2004

PACLIM

Climate Variability
of the
Eastern North Pacific
and
Western North America

Single copies of this report may be obtained without charge from:

State of California
Department of Water Resources
P.O. Box 942836
Sacramento, CA 94236–0001

Proceedings of the Twentieth Annual Pacific Climate Workshop

Asilomar Conference Grounds
Pacific Grove, California
April 6-9, 2003

Edited by
Scott W. Starratt and Nikki L. Blomquist

Technical Report 72
of the
Interagency Ecological Program for the
San Francisco Estuary

March 2004

PACLIM

Climate Variability
of the
Eastern North Pacific
and
Western North America

Contents

Authors

Clark Alexander
Skidaway Institute of Oceanography
10 Ocean Science Circle
Savannah, GA 31411

John A. Barron
US Geological Survey, MS910,
Menlo Park, CA 94025

Daniel Cayan
Scripps Institution of Oceanography, 0224
La Jolla, CA

Michael Dettinger
Scripps Institution of Oceanography, 0224
La Jolla, CA

Stephen Hager
United States Geological Survey
345 Middlefield Road, MS 496
Menlo Park CA 94025

Mike Hartman
Cooperative Institute for Research in Environmental Sciences
University of Colorado at Boulder
216 UCB, Boulder CO 80309-0216

Linda E. Heusser
Heusser & Heusser, Inc.
100 Clinton Rd.
Tuxedo, NY 10987

Mark Losleben
Mountain Research Station, University of Colorado
818 County Road 116
Nederland, CO 80466

Janet E. Mason
Pacific Fisheries Environmental Laboratory,
Southwest Fisheries Science Center / NMFS
1352 Lighthouse Ave.,
Pacific Grove, CA 93950

Jerrold G. Norton
Pacific Fisheries Environmental Laboratory,
Southwest Fisheries Science Center / NMFS
1352 Lighthouse Ave.
Pacific Grove, CA 93950

Nicholas C.Pepin
Department of Geography, University of Portsmouth, U.K.
Buckingham Building,
Lion Terrace, Southsea, U.K. P05 3NP

David Peterson
United States Geological Survey
345 Middlefield Road, MS 496
Menlo Park CA 94025

Maurice Roos
California Department of Water Resources
P.O. Box 942836
Sacramento, CA 94236-0001

Richard Smith
United States Geological Survey
345 Middlefield Road, MS 496
Menlo Park CA 94025

G. James West
United States Bureau of Reclamation
2800 Cottage Way
Sacramento, CA 95825

Statement of Purpose

In 1984, a workshop was held on the "Climatic Variability of the Eastern North Pacific and Western North America." From it has emerged an annual series of workshops held at the Asilomar Conference Grounds at Pacific Grove, California, or the Wrigley Institute for Environmental Studies at Two Harbors, Santa Catalina Island, California. These annual meetings, which involve 80-100 participants, have come to be known as the Pacific Climate (PACLIM) workshops, reflecting broad interests in the climatologies associated with the Pacific Ocean and western Americas in both the northern and southern hemispheres. Participants have included atmospheric scientists, hydrologists, glaciologists, oceanographers, limnologists, and marine and terrestrial biologists. A major goal of PACLIM is to provide a forum for exploring the insights and perspectives of each of these many disciplines and for understanding the critical linkages between them.

PACLIM arose from a growing concern about climate variability and its societal and ecological impacts. Storm frequency, snow pack, droughts and floods, agricultural production, water supply, glacial advances and retreats, stream chemistry, sea surface temperature, salmon catch, lake ecosystems, and wildlife habitat are among the many aspects of climate and climatic impacts addressed by PACLIM workshops. The workshops also address broad concerns about the impact of possible climate change over the next century. From observed changes in the historical records, the conclusion is evident that climate change will have major societal impacts through effects on global ecology, hydrology, geology, and oceanography.

Our ability to predict climate, climate variability, and climate change critically depends on an understanding of global processes. Human impacts are primarily terrestrial in nature, but the major forcing processes are atmospheric and oceanic in origin and transferred through geologic and biologic systems. Our understanding of the global climate system and its relationship to ecosystems in the eastern Pacific area arises from regional study of its components in the Pacific Ocean and western Americas, where ocean-atmosphere coupling is strongly expressed. Empirical evidence suggests that large-scale climatic fluctuations force large-scale ecosystem response in the California Current and in a very different system, the North Pacific central gyre. With such diverse meteorologic phenomena as the El Niño–Southern Oscillation and shifts in the Aleutian Low and North Pacific High, the eastern Pacific Ocean has tremendous global influences and particularly strong effects on North America. In the western United States, where rainfall is primarily a cool-season phenomenon, year-to-year changes in the activity and tracking of North Pacific winter storms have substantial influence on the hydrological balance. There are abundant climatic records, both instrumental and proxy, for this region. Recent research efforts are beginning to focus on better paleoclimatic reconstructions that will put present day climatic variability in context and allow better anticipation of future variations and changes.

The PACLIM workshops address the problem of defining regional coupling of multiple elements as affected by global phenomena. Because climate expresses itself throughout the natural system, our activity has been, from the beginning, multidisciplinary in scope. Our interdisciplinary group uses diverse time series, measured both directly and through proxy indicators, to study past climatic conditions and current processes in this region. The specialized knowledge from different disciplines has allowed for the synthesis of climatic records and process measurements to better understand the complete system.

Characterizing and linking the regional geosphere, biosphere, and hydrosphere provides a scientific analogue and, hence, a basis for understanding similar linkages in other regions and for anticipating the response to future climate variations. Our emphasis in PACLIM is to study the interrelationships among diverse data. To understand these interactive phenomena, we incorporate studies that consider a broad range of topics both physical and biological, time scales from months to millennia, and space scales from single sites to the entire globe.

Introductions

Editor's Introduction

Scott W. Starratt, US Geological Survey

In 2003, the Twentieth Annual PACLIM Workshop was held at the Asilomar State Conference Grounds at Pacific Grove, California. Situated on the beautiful windswept west coast, this was an ideal location for a conference on the climate of the eastern Pacific. Attended by more than 110 registered participants (see Appendix C, Attendees), this year's workshop included 39 scheduled talks and 32 poster presentations. As a twentieth anniversary bonus, a special dinner was held at the Monterey Bay Aquarium.

Following the United Nations designation of 2002 as the "International Year of the Mountain", the organizing committee (Mike Dettinger, US Geological Survey; Henry Diaz, Climate Diagnostics Center; Connie Millar, Pacific Southwest Research Station, Forest Service; Kelly Redmond, Western Regional Climate Center; Scott Starratt, US Geological Survey) assembled presentations aimed at evaluating past, present, and future trends in temperature and precipitation in the mountainous regions of western North America into a special session entitled "Integrated Climate Research in the Mountains" (see Appendix A, Agenda).

On the first evening, Kelly Redmond gave us an overview of the western weather and climate for the 2002-2003 "PACLIM YEAR" and Maury Roos presented the 2003 California Water Year report. In a change from the usual data-oriented presentations, Didier Sornette gave a more philosophical presentation on the endogenous and exogenous origins of crises, both natural and anthropogenic. In keeping with the theme of the special session, the Monday evening presentation by Lonnie Thompson explored recent contributions from ice cap records in Asia, South America, and Africa. For the Tuesday evening talk by Julio Betancourt, we moved toward the western coast of South America for a discussion of the late Quaternary history of the Atacama Desert and the Pacific slope of the central Andes.

Poster presentations were displayed throughout the meeting and time was set aside on Tuesday evening for their presentation and discussion (see Appendix B, Poster Presentations).

All presenters were invited to expand their abstracts into a manuscript for inclusion in the 2003 PACLIM proceedings volume, along with the abstracts from the oral and poster presentations. In this Proceedings volume, seven full-length papers are presented. The papers were not formally peer reviewed and editorial comments are generally limited to grammar, spelling, and format. Editorial comments on the content of some submissions have been offered, but any errors in fact or logic are the responsibility of the author(s).

Special Session Introduction—Integrated Climate Research in the Mountains

The goal of this year's special session was to highlight some of the recent work in past (pre-historic), historic past, and present rates and magnitudes of climate change in the western cordillera. Discussions covered all of the major mountains in western North America. General topics included:

1) overall variations in mountain climates and the means of monitoring these changes, 2) specific changes in the alpine cryosphere, 3) how do changes in mountain climates affect local and regional water flow and water quality, 4) what effect will these changes have on surficial processes, and 5) what impact will these changes have on the rate and magnitude of ecosystem transformation.

In Part I of this session ("Paleo Perspectives"), the majority of the presentations reviewed high elevation climatic variation through ecosystem change and the role played by fire. Ice core, glacier ice volume, tree-ring analysis, reconstructed stream flow variation, and lacustrine records rounded out the session. In Part II ("Rather Recent") instrumental records were discussed in the context of the causal mechanisms for regional temperature variations at low and high elevations, the role of snow pack in controlling high elevation temperatures, and the close relationship between hydrologic state variables and winter forecasts. Part III ("Looking Ahead") reviewed a number of the regional monitoring systems that were currently in place and ended with a panel discussion that looked at the options for expanding mountain climate research.

Acknowledgements

For two decades, PACLIM workshops have been run by volunteers who always manage to put together a timely and topically interesting gathering for a wide range of researchers. The 2003 workshop drew more than 100 participants with many first-time attendees, a strong indication that PACLIM continues to provide an exciting forum for new ideas, information, and concepts.

For 2003, thanks go to the following people and institutions: **Mike Dettinger** (US Geological Survey), Program Chair, **Henry Diaz** (Climate Diagnostics Center), **Connie Millar** (Pacific Southwest Research Station, Forest Service), **Kelly Redmond** (Western Regional Climate Center), **Scott Starratt** (US Geological Survey); and **Janice Tomson**, Meeting Organizer, who was ably assisted by **Canie Brooks**, **Olga Katsuk**, and **Keith Mootsey** (Long Beach City College).

Sponsorship and funding for the workshops come from a wide variety of sources. This year's PACLIM Workshop was sponsored by the US Geological Survey Water Resources Discipline (**Bill Kirby**), NOAA Office of Global Programs (**Harvey Hill**), CALFED Bay-Delta Science Program (**Sam Luoma**), US Navel Postgraduate School (**Tom Murphree**), California Department of Water Resources (**Zach Hymanson**), Forest Service Pacific Southwest Research Station (**Hilda Diaz-Soltero**), and US Geological Survey Geologic Discipline Earth Surface Dynamics Program (**Martha Garcia**).

For the sixth year Mike Dettinger oversaw the organization of the meeting program and maintained the website. As in previous years, Janice Tomson did a superb job of planning, organizing, and supervising the logistics of the meeting (getting us there, accommodated, and fed), and, with help from her Long Beach City College students, Janice ably handled the numerous details that need to be taken care of for a successful meeting. **Lucenia Thomas**, (U. S. Geological Survey Water Resources Discipline) arranged travel and assisted in the meeting organization. **Tom Murphee** (Naval Postgraduate School) provided and set up the audiovisual equipment. The seven meeting moderators (**Dan Cayan**, **Mike Dettinger**, **Henry Diaz**, **John Dracup**, **Connie Millar**, **Scott Starratt**, **Jim West**) are also gratefully acknowledged. Finally, we thank all our speakers and poster presenters (listed in the agenda) for their contributions and enthusiasm.

For the editing, production, and printing of the proceedings, thanks go to the California Department of Water Resources and the US Bureau of Reclamation's Interagency Ecological Program for the Sacramento-San Joaquin Estuary. This volume was produced by my co-editor, Nikki Blomquist, whom I thank for her special expertise and knowledge. John Barron and Elmira Wan greatly improved the introductory remarks.

The precedents for the 2003 volume were established by the previous editors of the PACLIM Proceedings: Dave Peterson (1984-1988), with the able assistance of Lucenia Thomas Julio Betancourt and Ana MacKay (1989-1990), Kelly Redmond and Vera Tharp (1991-1993), Caroline Isaacs and Vera Tharp (1994-1996), Ray Wilson and Vera Tharp (1997), Ray Wilson and Lauren Buffaloe (1998), and G. James West and Lauren Buffaloe (1999-2001), and James West and Nikki Blomquist (2002). It was Jim West's arm-twisting, starting at the American Quaternary Association meeting in August 2002, which resulted in the most recent change in editorship. Is there anybody's arm out there I can twist?

Scott W. Starratt
US Geological Survey
Menlo Park, CA

Water Year 2003: A Fairly Good Year in Northern California, But a Non-traditional El Niño

Maurice Roos

This paper is a review of the 2003 water year in northern California and how precipitation, snowpack, runoff, and water storage accumulated this season, with some comparisons to recent years. The water year (WY) started off with one big statewide storm in early November which pretty well caught us up to normal for that point in the season. December statewide precipitation was twice the average, and the snowpack was over 150% of the seasonal average at the end of the month on January 1, or about 60% of the April 1 average, which is the usual date of maximum accumulation. January turned out to be less than half the average except in the far north, which was wetter, especially on the Trinity River at about 80%. Many storms were unseasonably warm. By February 1, statewide seasonal snowpack percentages had dropped to average for the date and about 65% of the April 1 average. Precipitation in the southern half of the state was now less than normal. February storms were a disappointment except in the south, adding only 5 to 10% to the snowpack (about one-third of the average gain for the month) and forcing water supply forecasters to reduce the March 1 snowmelt runoff projections to about three-fourths of average. March precipitation was less than average, around 90% statewide, again lighter in the southern Sierra Nevada. Snowpack accumulation also lagged, with appreciable melting especially at lower elevations during the last week of the month. Instead of showing a gain, there was a net loss of about 5% during March, leaving about 65% of average statewide on April 1, the driest since 2001. On April 1 the forecasts called for about 70% for April through July snowmelt runoff. Water year runoff forecasts were 15% better than snowmelt percentages because of the above normal winter season runoff. These forecasts were below average, but not at drought level, and were somewhat better than conditions in much of the West. In-state major reservoir water storage on April 1 was near average overall. Most reservoirs in the north were somewhat above average, whereas those to the south and to the east side of the Sierra Nevada were below average.

Then came the surprise—a wet, cool April. Estimated statewide precipitation for the month was 230% of average. In the northern Sierra Nevada, April precipitation was the third wettest in some 80 years of record; only 1948 and 1963 were wetter. Instead of a normal decrease of 20% due to melting, the snowpack gained about 15% in water content and ended the month slightly over average at 105% of May 1 and 80% of the April 1 average (which is the normal date of maximum accumulation). As a result, the snowmelt and water year forecasts were updated to near average and a pretty good water year ensued. Most of the major foothill reservoirs filled, with the exception of several on the east side of the San Joaquin Valley and Lake Tahoe. Lake Tahoe started so low, at 0.8 foot above the natural rim, that the near normal rise only increased storage to about 2 feet above the rim or one-third of its water storage capacity.

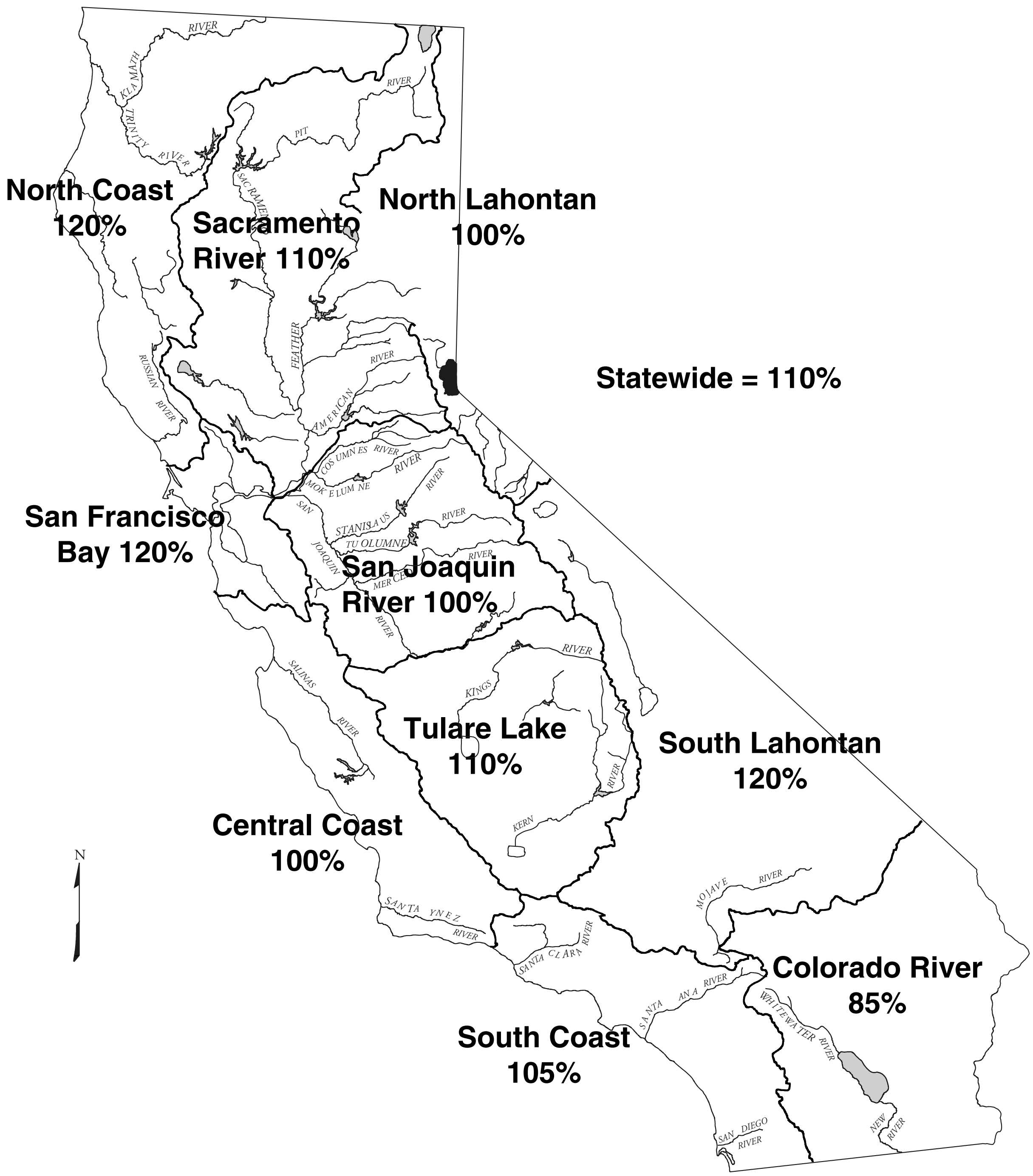

Figure 1 Seasonal precipitation by hydrologic region (in percent of average to date), October 1, 2002, through September 30, 2003

Figure 1 shows water year precipitation as of September 30 for the State's 10 hydrologic regions. Except for the southeastern desert regions, percentages changed little from that of June; on average, July through September precipitation statewide is only 37% of the yearly total. Figure 2 shows the snow water content. Notice the rapid buildup in December, then the late increase in April. The southern Sierra Nevada, San Joaquin through Kern Rivers, did not fare as well as in the north.

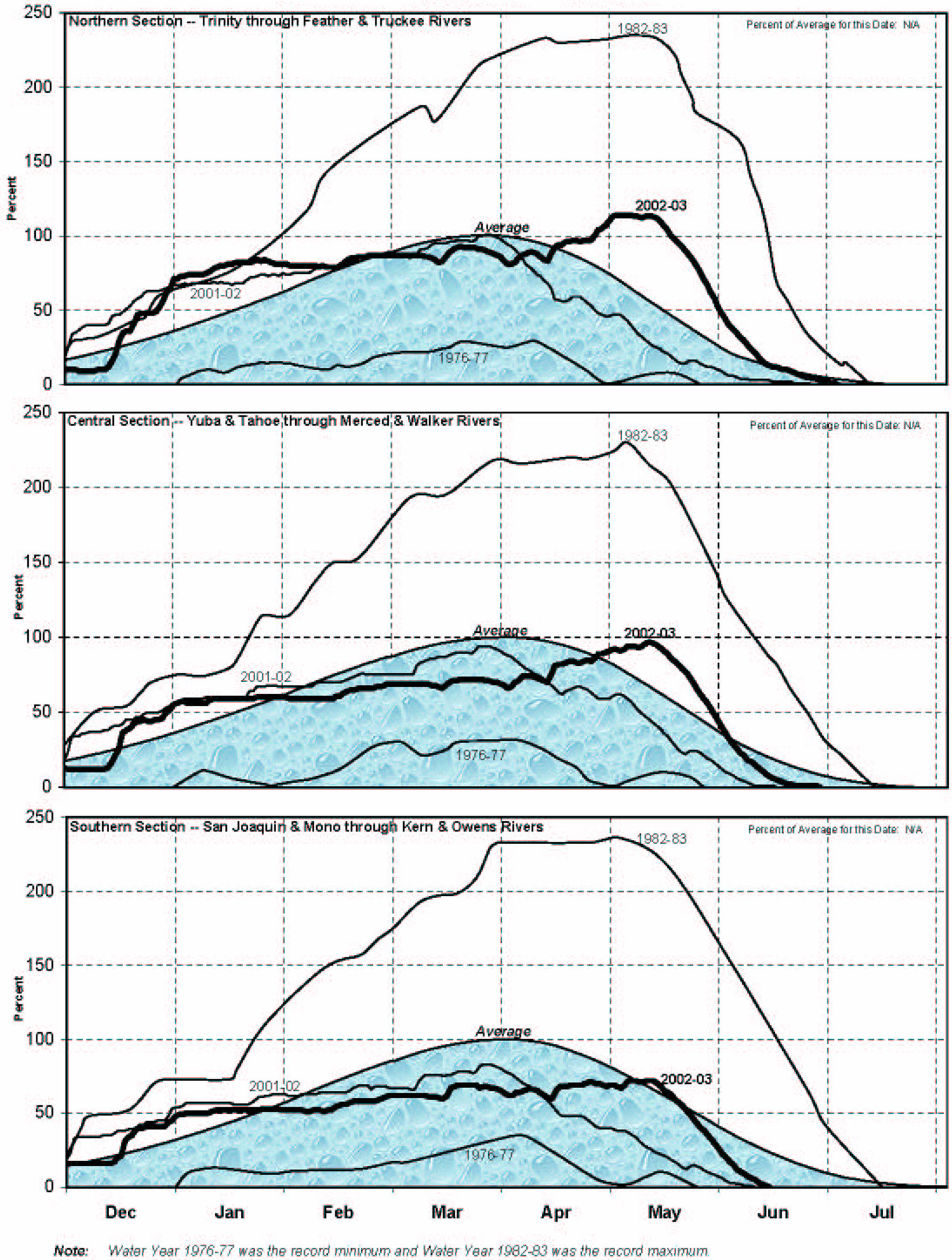

Figure 2 California snow water content for water year 2003, in percent of April 1 average (April 1 is the normal date of maximum accumulation for the season)

The next two charts (Figures 3 and 4) show northern Sierra Nevada precipitation—a monthly bar chart and a cumulative comparison. The month of December stands out; in fact, with 23.8 inches of precipitation, December accounted for half of our water year total on April 1 (the time of the PACLIM Workshop). In fact, storms over a 5-day period (December 13-17) added nearly 12 inches to the precipitation total, or about a quarter of the seasonal total. This just illustrates the importance of a few large storms to our water supply.

The mountain snowpack got off to a roaring start in December with 150% of average by New Year's Day. Then, as we have seen in other years, the water content curves flattened out with only a small net gain during the next three months. At the time of the PACLIM meeting it appeared that we had only a 65% snowpack April water content number for this year. Water year 2001, a dry year, was less at 60% and water year 1994, the last critical year, had 50%. The winter, particularly in January, was much warmer than average so some of the moisture, which would have otherwise come as snow, was winter rain and runoff. Actual stream runoff in January was above average. Some weir overflow from the Sacramento River into its flood bypass system occurred that month.

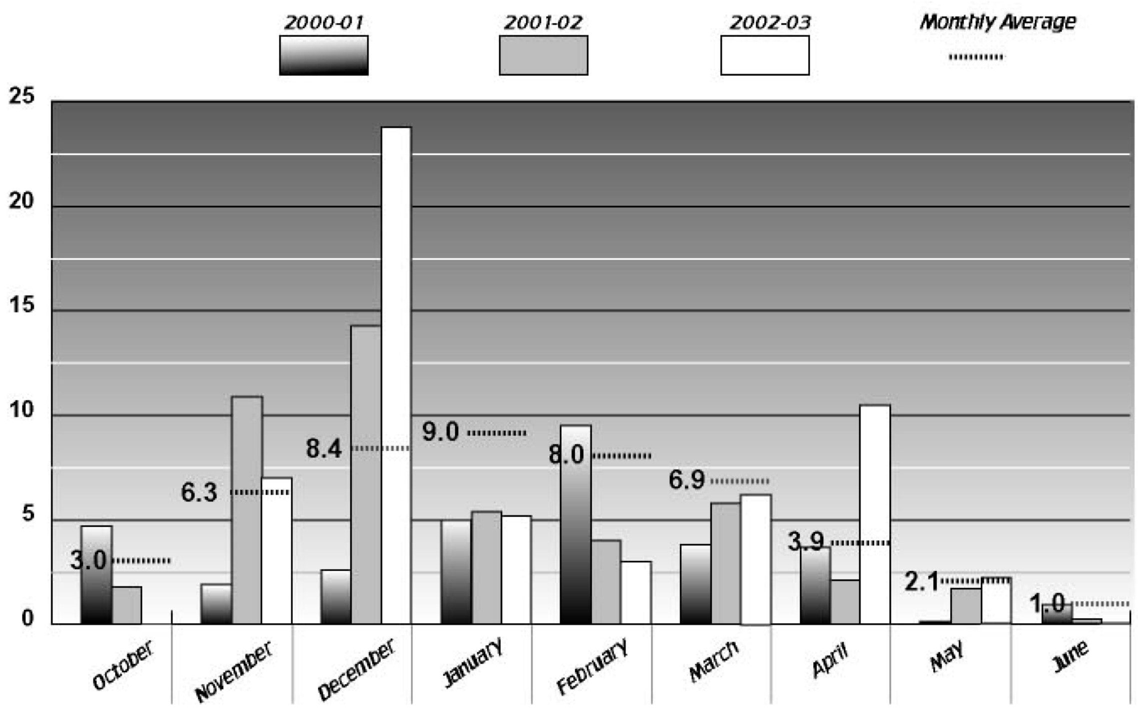

Figure 3 Northern Sierra Nevada precipitation in inches, by month

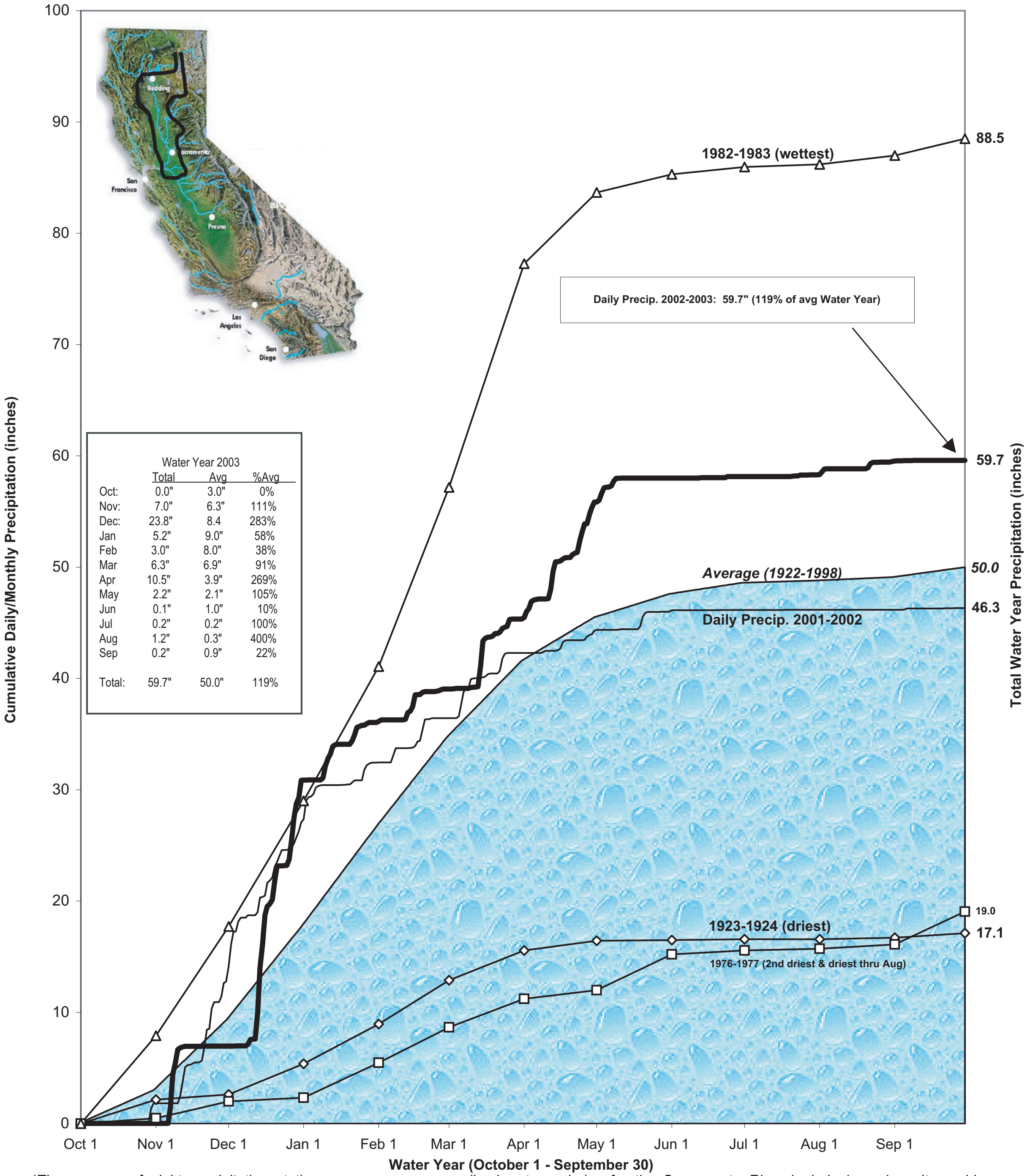

*The average of eight precipitation stations serves as a generalized wetness index for the Sacramento River hydrologic region. It provides a representative sample of the region's major watersheds: the upper Sacramento, Feather, Yuba, and American rivers, which produce inflow to some of California's largest reservoirs--the source of much of our water supply. The eight stations are: Blue Canyon, Brush Creek RS, Mineral, Mount Shasta City, Pacific House, Quincy RS, Shasta Dam, Sierraville RS. Official seasonal runoff forecasts are based on many more measurements than this index, including snowpack and prior streamflow. These seasonal forecasts are a much more accurate measure of water supply.

Figure 4 Northern Sierra Nevada precipitation for water year 2003: 8-Station Index

Runoff

With the wet April, statewide water year runoff was about average (see Table 1, which reflects the updated runoff average for 1951-2000). The runoff in the northern regions, North Coast and Sacramento River, was heavier than runoff in the southern Sierra Nevada, which was around 80% of average. For the four rivers of the Sacramento River region, the projected water year runoff of 19.1 million acre-feet (MAF) was just slightly above average, and much above the median amount (see Figure 5 for the complete water year record). On the San Joaquin River, where slightly less than 5 MAF occurred; nearly half of the years have been drier.

Table 1 Water Statistic

	Percentage of Average (unless noted)							
Statewide	*2003*	*2002*	*2001*	*2000*	*1999*	*1998*	*1997*	*1994*
Precipitation	110	80	75	100	95	170	125	65
April 1 Snowpack	65	95	60	100	110	160	75	50
Runoff	100	75	45	90	105	165	145	40
Reservoir storage, Sept. 30	103	86	86	108	115	133	101	71
Reservoir storage, MAF	(23.0)	(19.2)	(19.3)	(24.1)	(25.6)	(29.5)	(22.5)	(15.8)
Regional								
Northern Sierra Nevada Precipitation	120	93	66	113	110	165	138	64
8 Station Index, inches	(59.8)	(46.3)	(33.0)	(56.7)	(54.8)	(82.4)	(68.7)	(31.8)
Sacramento River	101	77	51	99	111	165	141	41
Unimpaired runoff, MAF	(19.1)	(14.6)	(9.8)	(18.9)	(21.2)	(31.4)	(25.4)	(7.8)
San Joaquin River	81	67	53	98	98	173	167	42
Unimpaired runoff, MAF	(4.9)	(4.1)	(3.2)	(5.9)	(5.9)	(10.4)	(9.5)	(2.5)

Note: 1951-2000 averages for runoff MAF=million acre-feet

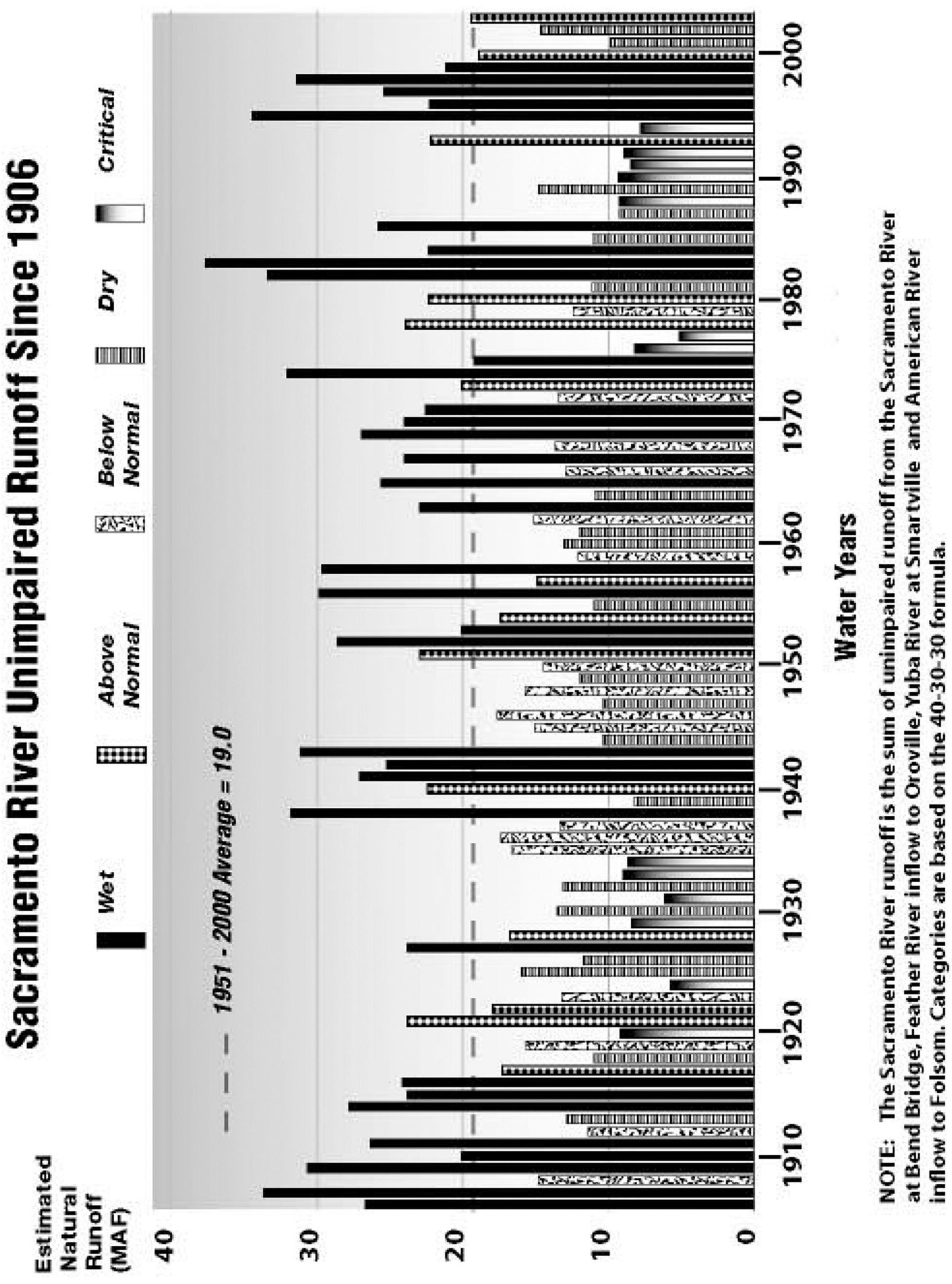

Figure 5 Sacramento River unimpaired runoff since 1906

Some significant amount of winter flood control releases were made from Shasta, Folsom, and Black Butte reservoirs. If conditions had been colder, some of this water would have come off later and probably would have been storable. Most of the large reservoirs in the north did fill. For all practical purposes, Shasta, Folsom, and Trinity reservoirs filled in May and Lake Oroville also filled in early June. San Luis Reservoir storage was about 96% full at its peak, but 70 thousand acre-feet (TAF) or so less than last year.

Full Central Valley Project (CVP) deliveries were available north of the Sacramento-San Joaquin Delta, but south of the Delta 75% of agricultural deliveries and 100% urban deliveries were available. Last year (2002), CVP agricultural deliveries south of the Delta were 70%. On December 1, an initial allocation of 20% was made for the State Water Project (SWP). This was raised to 45% (1.86 MAF) in mid-January in response to the wet December, raised to 50% in late March, and then eventually upped to a very good 90% or 3.7 MAF in mid-May. Last year's 2002 SWP deliveries, with an adjustment late in the season, turned out to be 2.89 MAF or 70% of entitlements.

El Niño Forecasts

In early winter, the long-lead seasonal forecast for December through February and January through March had forecast a typical El Niño with a wet Southwest and dry Pacific Northwest. In California, that would have meant a drier north and a wetter south, relative to normal. That did not happen; instead there was a pronounced wetter north, a drier south gradient with winter wetness extending into southwestern Oregon, and a mixed pattern in the southern deserts. A southern storm track did develop to some extent in February. One storm on February 12 brought heavy, although not unusual, rains in the Transverse Ranges of southern California after an extended mid-winter dry spell. The moisture for this storm originated unusually far to the south at about 5 °N of the equator and that storm went on to produce a major snowstorm in the northeast that Presidents' day weekend.

In California, the internal north-to-south gradient was quite pronounced with higher values for the Trinity and upper Sacramento River regions and the lower values for southern Sierra Nevada. Figure 6 shows the estimated actual April through July runoff percentages in the various rivers. Also of interest is the Upper Klamath River with snowmelt runoff forecasts in the 70% range, about 5% more than last year. However, winter runoff was enough to completely fill Upper Klamath Lake, which was making large releases in April.

Most of the west was dry, as Kelly Redmond has said. The final June forecast of the Colorado River inflow to Lake Powell was 4.0 MAF, 50% of average—much better than last year's dismal 1.1 MAF, but still much below average. (Preliminary estimates of actual inflows were 3.9 MAF, 49% of average.) It does not look like much of the record Denver snowstorm in March got over to the west slope of the continental divide. From what I have heard, it only increased the April 1 forecast of Colorado River runoff by 5% over the March 1 forecast at Lake Powell. Looking at the Pacific Northwest, the June Columbia River April-September runoff forecast of 81.4 MAF at the Dalles was 83% of average. That flow includes the Snake River, forecasted at 84% at lower Granite Reservoir. The Canadian portion of the Columbia was a little better at 89%.

This may be the year of truth on the Colorado River. As many of you know, California diversions have been reduced from 5.2 to 4.4 MAF as of January 1 because of lack of agreement on how to reduce Colorado River use. Previously we (and Nevada) had been furnished "interim surplus" which is basically upper basin state leftovers from their unused entitlements of 7.5 MAF. However, with the continuing drought on the watershed both Lakes Powell and Mead have been dipping to relatively low levels. Lake Mead's elevation was 1,143 feet at the end of August, some 2 feet below the 1,145-foot threshold for reducing the interim surplus by half. If it goes 20 feet lower, the interim surplus is supposed to end. So there is some question about whether California would have gotten a soft landing in its Colorado River diversion reduction after all. It depends on next year's precipitation and runoff from the Rockies.

Figure 7 shows the percentage of water year runoff during the snowmelt months, April through July, for the Sacramento River system. On April 1 it looked like the 2003 amounts would be quite low, around 4.6 MAF, which would give a forecasted 29% of the water year. The estimated actual snowmelt season runoff, boosted by the wet April, turned out to be near 7.7 MAF, and the percentage of the water year rose to 40%, the best since 1998. It was enough to flatten the best fit regression line by 1%.

One other thing was unusual this season. The summer in the interior was warmer than average, but the unusual aspect was the extent of southeasterly high level winds, which predominated from mid-July into the first week of September. There were four separate episodes of moist monsoonal air from the southeast which caused outbreaks of summer thunderstorms and scattered rain showers across the state with a large number of lightning-caused forest fires. August statewide precipitation in the northern Sierra Nevada was about four times the meager average amount of 0.3 inch. September precipitation, however, was much below average for the month.

The last chart (Figure 8) is one showing the distribution of northern Sierra Nevada precipitation this season (October-May). About 45% of the days, 110 of 243, had measurable precipitation of 0.01 inch or more. Only a relatively few days, 17 in all, had precipitation over 1 inch, but these 17 days accounted for about two-thirds of the quantity. The difference is even more striking for the 6 days with precipitation exceeding 2 inches. These 6 days accounted for 36% of the precipitation total for the October through May season. We have known all along that a few good orographic storms make the difference between a dry and wet water year, with perhaps 5 to 7 a "normal" number. A few extra big storms make a wet year and a few less make a dry year. I did review the dry year 2001 to see how many wet days there were over 2 inches. To no surprise, none happened that year, although there were 10 days in the 1- to 2-inch category.

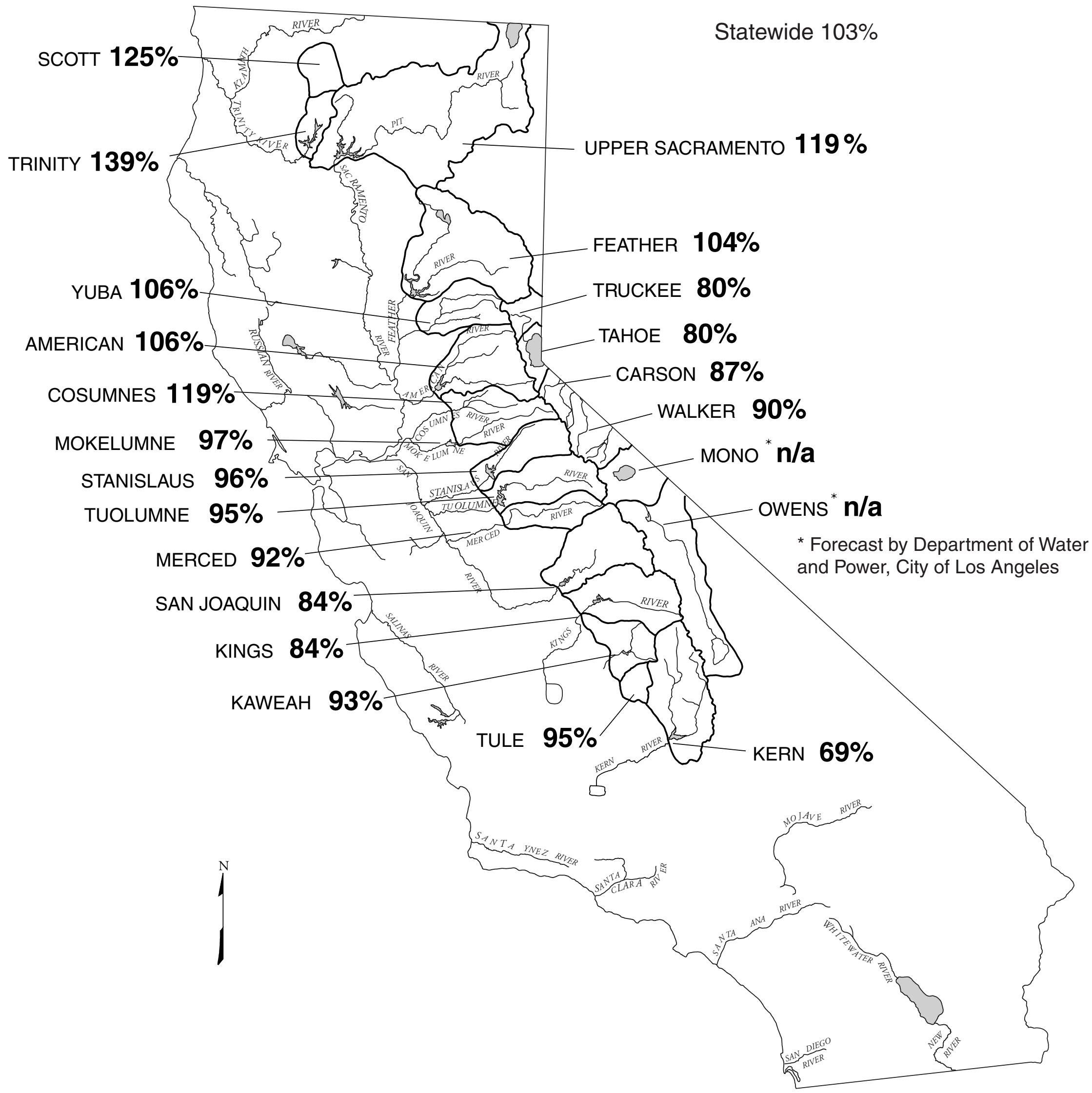

Figure 6 Observed April-July Runoff for water year 2003

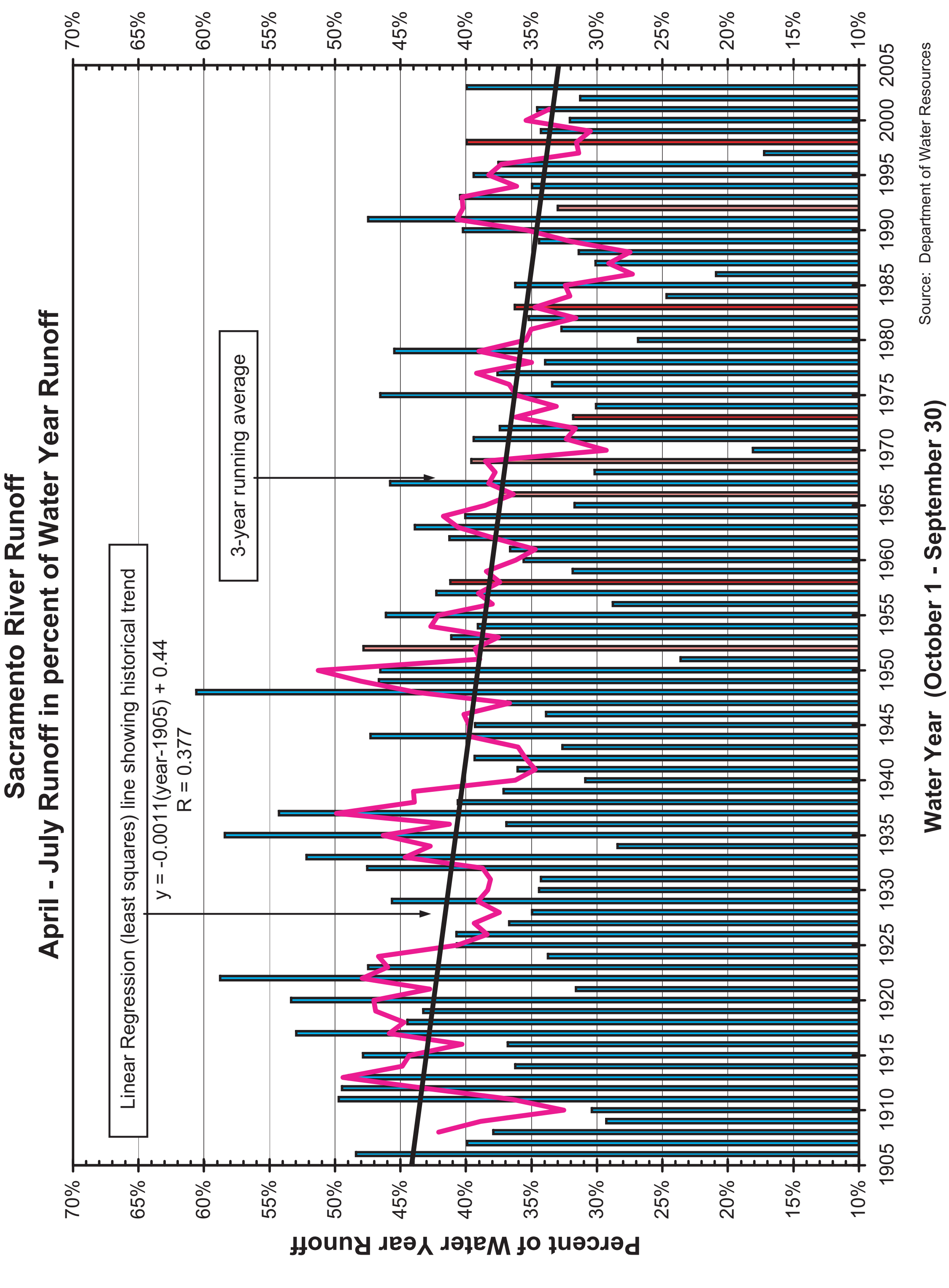

Figure 7 Sacramento River Runoff, April-July Runoff in percent of water year runoff

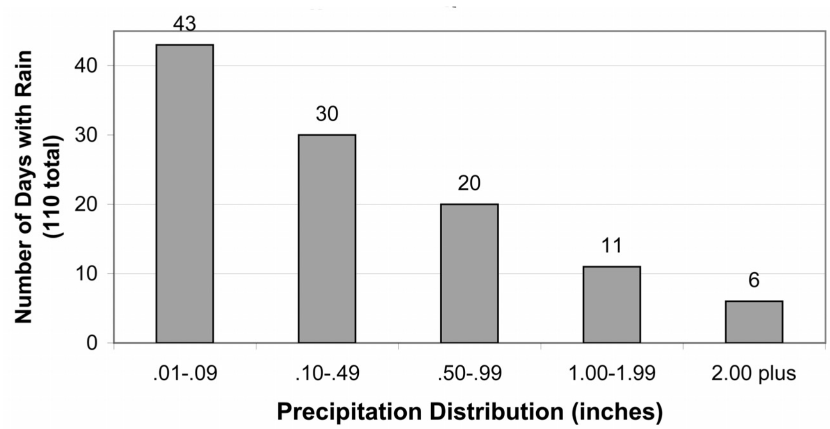

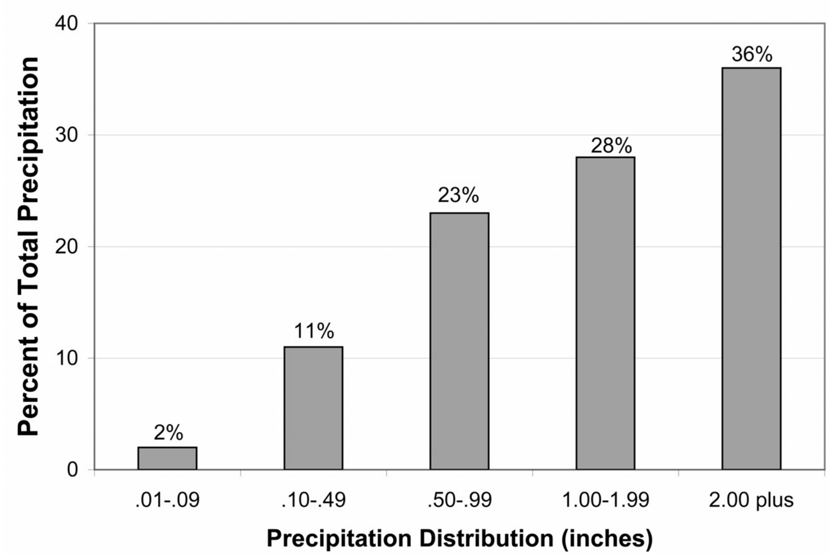

Figure 8 Northern Sierra Nevada Daily Precipitation Distribution

High Resolution Climate of the Past 3,500 Years of Coastal Northernmost California

John A. Barron, Linda E. Heusser, and Clark Alexander

Abstract

Diatom data suggest that a late Holocene trend toward warmer fall sea surface temperatures (SST) began approximately 1,000 years earlier (ca. 3,400 cal yr BP) at Ocean Drilling Program (ODP) Site 1019 (60 km offshore) than it did in the more coastal site of piston core TN062-0550 (33 km offshore). A pronounced offshore-nearshore SST gradient appears to have existed between these two core sites until ca. 1,400 cal yr BP (or AD 600), after which it abruptly collapsed. Coincident with this collapse, Douglas fir pollen abruptly increased from ca. 15% to nearly 40% of the pollen assemblage in Schelling's bog in the nearby Coast Ranges of northern California, arguing for a sudden increase in summer moisture. Regional cooling may have caused a shift in the mean summer position of the Subtropical High further to the south between ca. AD 500 and 600. During the past 1,400 years, diatom data suggest cooling of SST between ca. AD 600 and 900, a pronounced warming between ca. AD 950 and 1200 (the Medieval Warm Period?), and another cooling between ca. AD 1350 and 1800 (the Little Ice Age?). In general, greater relative abundance of Douglas fir pollen in the Schelling's bog record coincident with these cooler SST intervals implies increased summer moisture onshore. Increased relative abundance of oak pollen between ca. AD 850 and 1050, and AD 1150 and 1200 suggest that drier summer conditions coincided with warmer fall SST offshore.

Introduction

In a study of the high resolution climatic evolution of coastal northern California during the past 16,000 years, Barron and others (2003) concluded that modern oceanographic conditions, including enhanced ENSO-like cycles, only evolved in the region during the past 3,500 years. They compared proxy SST records from alkenones and diatoms with records of onshore vegetation from pollen at DSDP Site 1019 (41.682°N, 124.930°W), which is about 60 km off the coast at a 980 m water depth. Barron and others (2003) argued that higher amplitude and more frequent cycles of pine pollen alternating with increased alder and redwood pollen in the ODP 1019 record after 3,500 cal yr BP were evidence of rapid changes in effective moisture and seasonal temperature (enhanced ENSO cycles). At ca. 3,200 cal yr BP, they reported a permanent ca. 1 °C increase in alkenone SST and three-fold increase in the subtropical diatom *Pseudoeunotia doliolus*, which they suggested signaled a warming of fall and winter SST and the establishment of modern oceanographic conditions.

It seems appropriate to examine in greater detail the climatic record of the past 3,500 years of coastal northernmost California using additional cores from the area. To do this, we have selected two cores from high-sedimentation sites. Core TN062-0550 is located about 33 km west of the mouth of the Mad River, and a terrestrial core (SB70-1) is located about 60 km southeast of Eureka between the upper reaches of the Mad River and the Van Duzen River.

The diatom record of the past 3,300 years from core TN062-0550 was compared with that of ODP Site 1019 to establish regional differences and similarities. Both were then compared with a high resolution pollen record from core SB70-1 from a bog located in the Coast Ranges southeast of Eureka in an effort to correlate marine and continental climatic trends.

Materials and Methods

Piston core TN062-0550 was collected by the U.S. Geological Survey in 1996 as part of the STRATIFORM project. This core is located at 40.866°N 124.572°W, at a water depth of 560 m (Figure 1). The core site lies seaward of a preferred path of seaward sediment dispersal to the slope and contains relatively fine-grained sediments that appear to be free of distinct turbidites (Homa Lee, written communication, 2002). Radiocarbon (AMS) dates on planktic and benthic foraminifers collected from this 7-m-long piston core argue for a near uniform sediment accumulation rate of ca. 100 cm/1,000 years (1mm/yr).

Core SB70-1 was taken in an undisturbed bog in the mixed evergreen forest of the northern Coast Range near McClellan Mountain (40.28°N, 123.36°W, 910 m altitude) (Figure 1). The bog lies on private property owned by R. Schelling and the core was collected in 1970 by Linda and Calvin Heusser using a modified Hiller corer. Radiocarbon dates on bulk material from the 10.3-m-long core yield an average sediment accumulation rate of ca. 250 cm/1,000 years (2.5 mm/yr).

The upper 300 cm (last 3,280 years) of core TN062-0550 were collected for diatom studies at 5 cm (=ca. 50 years) intervals. Samples were disaggregated in distilled water and then placed in a vial containing at least 7-10 times as much distilled water as sample. No chemical processing was used. To prepare slides, the vial was shaken and a drop of the suspension was taken after 5-10 seconds of settling from near the top of the vial, transferred to a 22x30 mm cover slip and allowed to dry on a warming tray. Slides were then mounted in Naphrax (index of diffraction=1.71). At least 300 individual diatoms were counted using the counting techniques of Schrader and Gersonde (1978) by making random traverses of the slide under the light microscope at 1250X. Complete diatom data are available from John Barron.

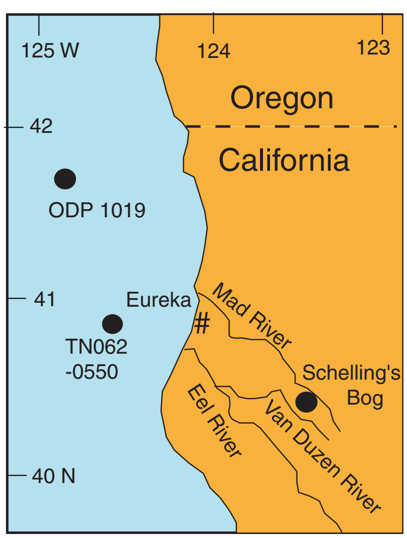

Figure 1 Generalized map of localites discussed in the Eureka area of northern California.

Resting spores of *Chaetoceros* dominate the Holocene diatom assemblage of TN062-0550, so following the practice of Barron and others (2003), other diatom taxa were tabulated on a *Chaetoceros*-free basis based on counts of at least 300 other individuals. *Chaetoceros* spores are easily transported downslope and tend to be more resistant to dissolution than many diatom taxa. Their inclusion in assemblage data can obscure environmental interpretations suggested by other diatom taxa.

Samples, roughly 10 cm^3 in size, were collected every 10 cm throughout the 10.3 m length of the Schelling's bog core (SB70-1). Standard processing procedures (KOH and HF digestion and acetolysis) were preceded and succeeded by sieving through 7-µm nylon screening (Heusser and Stock 1984). An exotic tracer (*Lycopodium*) was used to determine pollen concentration. Taxonomic identification of pollen was based on comparison with modern pollen reference collections from western North America. At least 300 pollen grains were identified from each sample. Complete pollen data are available from L. Heusser.

Age Models

The radiocarbon dates (AMS, Woods Hole Oceanographic Institution) of three samples from core TN062-0550 of mixed planktic foraminifers are corrected to calendar years on Table 1 using the CALIB 4.3 program (Stuiver and others 1998). A reservoir age of 800 years for planktic foraminifers was used following Southon and others (1990).

Peat was radiocarbon dated by Minze Stuiver (University of Washington) from three levels of the Schelling's bog core (Table 1). These radiocarbon dates are converted to calendar years using the CALIB 4.3 program (Stuiver and others 1998) and confirming age estimates using the calibration curves of Stuiver and Becker (1993) to tree ring chronologies.

Table 1 Radiocarbon age data from piston core TN062-0550 and Schelling's bog core SB70-1 and calculated calendar ages

	Material	*Radiocarbon yr BP*	*Calendar yr BP*
Core TN062_0550		(Stuiver and others 1998)	
102-105 cm	mixed planktics	1,770±70	1,001±80
302-305 cm	mixed planktics	3,750±75	3,219±100
670-673 cm	mixed planktics	7,030±120	7,252±120
Schelling's Bog -surface=1970 AD		(Stuiver and Becker 1993)	
230 cm	peat	680±160	654±160
390 cm	peat	1,570±170	1,480±170
ca. 1.0 m	peat	ca. 4,000	4,540±340

Results and Discussion

Diatoms of TN062-0550

Figure 2 shows the relative percentage contributions of *Thalassionema nitzschioides*, *Pseudoeunotia doliolus*, and *Thalassiosira pacifica* (on a *Chaetoceros*-free basis) in piston core TN062-0550 for the past 3,300 years.

Thalassionema nitzschioides is a temperate to subtropical taxon that represents spring-season production within a broad region extending seaward from the coastal zone (Sancetta 1992). The species is most abundant in the Midway Mulitracers sediment trap during the early spring (March-April) according to Sancetta (1992), and may be indicative of the oceanic upwelling that occurs at that time. Prior to ca. 400 BC (2,400 cal yr BP), *T. nitzschioides* comprises 60% to 70% of the *Chaetoceros*-free diatom assemblage in TN062-0550. After ca. 300 BC (2,300 cal yr BP), relative percentage values of *T. nitzschioides* fall to 40% to 55%, before dropping again to values ranging between 30% and 45% after ca. AD 1600 (Figure 2).

Pseudoeunotia doliolus is associated with the warm-water Central Gyre that enters coastal waters off northern California and southern Oregon from late August to October, when the California Current relaxes (Sancetta 1992). In the Multitracer sediment trap series, it is most common at the Gyre site (17%) and decreases shoreward (7% at Midway and 3% at Nearshore) (Sancetta 1992). *Pseudoeuntia doliolus* appears to represent warm, strongly stratified waters with low nutrient availability. Prior to ca. 400 BC (2,400 cal yr BP), *P. doliolus* makes up typically 5% or less of the *Chaetoceros*-free diatom assemblage of core TN062-0550 (Figure 2). Its contribution rises abruptly to ca. 15% between 400 and 300 BC, coincident with a ca. 20% drop in the relative percentages of *T. nitzschioides*, the diatom indicative of oceanic upwelling (Figure 2). Between 300 BC and AD 1300 (2,300 to 700 cal yr BP) *P. doliolus* typically constitutes 10% to 15% of the *Chaetoceros*-free diatom assemblage, whereas after AD 1300, its relative percentage values range between 10% and 5% (Figure 2).

Thalassiosira pacifica is typical of coastal upwelling bloom conditions, clustering with other coastal diatoms in Sancetta's (1992) sediment trap and sediment data. In core TN062-055, *T. pacifica* varies from 0% to 7% of the *Chaetoceros*-free diatom assemblage prior to about AD 1300 (Figure 2). After about AD 1300, the relative abundance of *T. pacifica* displays an increasing trend towards maximum values of ca. 25% at about AD 1900. This increasing trend coincides with a decreasing trend in *P. doliolus* and might be interpreted as a cooling of waters above TN062-0550. It would be tempting to correlate the sharp (ca. 15%) increase of *T. pacifica* between ca. AD 1800 and 1900 as a response to increasing nutrient levels in the Eel and Mad rivers as a result of logging. However, this increase in the relative percentage of *T. pacifica* occurs at a depth of 20 cm in the core, more or less coincident with the transition to the soupy, less compacted sediments at the top of the core. Additional proxy studies (e.g., total organic carbon and other nutrient proxies) are needed from TN062-0550 to further evaluate this potential relationship.

Comparison of the *T. nitzschiodes* and *P. doliolus* relative percentage data of TN062-0550 with that of ODP 1019 (Barron and others 2003), which lies 27 km further offshore, should reveal regional similarities and differences. On Figure 3a, the ratio of *P. doliolus* to *T. nitzschioides* is compared between ODP 1019 and TN062-0550 for the past 3,500 years. Because these two diatoms have distinctly different ecological preferences and because they are roughly equal in size, this ratio is used so that variations in the sample preparation technique should be diminished.

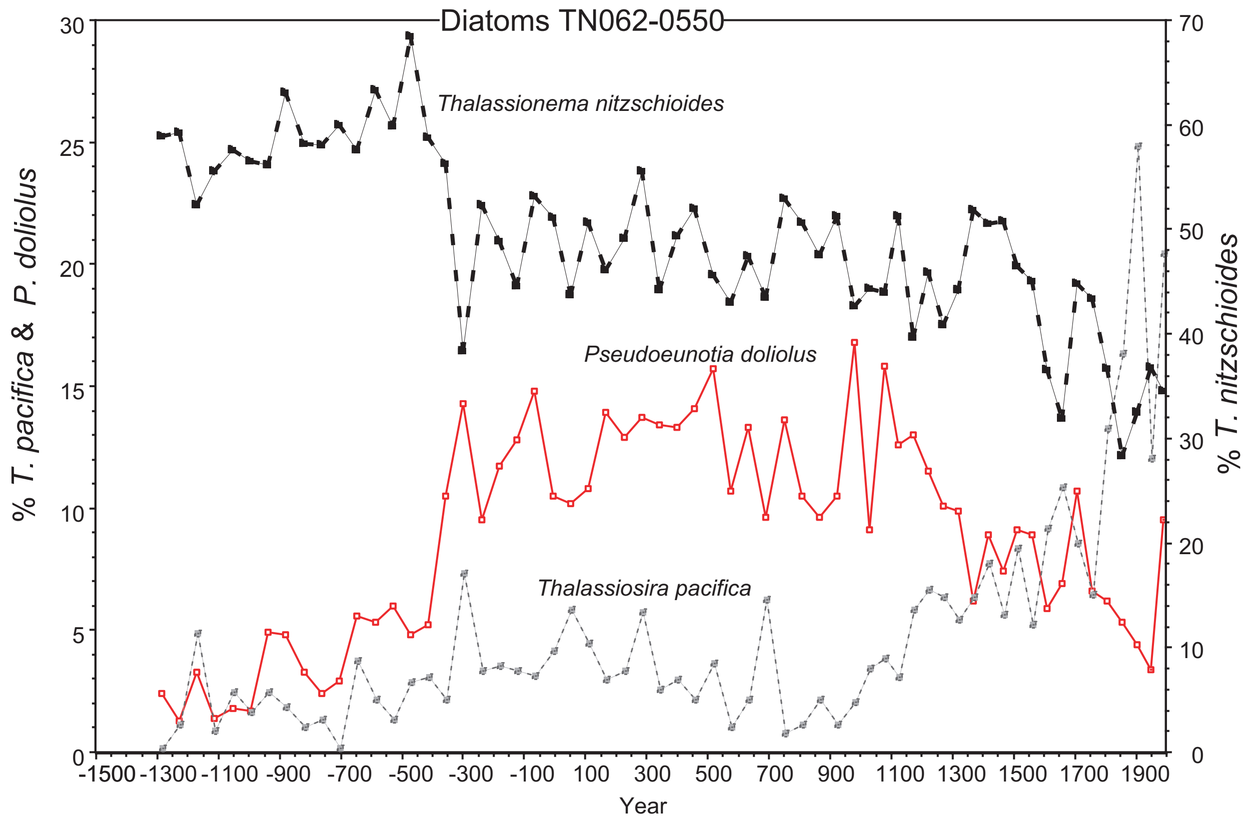

Figure 2 Relative percentage of key diatom taxa in core TN062-0550 during the past 3,300 years.

Marine Climatic Gradients

The *P. doliolus/T. nitzschioides* ratio is a measure of the influence of the Central Gyre at a particular site, so it is not surprising that this ratio is typically higher at offshore ODP Site 1019 than it is in core TN062-0550. The *P.doliolus/T.nitzschioides* ratio begins a late Holocene increase above values of 0.1 at ca. 3,400 cal yr BP (1400 BC) at ODP 1019, but a similar increase is delayed until ca. 2,400 cal yr BP (400 BC) at more inshore core TN062-0550 [Figure 3a (1)]. Between ca. 100 BC and AD 500 (2,100 and 1,500 cal yr BP), an east-west (or onshore-offshore) gradient is apparent [Figure 3a (2)], with values of the *P.doliolus/T.nitzschioides* ratio typically 0.1 greater at ODP 1019 than they are in core TN062-0550. This E-W gradient appears to have collapsed rather abruptly between ca. AD 500 and 600 [Figure 3a (3)], resulting in *P. doliolus/T. nitzschioides* ratios that are roughly similar between the two sites. Subsequently, general cool intervals between ca. AD 600 to 900 and ca. AD 1450 to 1900 bracket a relatively warmer interval (ca. AD 950-1200) in a manner that recalls such global climate patterns such as the Dark Ages Cold Period, Medieval Warm Period, and the Little Ice Age (Denton and Karlen 1973, Wigley 1988, McDermott and others 2001).

Are these marine climate trends real and can they be related to climate trends on the nearby continent? In order to investigate this, we turn now to the pollen record from Schelling's bog, which lies in the Coast Ranges about 60 km southeast of Eureka.

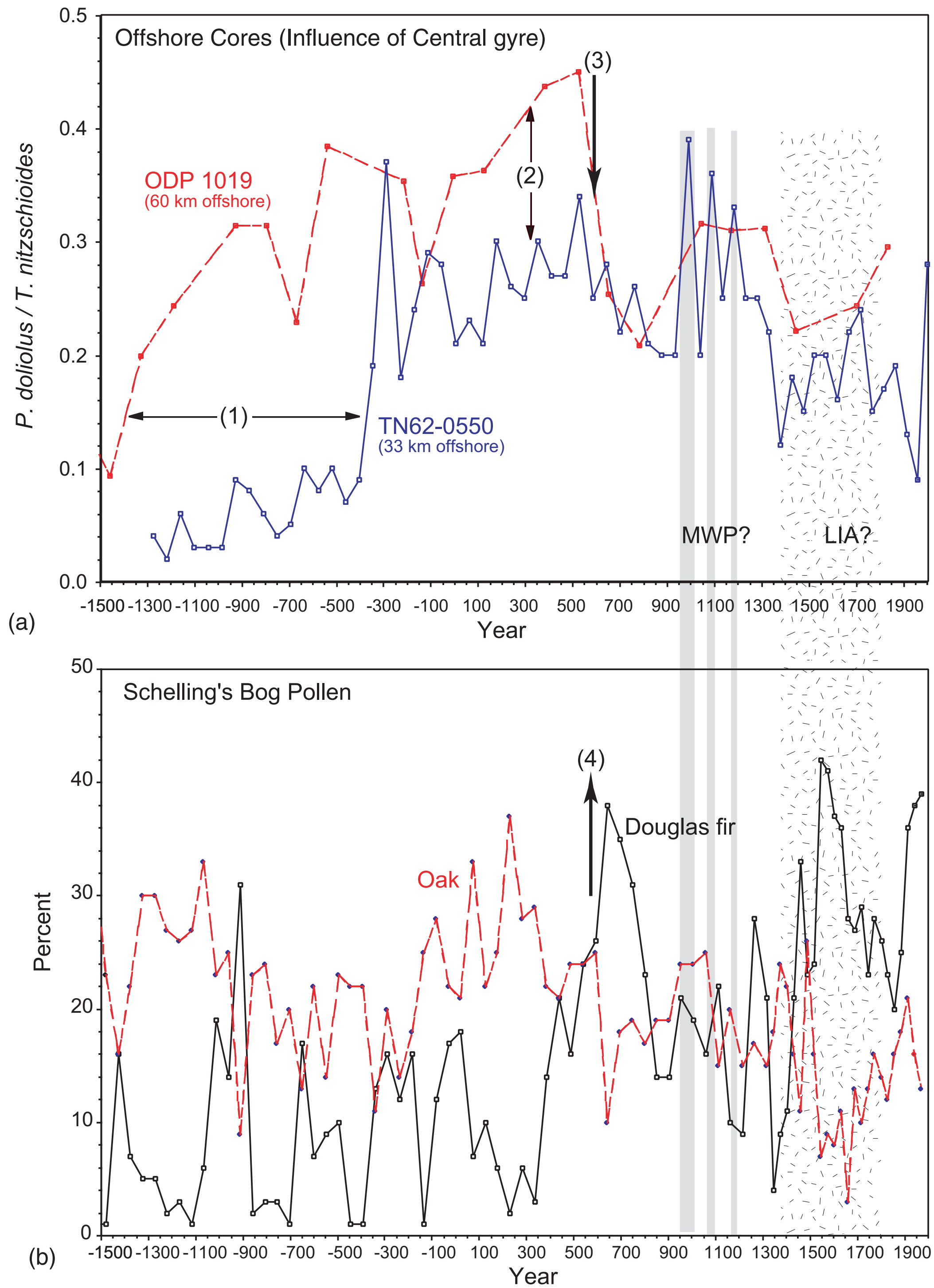

Figure 3(a) Comparison of the ratio of the diatoms *Pseudoeunotia doliolus* to *Thalassionema nitzschioides* in offshore cores ODP 1019 and and TN062-0550 during the past 3,300 years. (1) Lag warming response in TN062-0550; (2) E-W gradient; (3) Collapse of E-W gradient. Figure 3(b) record of Douglas fir and oak pollen in Schelling's bog core SB70-1 during the past 3,500 years; (4) Large increase in Douglas fir pollen at ca. AD 600 coincides with collapse of the E-W gradient. LIA=Little Ice Age; MWP=Medieval Warm Period.

Pollen from Core SB70-1

Pollen in the core from Schelling's bog (SB70-1) derives from the local montane communities of mixed evergreen forest, forests that are dominated by Douglas fir (*Pseudotsuga menziesii*), and include sclerophyllous (hard-leaved) oaks (primarily *Quercus chrysolepis*), as well as incense cedar *(Calocedrus decurrens*), Ponderosa pine (*Pinus ponderosa*), and fir (*Abies grandis*). The mixed evergreen forest communities form a complicated mosaic with the xeric communities of northern oak woodland, grassland, and chaparral. Oak dominance increases on drier, upland soil, forming pure stands on drier ridges. Douglas fir develops on rocks of the Franciscan Complex, which maintain high water availability throughout summer drought (Sawyer and others 1977). Spatial distribution of vegetation is closely related to variation in seasonal distribution of effective moisture and temperature (Barbour and others 1980).

Figure 3b shows the clear fluctuations in the relative contributions of *Pseudotsuga menziesii* and *Quercus* pollen in core SB70-1 for the past 3,300 years. Using present vegetation and climate relationships as our model, we interpret increased oak, which is associated with increased herbs, as indicative of warm dry conditions. Increased *P. menziesii* would suggest a more closed forest with increased summer moisture. Prior to ca. AD 550 (ca. 1,450 cal yr BP), oak pollen dominates, with the exception of a brief period at about 900 BC. During this period between ca. 3,500 to 1,450 cal yr BP, overall, comparatively warm, dry summers prevailed in the northern Coast Range. A major increase in Douglas fir pollen from roughly 15% of the pollen assemblage at ca. AD 500 to nearly 40% at ca. AD 600 [Figure 3b (4)] coincides with the collapse in the E-W gradient of *P. doliolus/T. nitzschioides* values in the offshore cores [Figure 3a (3)]. After ca. AD 600, Douglas fir pollen dominates, except for selected intervals between ca. AD 850 and 1350. These warm, dry intervals may coincide with droughts of the Medieval Warm Period. An increase in effective precipitation during the Little Ice Age concurs with evidence from glacial deposits from California, Washington, and Oregon (Grove 1988). It would appear that collapse of the E-W offshore gradient coincides with increasing summer moisture at Schelling's bog in this maritime, summer-dry, winter-wet Mediterranean climate, which is primarily controlled by zonal circulation over the Pacific Ocean. Presumably, regional cooling shifting the summertime position of the Subtropical High further to the south might be responsible for these patterns.

Douglas fir is most dominant over oak between ca. AD 600 and 800, and again between ca. AD 1550 and 1800. Intervals of dominance of oak over Douglas fir between ca. AD 850 and 1050, AD 1150 and 1200, and AD 1350 and 1400 (Fig. 3b) may reflect a northward shift in the summertime position of the Subtropical High and deflection of summer storms to the north.

Other Northern California Climate Records

Onshore Precipitation

The suggestion of drought in northern California during the Medieval Warm Period is not new. In the White Mountains of eastern California, Hughes and Graumlich (1996) constructed a 7,979-yr-long record of annual (July-June) precipitation using ring records from bristlecone pines. During the Medieval Warm Period, they documented two multi-decadal droughts centered on AD 924 and AD 1299. Elsewhere in California, coincident evidence of drought during the Medieval Warm Period is inferred from relict tree stumps in Mono Lake (Stine 1994). Stine (1994) has shown that for 70 years before AD 1093, the lake stood at least 13 m below its outflow spillway, and for 141 years before AD 1333, it stood at least 11 m below its spillway. He concluded that late in the Medieval Warm Period, California experienced several decade-long periods of profound drought, which was attributed to reorientation of mid-latitude storm tracks.

Similarly, the high freshwater flow from the Sacramento-San Joaquin watershed into San Francisco Bay between AD 1550 and 1850 that is suggested by Byrne and others (2001) and Starratt (2002) coincides with a period of higher relative abundance of Douglas fir pollen compared with oak pollen in the Schelling's bog core, arguing for increased effective moisture in northern California during this interval of the Little Ice Age.

Sea Surface Temperature

Other SST records for offshore northern California and southern Oregon generally lack the detail of those from ODP 1019 and TN062-0550. Oxygen isotopes in mussel shells from central California coastal archaeological sites record SST that were 2-3 °C cooler than present between 300 and 500 years ago (AD 1500 to 1700) according to Jones and Kennett (1999), generally supporting the diatom proxy SST data of this report (Figure 3a). On the other hand, Jones and Kennett (1999) suggest that SST ranged both above and below values of the present between AD 1300 and 1500, during a period that the diatom proxy SST data of ODP 1019 and TN062-0550 suggest was relatively cool (Figure 3a).

In San Francisco Bay, McGann (2002) argued that water temperatures were ca. 1 °C warmer than present between ca. AD 680 and 1270 based on oxygen isotopes measured in specimens of the benthic foraminifer, *Elphidium excavatum*. McGann (2002) suggested that this warm interval of the Medieval Warm Period, which coincided with widespread drought in the Sierra Nevada, was abruptly followed by cooler and wetter conditions.

To the south in the Santa Barbara Basin, Baumgartner and others (1992) published a detailed record of sardine and anchovy abundance during the interval between AD 300 and 1970. During the ca. 1,700-yr-long record, they recorded 22 cycles of alternation in the two species (sardine vs. anchovy). They argued that sardines dominate during warm coastal ocean phases and diminished northerly winds, while anchovies dominate during the opposite ocean-atmospheric phase. Spectral analyses of these data indicated strong peaks at ca. 60 year periods, suggesting that they are caused by the Pacific Decadal Oscillation (PDO). A major peak in sardine abundance in the Santa Barbara Basin between ca. AD 950 and 1040 coincides with higher values of the *P. doliolus/T. nitzschioides* ratio in core TN062-0550 (Figure 3a), suggesting warmer SST along the California coast during this interval of the Medieval Warm Period. On the other hand between ca. AD 1300 and 1850, sardine abundance in the Santa Barbara Basin was anomalously low (except for a brief event in the early 16th century), suggesting cooler SST during the Little Ice Age, similar to SST suggested by the diatom proxy data of core TN062-0550 (Figure 3a).

Conclusions

High resolution diatom records of the past 3,500 years in marine cores ODP 1019 and TN062-0550, located 60 and 33 km, respectively, off the coast of northernmost California, reveal that late Holocene warming of fall SST began about 1,000 years earlier (at ca. 3,400 cal yr BP) in more offshore waters than it did in more nearshore waters. Between ca. 3,400 and 1,400 cal yr BP, a pronounced offshore-nearshore SST gradient apparently existed during the fall in waters off northernmost California. This

SST gradient abruptly collapsed shortly after ca. 1,400 cal yr BP, possibly as a result of regional cooling.

The regional nature of this ca. 1,400 cal yr BP climate event is supported by a coincident switch from the dominance of oak pollen to the dominance of Douglas fir pollen in core SB70-1 from Schelling's bog pollen in the nearly California Coast Ranges, implying increased summer moisture onshore.

During the past 1,400 years, diatom proxy data suggest cooling of fall SST between ca. AD 600 and 900, followed by a pronounced warming between ca. AD 950 and 1200, which is coincident with the Medieval Warm Period. Between ca. AD 1350 and 1800 (the Little Ice Age?), reduced relative numbers of the warm-water diatom *Pseudoeunotia doliolus* argue for cooling of fall SST. Between AD 1800 and 1900, *Thalassiosira pacifica*, a diatom indicative of coastal upwelling, increased sharply (by ca. 15%) in relative abundance in the coastal core TN062-0550, possibly indicating increased nutrient levels in nearshore waters.

In general, during the past 1,400 years, intervals of greater relative abundance of Douglas fir pollen in Schelling's bog core SB70-1 match intervals of reduced relative abundance of *P. doliolus* in the offshore cores, implying that cooling of fall SST coincides with increased summer moisture onshore. Dominance of oak pollen over Douglas fir pollen between ca. AD 850 and 1050 and again between AD 1150 and 1200 suggest that drier summer conditions corresponded with warmer fall SST during parts of the Medieval Warm Period.

Acknowledgments

We are grateful to Homa Lee for suggesting study of piston core TN062-0550 and to the Tara Kneeshaw for technical assistance in preparing the diatom data. This manuscript benefited from the reviews of Scott Starratt and Mary McGann of the U.S. Geological Survey.

References

Barbour, M.G., J.H. Burk, and W.D. Pitts. 1980. *Terrestrial Plant Ecology:* The Benjamin/Cummings Company, Menlo Park, CA, 604 pp.

Barron, John A., L. Heusser, T. Herbert, and M. Lyle. 2003. High-resolution climatic evolution of coastal northern California during the past 16,000 years. *Paleoceanography* 18(1):20(1-19).

Baumgartner, T., A. Soutar, and V. Ferreira-Bartrina. 1992. Reconstruction of the history of Pacific sardine and northern anchovy populations over the past two millennia from sediments of the Santa Barbara Basin, California. *CalCOFI Reports*. 33:24-40.

Byrne, R., B.L. Ingram, S. Starratt, F. Malamud-Roam, J.N. Collins, and M.E. Conrad. 2001. Carbon isotope, diatom, and pollen evidence for Late Holocene salinity change in a brackish marsh in the San Francisco estuary. *Quaternary Research* 55:66-76.

Denton, G.H. and W. Karlen. 1973. Holocene climatic variations - Their pattern and possible cause. Quaternary Research 3:155-205.

Grove, J.M. 1988. *The Little Ice Age*. Methuen, New York, 498 pp.

Heusser, L.E. and C.E. Stock. 1984. Preparation techniques for concentrating pollen from marine sediments and other sediments with low pollen density. *Palynology* 8:225–227.

Hughes, M.K. and L.J. Graumlich. 1996. Climatic variations and forcing mechanisms of the last 2000 years. Volume 141. Multi-millenial dendroclimatic studies from the western United States. NATO ASI Series, pp. 109-124.

Jones, T.L. and D.J. Kennett. 1999. Late Holocene sea temperatures along the Central California Coast. *Quaternary Research* 51:74-82.

McDermott, F., D.P. Mattey, and C. Hawkesworth. 2001. Centennial-scale Holocene climate variability revealed by a high-resolution speleothem d^{18}O record from SW Ireland. *Science* 294:1328-1331.

McGann, M. 2002. Faunal and isotopic evidence of the Medieval Warm period in San Francisco Bay, California. EOS Transactions, American Geophysical Union (Fall Meeting Supplement, Abstract) 83(47):F917.

Sancetta, C. 1992. Comparison of phytoplankton in sediment trap time series and surface sediments along a productivity gradient. *Paleoceanography* 7:183-194.

Sawyer, J., D. Thornburgh, and J. Griffin. 1977. Mixed evergreen forrest. Pages 359-381 in *Terrestrial Vegetation of California.* Barbour, M.G., and Major, J., editors. Wiley, New York.

Schrader, H.-J., and R. Gersonde. 1978. Diatoms and silicoflagellates. Pages 129-176 in *Micropaleontological counting methods and techniques - an exercise of an eight meter section of the lower Pliocene of Cap Rossello, Sicily.* W.J. Zachariasse, W.R. Riedel, A. Sanfilippo, R.R. Schmidt, M.J. Brolsma, H.-J. Schrader, R. Gersonde, M.M. Droeger, and J.A. Broekman, editors. *Utrecht Micropaleontological Bulletins, 17*.

Southon, J.R., D.E. Nelson, and J.S. Vogel. 1990. A record of past ocean-atmosphere radiocarbon differences from the Northeast Pacific. *Paleoceanography* 5:197-206.

Starratt, S.W. 2002. Diatoms as indicators of freshwater flow variation in central California. Pages 129-144 in *Proceedings of the Eighteenth Pacific Climate Workshop*. G.J. West and L.D., Buffaloe, editors. Technical Report 68 of the Interagency Ecological Program for the San Francisco Estuary.

Stine, S. 1994. Extreme and persistent drought in California and Patagonia during mediaeval time. *Nature* 369:546-8.

Stuiver, M., and B. Becker. 1993. High-precision calibration of the radiocarbon time scale AD 1950-6000 BC *Radiocarbon* 35:35-65

Stuiver, M., P.J. Reimer, E. Bard, J.W. Beck, G.S. Burr, K.A. Hughen, B. Kromer, F.G. McCormac, J.V.D. Plicht, and M. Spurk, 1998. INTCAL98 radiocarbon age calibration, 24,000-0 cal BP. *Radiocarbon* 40:1041-1083.

Wigley, T.M.L. 1988. The climate of the past 10,000 years and the role of the sun. Pages 209-224 in *Secular Solar and Geomagnetic Variations in the Last 10,000 Years.* F.R. Stephenson and A.W. Wolfendale, editors. Kluwer, Dordrecht.

Spatial and Temporal Variability in Snowpack Controls: Two Decades of SnoTel Data from the Western U.S.

Mark Losleben and Nicholas Pepin

Snowpack is a crucial, and often primary, water resource in much of the western United States (U.S.). Thus, its variability and sensitivity to changes in climate are important issues. We attempt to describe characteristics of snowpack development related to these issues. Toward this end, two indices are developed for this study. First, a snowpack index (SI) is used to evaluate the role of non-precipitation factors in snowpack development. The SI is derived from the percent of average snow water equivalent (SWE) and cumulative precipitation on April 1. An SI of one indicates the average amount of winter precipitation is sequestered in the snowpack. An SI of greater than one indicates more than average winter precipitation is sequestered, and an SI of less than one indicates less than the average amount of precipitation is sequestered in the snowpack. The second index, FASTDIF, is the difference between surface and derived elevationally equivalent free air temperatures for the same locations as the SnoTel sites. The snowpack index eliminates the variability in snowpack development related to precipitation, and the FASTDIF suggests changes in surface to free air feedback processes (radiation balance and related factors, for example).

The spatial scope of this study is the mountainous western U.S., reported both as a whole unit and as eight separate mountain sub-regions. However, the California group of sites is limited to a small area near the Nevada border, and thus cannot be construed as representative of the Sierra Nevada as a whole.

Data used in this study are the April 1 SWE, cumulative winter precipitation, and maximum and minimum Oct. 1-Apr. 1 temperatures from the National Resources Conservation Service (NRCS) SnoTel network (1979-1999) of several hundred sites (Figure 1). FASTDIF uses both SnoTel and NCAR-NCEP (National Center for Atmospheric Research-National Centers for Environmental Prediction) reanalysis data.

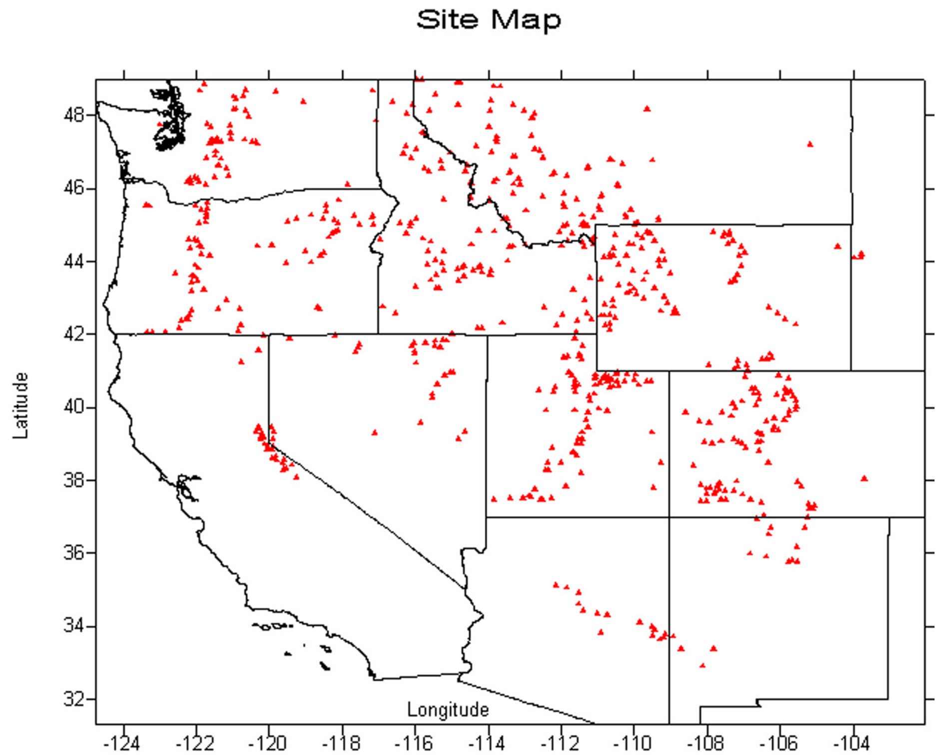

Figure 1 Site Map. Triangles indicate the mountain locations of SnoTel sites used in this study. The western U.S. as a whole and eight sub-regions are utilized.

Results

Our results include trends in snowpack, precipitation, the SI, and temperature, as well as variability over time and by elevation of these parameters.

These results show:

- SI trends (Figure 2) are negative in all regions except Wyoming and the California group (95% sig. level), indicative of an increase in factors detrimental to snowpack development under conditions of constant precipitation. These negative trends are greatest in the mountains of Arizona followed (in decreasing negativity) by northern New Mexico/southern Colorado; Utah; the western U.S. as a whole; Oregon and Washington; and Colorado.
- Trends in minimum Oct. 1-Apr. 1 temperature (95% sig. level) are increasing in the mountains of northern New Mexico/southern Colorado, Idaho/Montana, and Utah (Figures 3d, 3f, 3h, and 4b). They are decreasing in Wyoming, Colorado, and the western U.S. as a whole (Figures 3i, 3e, and 4b).

  Maximum temperatures are increasing in the mountainous California group, northern New Mexico/southern Colorado, Utah, Oregon/Washington, and the western U.S. as a whole (Figures 3c, 3d, 3h, 3g, 3a, and 4b).

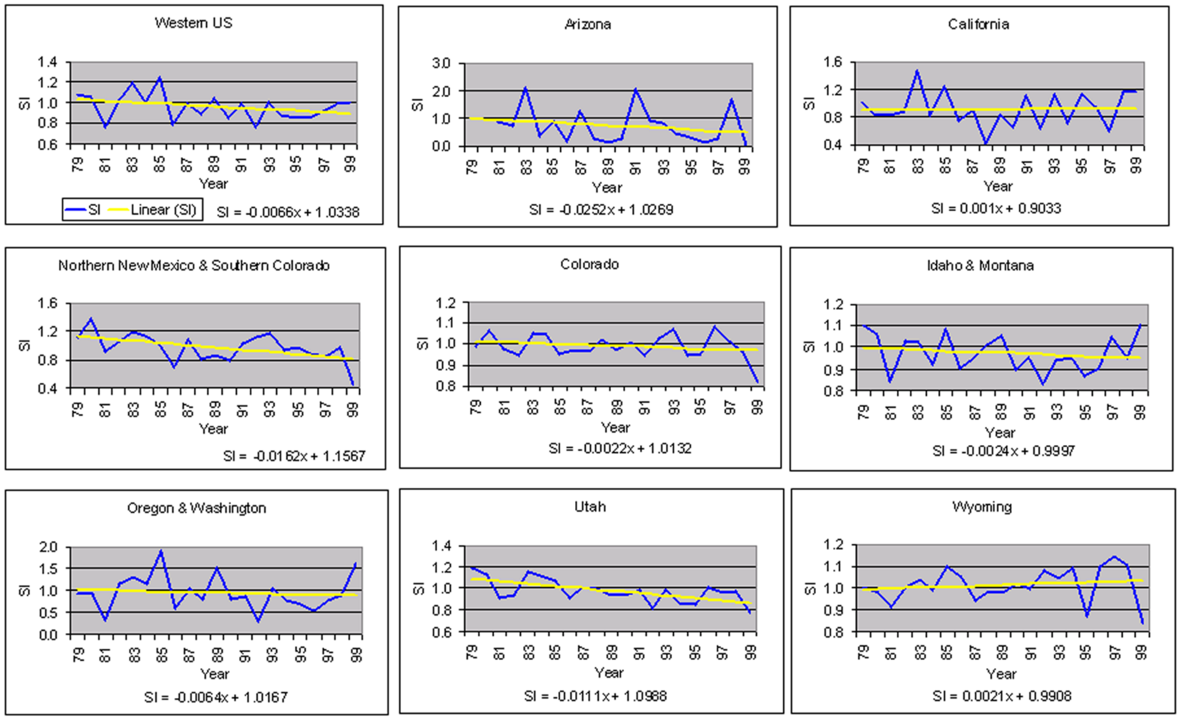

Figure 2 Time-series graphs of the snowpack index (SI) for conditions on April 1, and linear trends for the western U.S. and the eight sub-regions. Only Wyoming and the California group show positive trends.

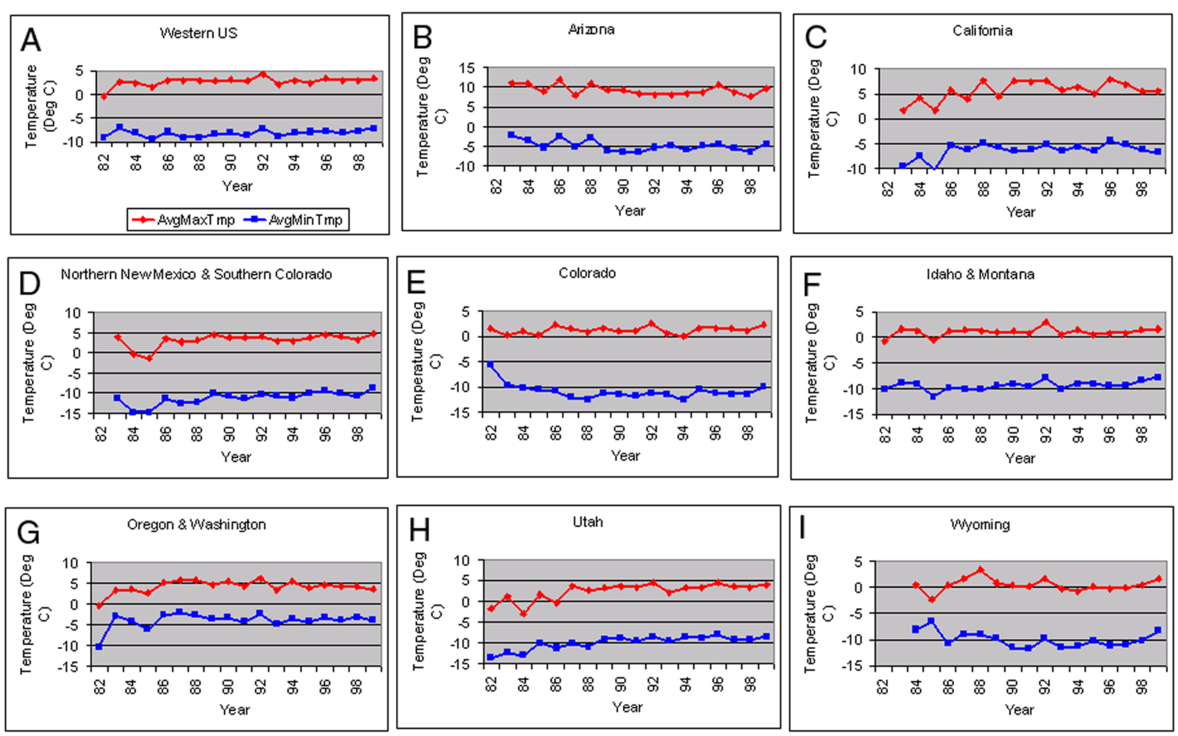

Figure 3 Time series of winter (Oct. 1-Apr. 1) average maximum (upper line) and minimum (lower line) temperatures for the same nine groupings of sites as in Figure 1.

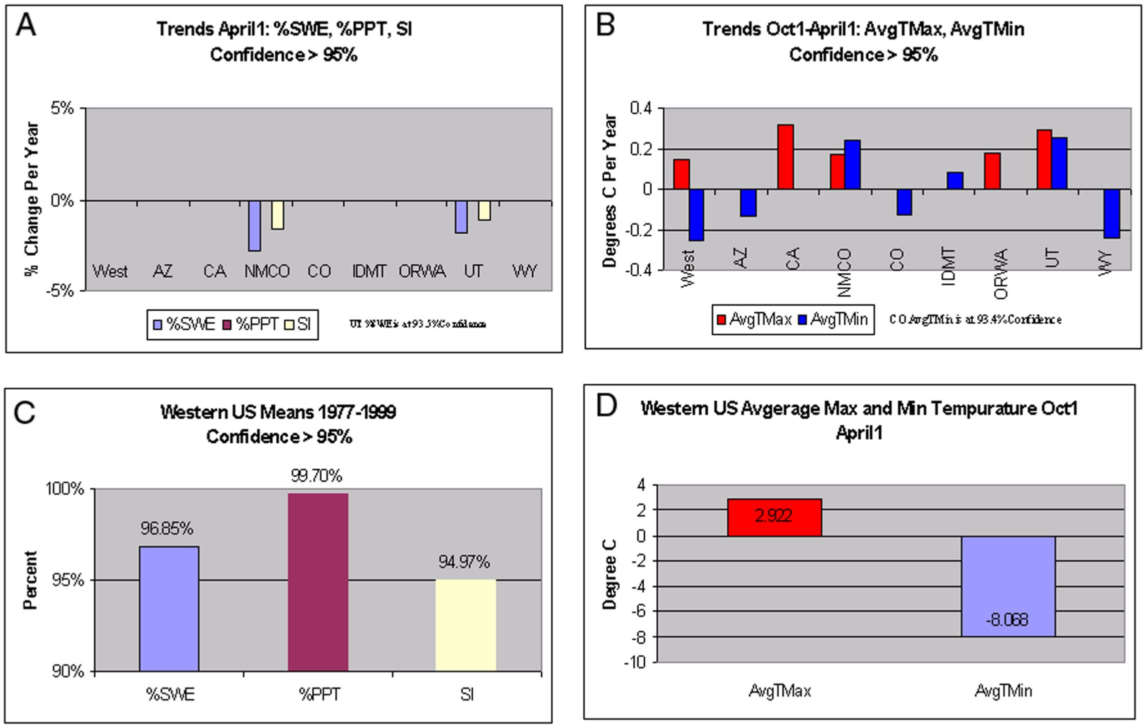

Figure 4 Significant (95% level) trends (a and b), mean percent of average snow water equivalent (SWE), cumulative winter precipitation, snowpack index (SI) for the western U.S. (c), and the average maximum and minimum temperatures for the western U.S. (d). All (a-d) are for April 1 conditions. The only significant moisture-related trends are negative SWE and SI in northern New Mexico/southern Colorado, and Utah (a). In the western U.S. as a whole, the April 1 cumulative winter precipitation is near average, but both snowpack and SI are below average.

- The SI shows a slight tendency to be greater than one in the more continental (interior) regions of the western U.S. (Figure 5a).
- Variability in the SWE and cumulative winter precipitation are greatest near the Pacific coast (California, Oregon, and Washington are the most variable), and least inland (Wyoming, Colorado, eastern Montana are the least variable) (Figures 5b and 5c).
- The variability of the SWE tends to be more temporal in Arizona and the California group (Figures 6a and 6g), and more elevational in most of the other regions (Figures 6b, 6c, 6d, 6e, and 6h). However, there is both a temporal and elevational variability component in the Utah and Oregon/Washington regions (Figure 6f).

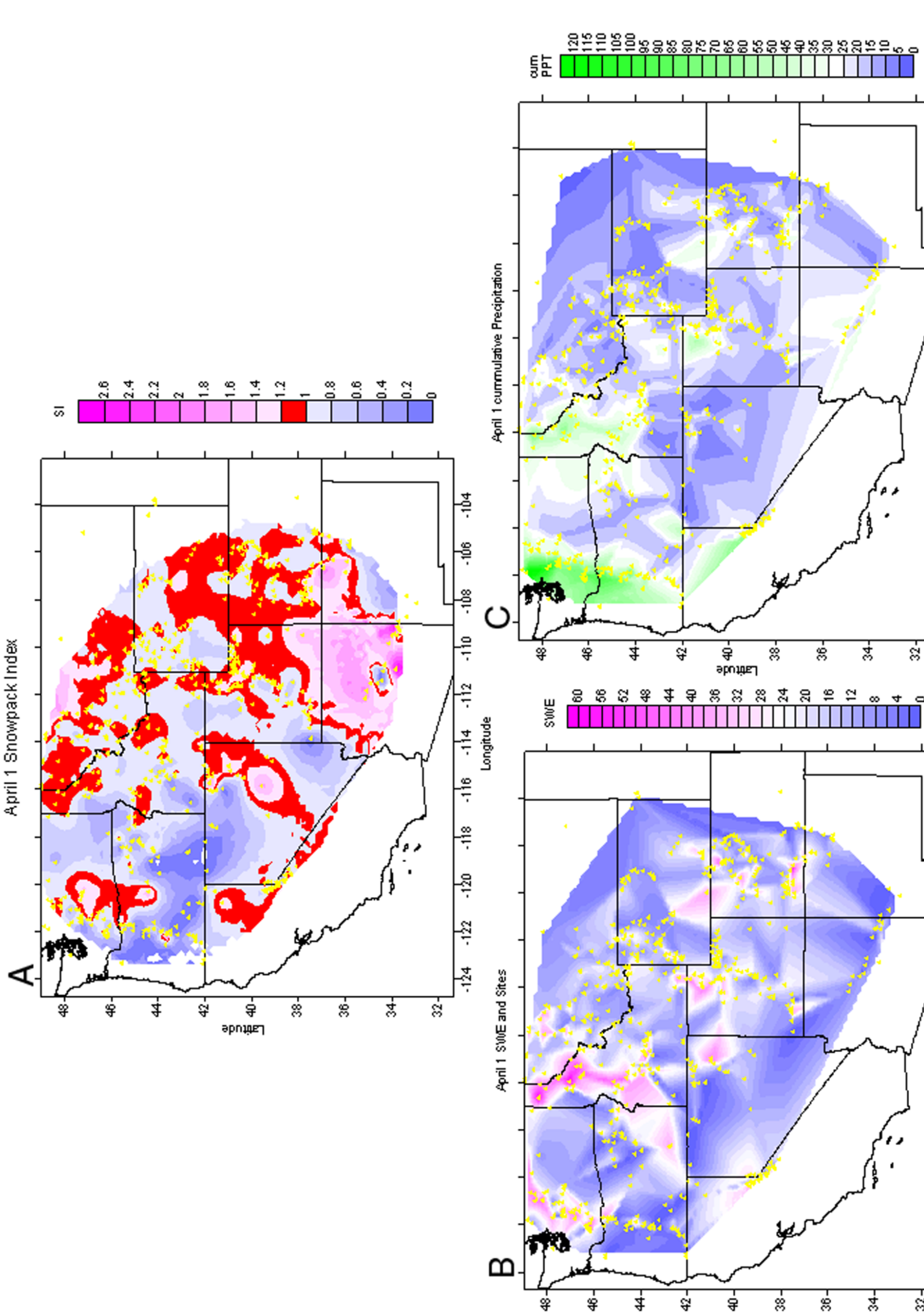

Figure 5 Spatial representation of SI (a), and the standard deviations of snow water equivalent (SWE) (b), and cumulative winter precipitation (c) as of April 1. The greatest variability of SWE and precipitation occurs in the Pacific Northwest, but there is also considerable precipitation variability in the southwestern U.S.

- The SI varies more by elevation in Colorado and at the higher elevations of California and Wyoming (Figures 7c, 7g, and 7h), and more over time in mountainous Arizona, northern New Mexico/southern Colorado, Oregon/Washington, and the lower elevations of California and Wyoming (Figures 7a, 7b, 7f, 7g, and 7h). Less distinct patterns of variability are seen in the Utah and Idaho/Montana mountains.
- Variability in precipitation is elevational in Colorado and northern New Mexico (Figures 8c and 8b), temporal in the California group (Figure 8g), and both in the other regions (Figures 8a, 8d, 8e, 8f, and 8g).
- Non-precipitation and non-temperature dependent variability is greater in Arizona, Oregon/ Washington, and Wyoming (Figures 9a, 9f, and 9h); is less in Idaho/Montana and Utah; and occurs at lower temperatures in Colorado (Figures 9e, 9d, and 9c).

These results may identify mountain snowpacks vulnerable to changes in climate factors other than precipitation. In this regard, the more vulnerable snowpacks appear to be in the mountains of Arizona/southern New Mexico and Oregon/Washington, whereas the less vulnerable snowpacks are in the mountains of Wyoming and northern Colorado.

In conclusion, the areas of greatest variability in the western United States tend to be those with the highest and lowest precipitation, and warmer winter temperatures (the marine and desert climate zones). By implication, these would also be the areas whose water supplies are most vulnerable to climatic change. The continental (interior) regions of the west are less variable, with their lower winter temperatures and low-to-intermediate amounts of precipitation, such as the Rocky Mountains of Colorado and Wyoming.

Snowpack SWE variability appears to be influenced by factors other than precipitation and temperature, particularly in the mountain areas of Oregon/Washington, Arizona, and Wyoming. Thus, other indices like FASTDIF, which relates to radiation balance, may be useful in future work to identify factors affecting snowpack development.

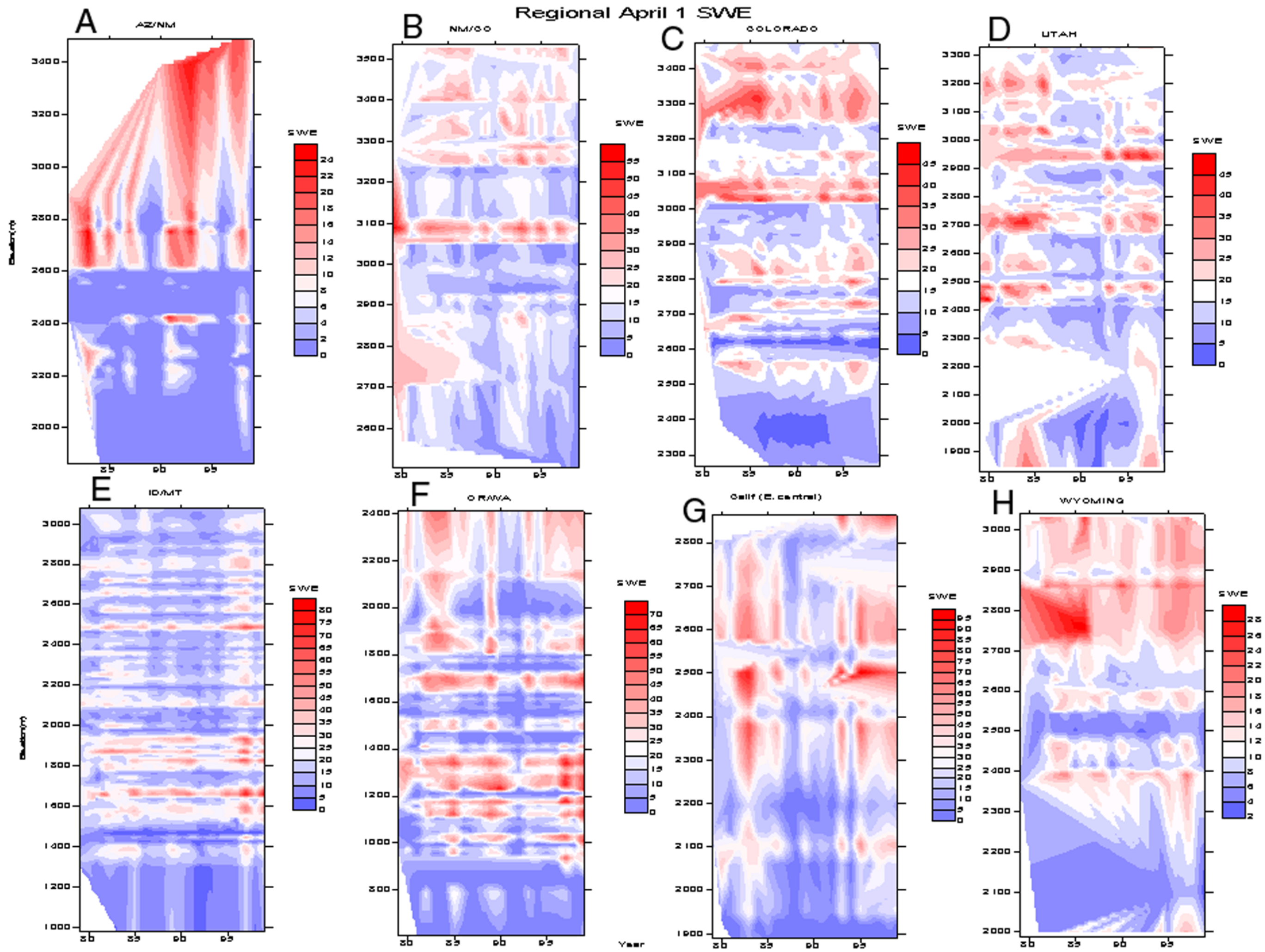

Figure 6 Time and elevation depictions of April 1 snow water equivalent (SWE) in the eight sub-regions. Each of these pictures indicate whether SWE variability is greater across time (dominance of vertical patterns), or by elevation (dominance of horizontal patterns). Temporal variability appears to be greater than elevational in Arizona/New Mexico and the California group. The opposite is the case in the other regions, but Utah and Oregon/Washington show both.

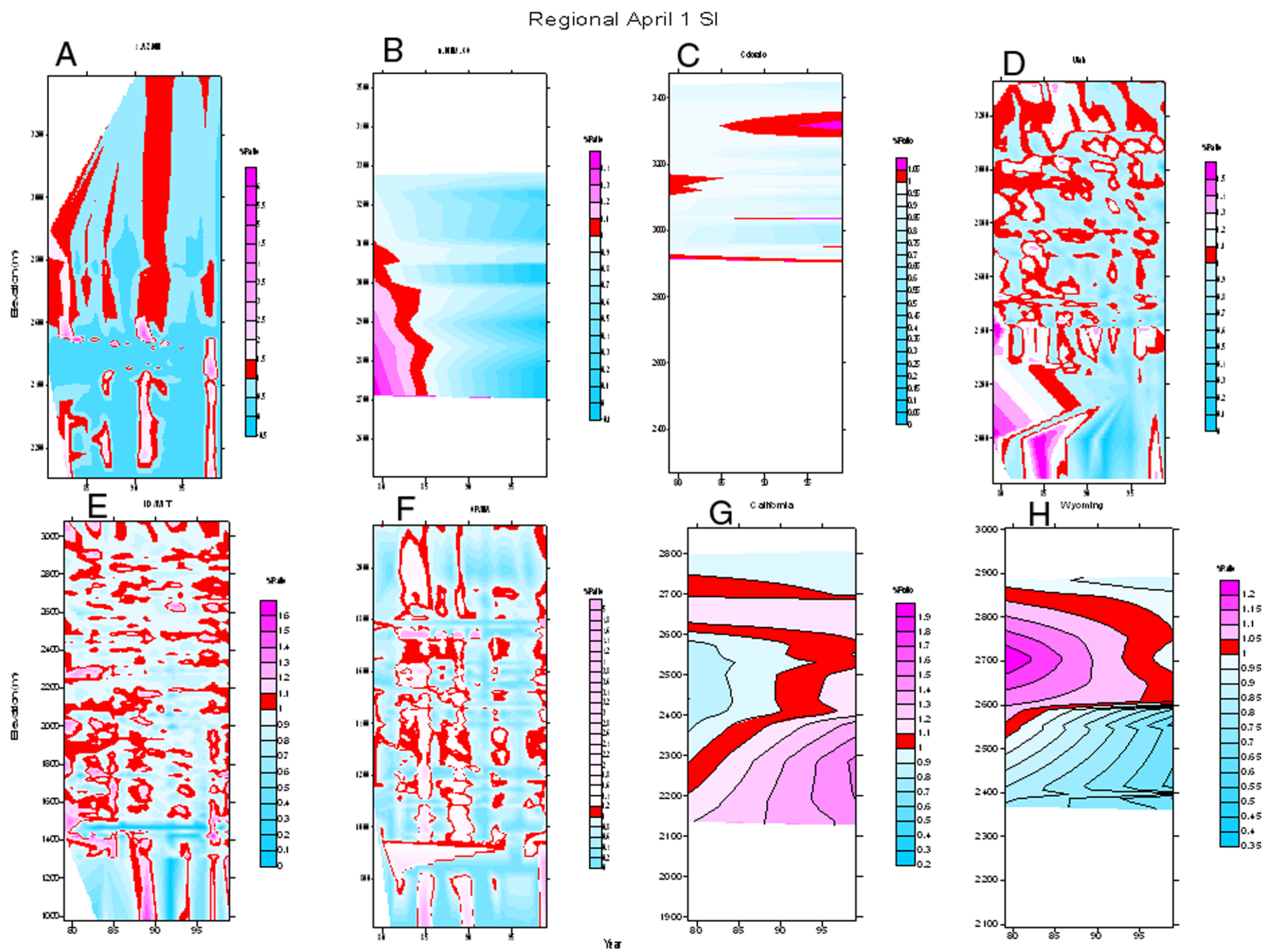

Figure 7 Time and elevation pictures as in Figure 6, but for the April 1 snowpack index (SI). Climatic conditions, excluding precipitation variability, appear to be increasingly favorable to snowpack development at the higher elevations of Colorado and at all elevations in the California group of sites. The opposite appears to be the case in northern New Mexico/southern Colorado, and Wyoming. Considerable temporal variability is also seen in the mountains of Arizona and Oregon/Washington.

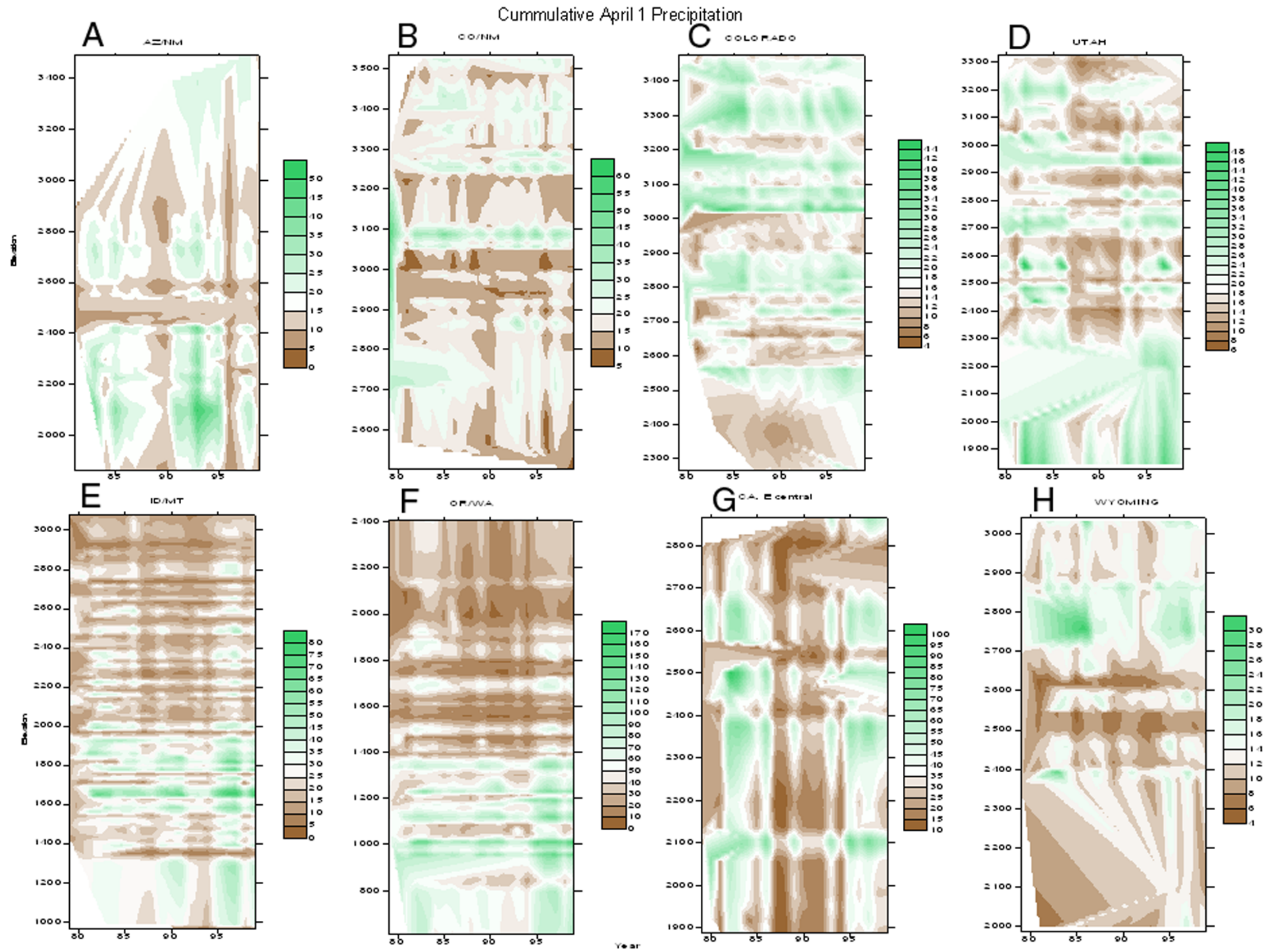

Figure 8 Time and elevation diagrams as in Figures 6 and 7, but for cumulative winter precipitation (Oct. 1-Apr. 1). Strong elevational variability is seen in Colorado, Utah, Idaho/Montana, and Oregon/Washington; whereas temporal variability appears to be more dominant in the California group, Wyoming, and somewhat in the Arizona mountains.

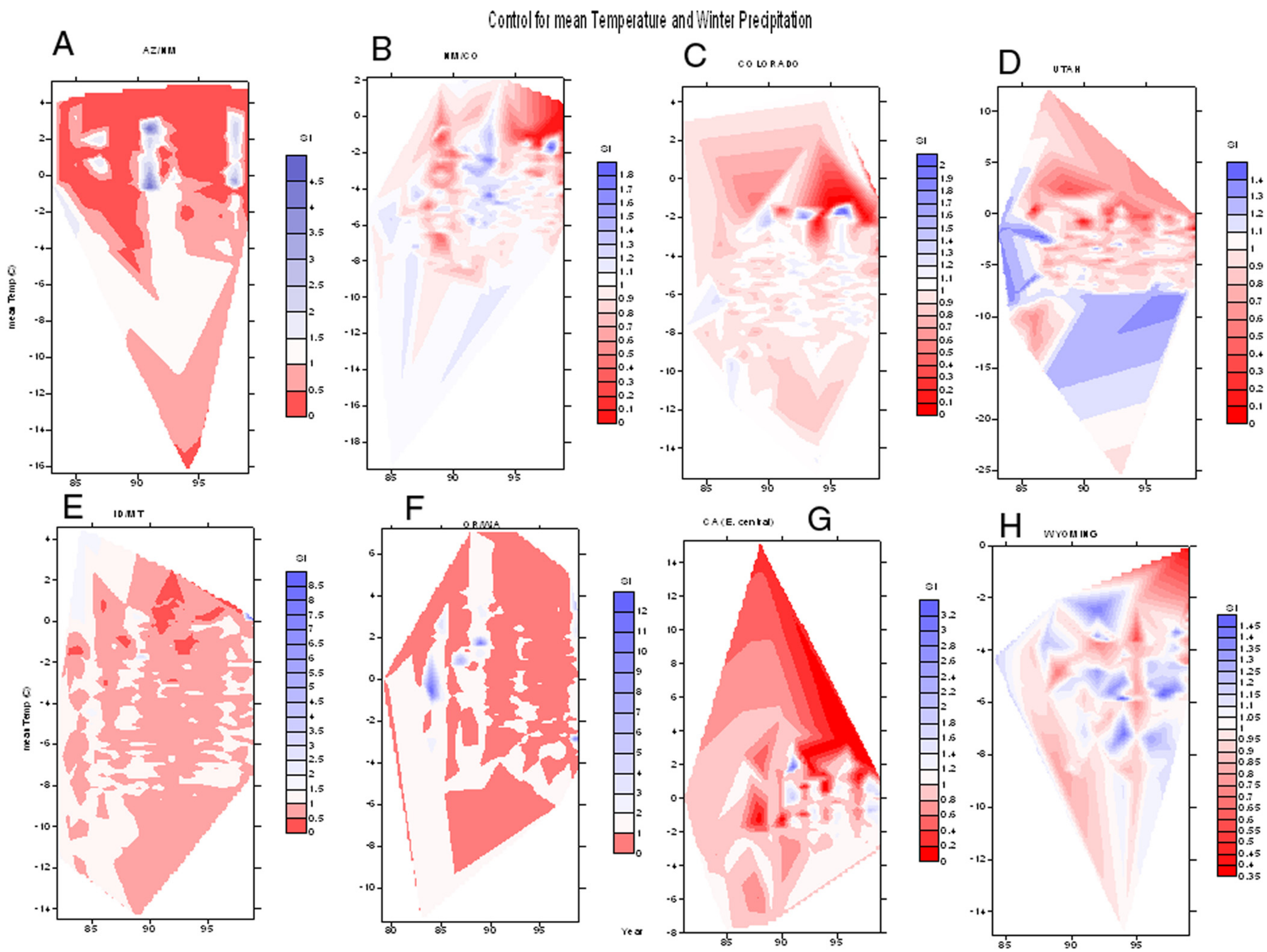

Figure 9 Time versus mean temperature for snowpack index (SI) conditions on April 1. These pictures are interpreted in the same manner as Figures 6-8, but looking at the role of temperature instead of elevation. Constant temperature conditions can be viewed for each region by reading horizontally across the pictures. Therefore, the role of climatic factors, excluding precipitation and temperature, can be assessed by tracking the change in SI at any given temperature contour. This is because SI controls for precipitation and a horizontal reading controls for temperature. Thus, those regions with a dominance of vertical patterns are those where non-precipitation and non-temperature effects on snowpack development are greatest. The Oregon/Washington region is an example, and perhaps to a lesser degree, so are Arizona and Wyoming.

Assessment of Environmental Influences on California Commercial Fish and Invertebrate Landings

Jerrold G. Norton and Janet E. Mason

Records of the commercial harvest of fish and invertebrates from California waters have been converted from California Department of Fish and Game documents to computer accessible formats (CACom data). Empirical orthogonal function (EOF) analysis of the log-transformed data indicates two robust modes of change in species composition. Together, the first two EOFs explain more than 45% of the variance in CACom data sets that included annual landings of 25, 29, or 43 market groups through the 1930-2001 period. Some market groups include several species, but 29 single-species market groups have been consistently landed and specifically recorded throughout the 71-year period examined. The EOFs and time variable coefficients (*C*), also known as principal components, are similar for each of the three ensembles of market groups (Figure 1). Since time-variation in the EOFs show the persistence (autocorrelation) that is characteristic of specific catch series, indices showing persistence in physical processes were developed from published data sets by accumulating anomalies from overall monthly means (Norton and McLain 1985; Klyashtorin 2001; Hanley and others 2002). Correlation coefficients (r) larger than 0.8 between time variation in the EOFs and environmental series strongly suggest that changes in catch composition are affected by persistent environmental conditions (Figures 2 and 3). The EOF1-species composition changes through the 1930-2000 period (*C*1) are closely related to persisting anomalous conditions in southern California (La Jolla) sea surface temperature (CaSST), the Pacific decadal oscillation index, and related variables (Figure 2). The EOF2-species composition changes (*C*2) are more closely related to local California southward wind stress (SWS) regimes (Figure 3). *C*2 also corresponds to variation in concentration of fish larvae and other zooplankton in California waters over the 1950-2000 period (Roemmich and McGowan 1995, McGowan and others 1998).

The CaSST and *C*1 values are closely related to equatorial atmosphere-ocean processes (Figure 4). The accumulated sea level pressure anomaly at Darwin, in northern Australia, and the accumulated sea surface temperature anomaly of an area in the eastern equatorial Pacific Ocean bounded by 4 °N-4 °S and 90 °W-150 °W (Hanley and others 2002) have overall variability similar to that found in CaSST and *C*1 ($r > 0.80$). The CaSST and *C*1 lag equatorial events during specific intervals (e.g. 1956-1961) suggesting that some California current physical and biological events are the result of changes occurring first in the equatorial ocean (Figure 4).

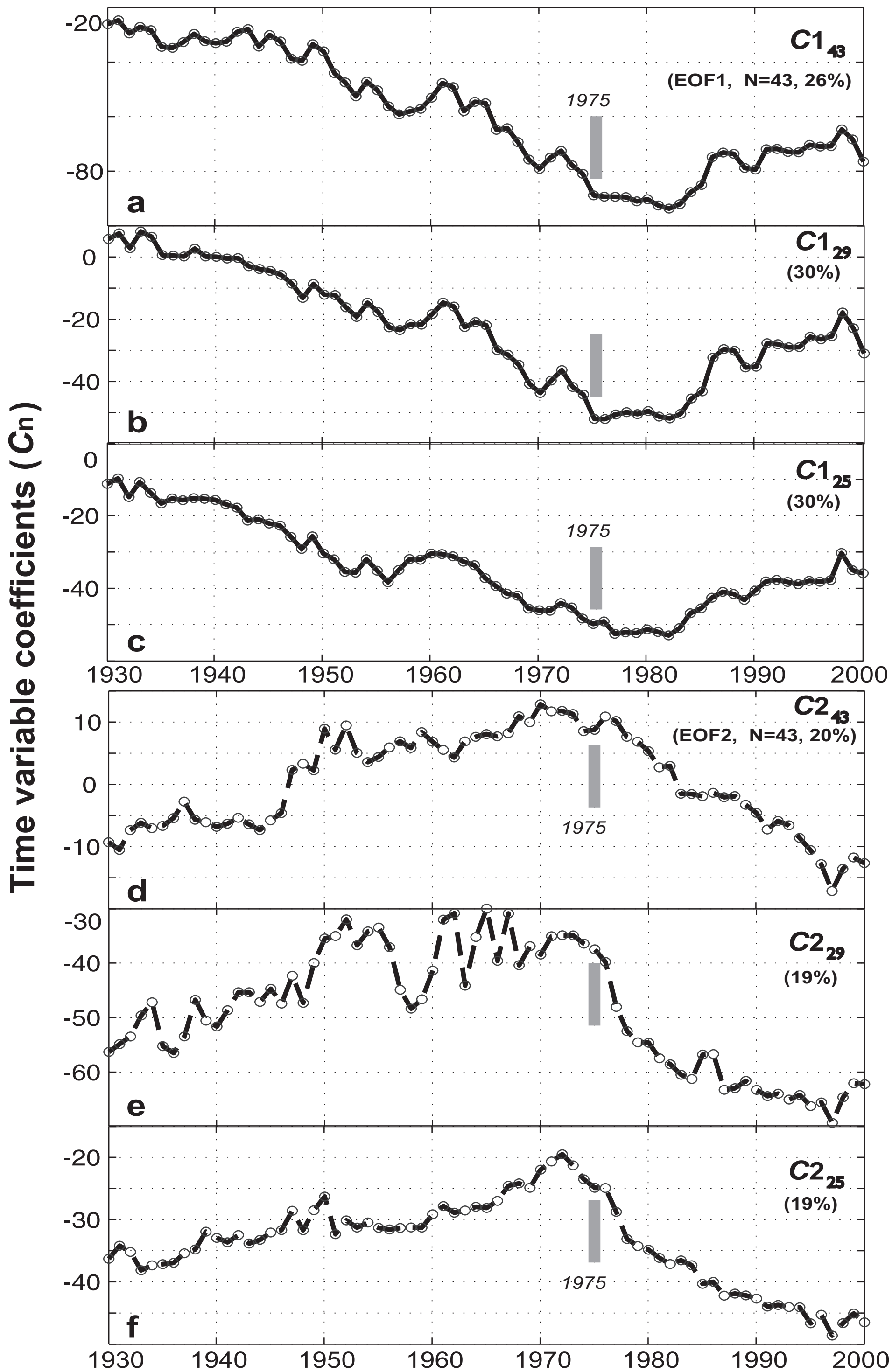

Figure 1 Time-variable coefficients (*C*) for the ensemble of the 43, 29, and 25 market groups having landings throughout 1930-2000. Time variable coefficients for EOF1 (*C*1, solid line) are at the top (a, b, c). Panels d, e, and f give the time-variable coefficients for EOF2 (*C*2, broken line). *C*-values for each year are shown by circles. Only the connecting lines are used in the following graphs.

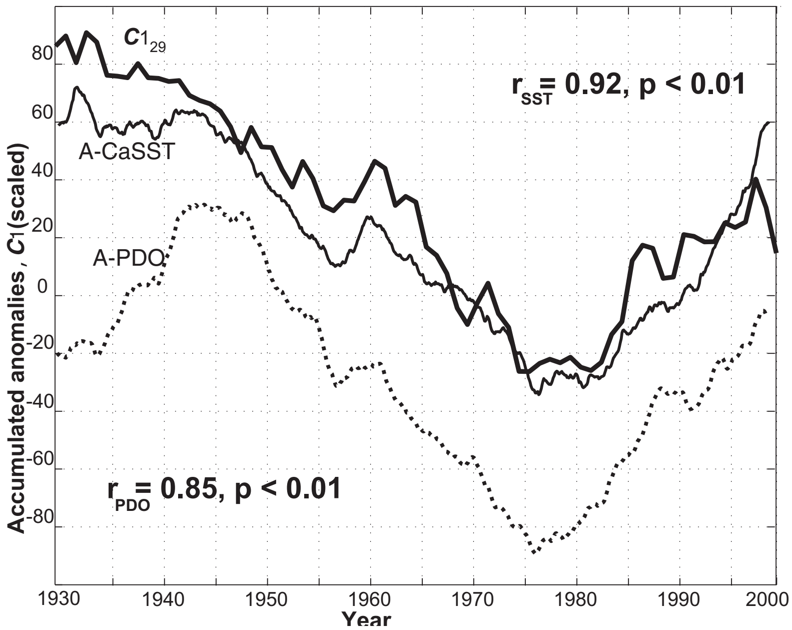

Figure 2 Accumulated monthly anomalies of the environmental indices and annual $C1_{29}$ values for $EOF1_{29}$ (heavy solid line) are scaled to show similarities. The accumulated sea surface temperature anomaly from the La Jolla shore station (A-CaSST) is the thinner solid line. The accumulated Pacific Decadal Oscillation (A-PDO) is the dotted line.

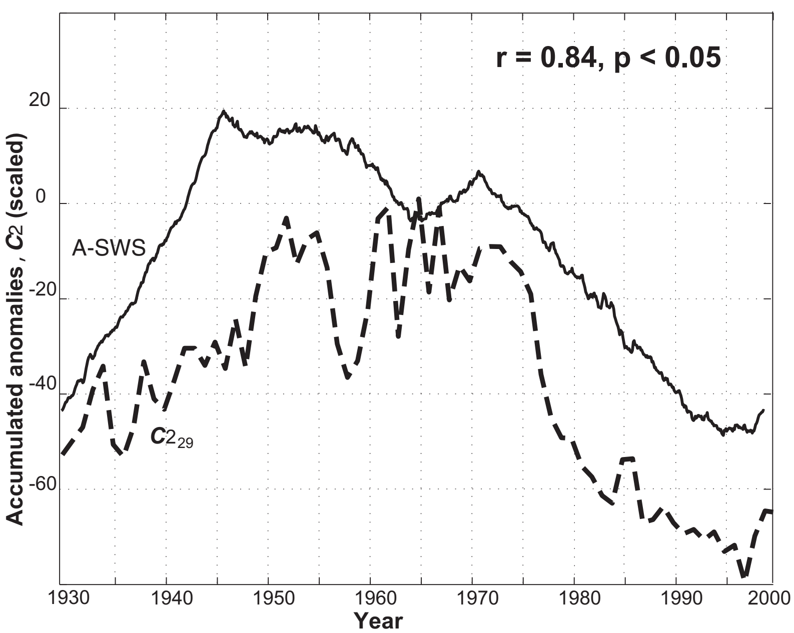

Figure 3 Accumulated monthly anomalies of southward wind stress and annual time variable coefficients ($C2_{29}$) values for $EOF2_{29}$ (heavy, broken line) are scaled to show similarities. The accumulated central California southward wind stress anomaly (A-SWS) is the thinner solid line. Scaling and offsets are as follows: $C2_{29}$ x 2, +60; A-SWS x 10 Pa.

The *C*1 and *C*2 species compositions follow well-known patterns of physical change in the California current environment (Norton and others 1985, Roemmich and McGowan 1995, Parrish and others 2000, Norton and Mason 2003). First, Parrish and others (2000) showed independent variation in central California SST and SWS over the 1881-1995 period. The uncorrelated temporal patterns in *C*1- and *C*2-series and their apparently unique correlation to A-CaSST and A-SWS is consistent with the Parrish and others (2000) result. Second, some of the highest coastal CA SST means of the 20th century occurred during 1957-1962, a period marked by a trend in *C*1 to more positively loaded species. Third, the northeastern Pacific climate change of 1973-1982 is indicated by negative trend in *C*1 during the early 1970s, followed by a relatively stable period (Figure 2). The *C*2 species compositions show the 1973-1982 climate shift by continuous change to more negatively loaded species (Figure 3). Finally, *C*1 and *C*2 have trend changes in response to the cooler ocean climate following the 1997-1998 California El Niño period. The *C*1 and *C*2 species compositions are less closely related to temporal fluctuations in total boats making landings and the total value of the catch adjusted for inflation than to the environmental variables, suggesting that the variation in catch composition is not entirely the result of either overall effort or the fisher's gross income (Norton and Mason 2003). The harvest from California waters appears to depend largely on the fish available, which in turn appears highly dependent on environmental factors.

When each species is examined in terms of EOF1 and EOF2 loading values, a progression of species dominance through the 1930-2000 period is indicated (Figure 5). The 1930s and 1940s (center right in Figure 5) were dominated by the sardine fishery, but scorpionfish, barracuda, and yellowtail were also at their maximum abundance. In the 1950s and 1960s (upper left) landings of jack mackerel and albacore were high. During the 1970s (center left in Figure 5) anchovy and sablefish were near their maximum abundances in the landings. Landings during the 1980s and 1990s (lower left and center) were characterized by several species, including Pacific mackerel, hake, and herring. Finally, in the 1990s and 1930s (lower and center right in Figure 5), the cycle of availability appears to be completing, with sardine, ocean whitefish, and sheephead increasing in the landings. Arrows at the top and the right sides of Figure 5 show correspondence of positive EOF1 loading values to persisting positive sea surface temperature (CaSST, top) and negative EOF2 to anomalously strong southward wind stress (SWS, right). The relationships of EOF loading values to persistence in environmental anomaly may provide alternate means of assessing the ability of species groups to withstand continued harvest pressure.

The *C*1 and *C*2 values indicate that species composition in the landings have changed continuously throughout the 71-year period, with general trends over intervals lasting from 6 to 36 years. These are the time scales of significant fisheries-climate interactions. Some species groups have occurred together under specific environmental conditions during the 1930-2000 period. This result may provide a basis for proactive ecosystem management that establishes harvest regulations, increasing or decreasing the catch of particular species which are dependent on ongoing environmental conditions.

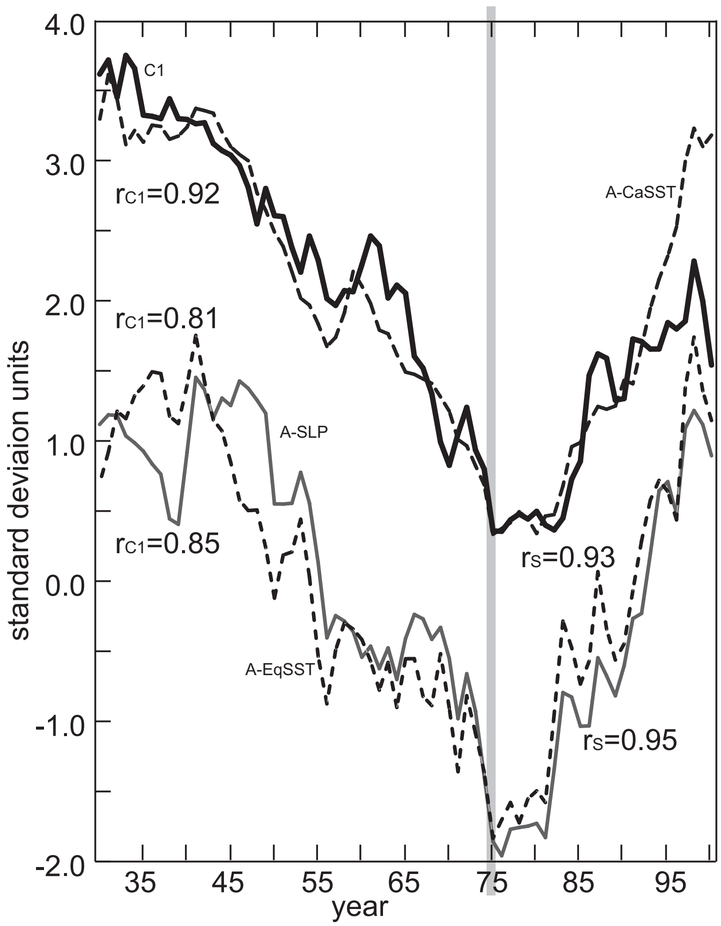

Figure 4 Comparison of $C1_{29}$, (upper solid line) to accumulated southern California SST anomalies (A-CaSST, upper broken line), accumulated equatorial sea surface temperature anomaly (A-EqSST) from 4 °N - 4 °S by 90 °W to 150 °W (lower broken line), and accumulated average sea level pressure anomaly at Darwin, Australia (A-SLP). All values are scaled by standardization; two units have been added to the upper two-time series.

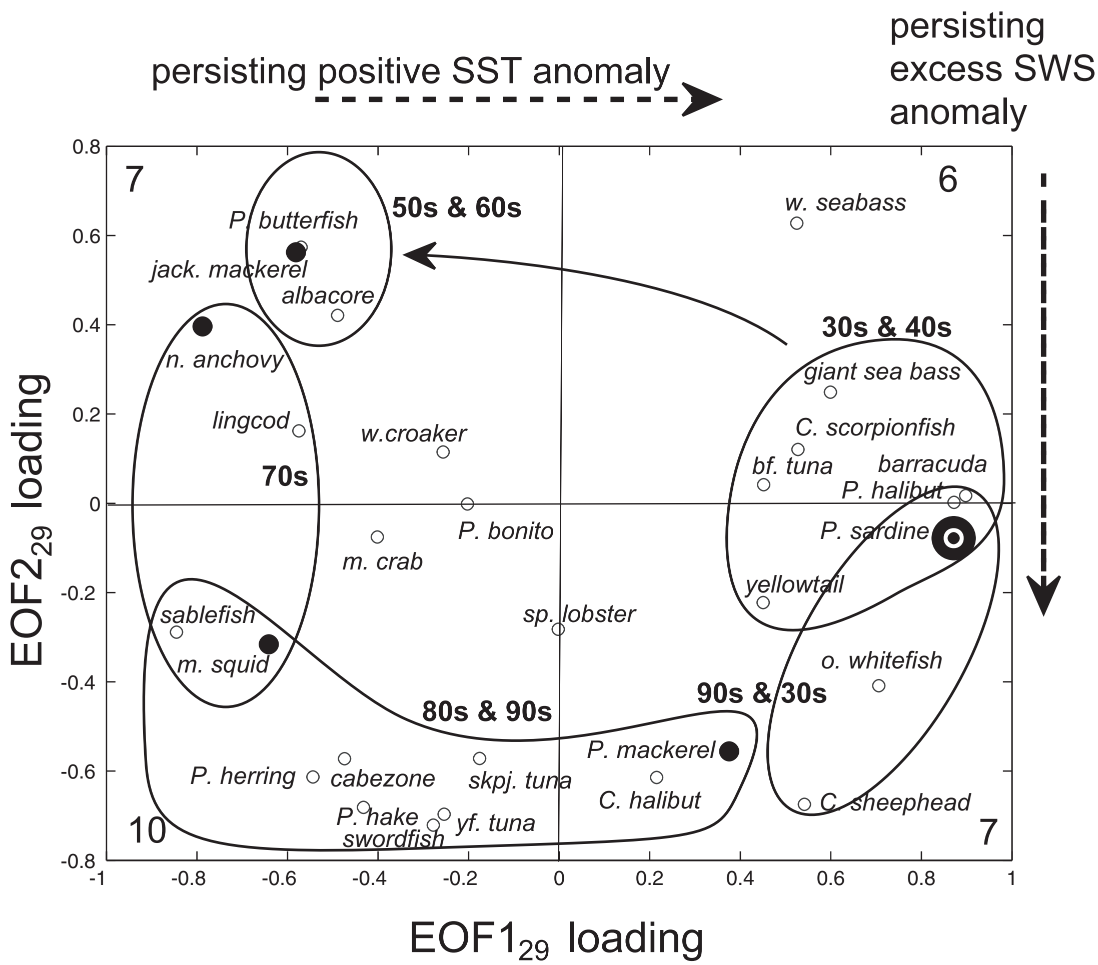

Figure 5 Comparison of EOF1 and EOF2 loading values for each species, with EOF1 on the abscissa and EOF2 on the ordinate. The number of species in each quadrant is given by bold numbers in the corners. Species locations are shown by circles. Filled circles indicate landings of more than a million metric tons during the 1930-2000 period. Sardine landings have exceeded eight million metric tons. Arrows at the top and the right side show correspondence of the "EOF-space" to persisting anomalous sea surface temperature and persisting anomalous southward wind stress, respectively. Species dominant in the landings relative to their own range of variability in the 1930s and 1940s (center right), the 1950s and 1960s (upper left), 1970s (center left), 1980s and 1990s (lower left and center), and the 1990s and 1930s (lower and center right) are indicated.

References

Hanley, D.E., M.E. Bourassa, J.J. O'Brien, S.R. Smith, and E.R. Spade. 2002. A Quantitative evaluation of ENSO indices. *J. Climate*, 16: 1249-1258.

Klyashtorin, L.B. 2001. Climate change and long-term fluctuations of commercial catches, *FAO Fish. Tech. Paper* 410, 86 pp.

McGowan, J.A., D.R. Cayan and L.M. Dorman. 1998. Climate-ocean variability and ecosystem response in the Northeast Pacific. *Science* 281: 210-217.

Norton, J.G., and D.R. McLain. 1985. Coastal ocean monitoring using daily sea surface temperatures from shore stations. *EOS, Trans. Am. Geophys. Union.* 66: 923.

Norton, J.G., D.R. McLain, R.E. Brainard and D.M. Husby. 1985. El Niño event off Baja and Alta California and its ocean climate context. Pages 44-72 in *Niño effects in the eastern subarctic Pacific Ocean*. W.S. Wooster and D.L. Fluharty, editors. University of Washington, Seattle.

Norton, J.G., and J.E. Mason. 2003. Environmental influences on species composition of the commercial harvest of finfish and invertebrates off California. *Calif. Coop. Oceanic Fish. Invest.* (CalCOFI) *Reports*, vol. 44 (in press).

Parrish, R.H., F.B. Schwing, and R.Mendelssohn. 2000. Mid-latitude wind stress: the energy source for climatic shifts in the North Pacific Ocean. *Fish. Oceanogr.* 9: 224-238.

Roemmich, D., and J. McGowan. 1995. Climatic warming and the decline of zooplankton in the California current. *Science* 267: 1324-1326.

A Comparison of Free-Air and Surface Temperature Trends at High Elevations in the Mountainous West of the U.S.

Nicholas C. Pepin, Mark Losleben, and Mike Hartman

Introduction

Concern over the impact of global warming at high elevation sites has increased over the last few years, leading to recent international workshops (e.g., HIGHEST II, 2001) and the declaration by the United Nations of 2002 as the "International Year of the Mountain" (Becker and Bugmann 2001). One area of particular concern in studies of cryospheric change is the role that mountain glaciers and seasonal snowpack play in providing water resources for mountain communities. The rapid retreat of many glaciers (Thompson 2000) has been cited as proxy evidence for a rapid increase in surface temperatures (Houghton and others 2001). However, there is extremely limited long-term surface temperature data at high elevation sites due to logistical problems of instrument maintenance in remote environments. For this reason, most studies of temperature variability in the middle troposphere are based on satellite and radiosonde data.

Systematic examination of the horizontal differences between temporal trends in surface temperature observations at high elevations and free-air equivalent temperatures (from both radiosonde and satellite data) has so far received less attention than the vertical comparison between the low elevation surface and lower and middle troposphere. This issue is important for two main reasons:

a. It could shed light on the apparent discrepancy between rapid glacier retreat and lack of strong free-air warming in the middle troposphere. It may be that the surface is warming at a faster rate than the free-air, or it may be that factors other than temperature change are more influential in causing glacier retreat.

b. Most General Circulation Models (GCM) used to develop scenarios of future climate represent surface mountain conditions poorly due to the complex interaction between topography, surface characteristics, and the atmosphere. The atmosphere above mountains in GCM often responds to radiative forcing in contrasting ways to lowland areas (Giorgi and others 1997) through complex feedback processes. However, simulated free-air temperatures are usually very different from temperatures experienced on the surface, and this difference is handled badly in models. Thus global warming scenarios in mountain regions using model output are often potentially unrealistic.

A few studies have begun to compare long-term records of surface and free-air equivalent temperatures (at the same elevation). Pepin and Losleben's (2002) studies in the Colorado Front Range show that divergent trends result in the surface becoming an increasing heat sink relative to the free-air. Possible explanations include increased instability leading to higher snowfall selectively at high elevations, thus depressing surface temperatures (Barry 1990). Preliminary analysis in other mountain locations (Pepin and Losleben 2001) fails to replicate this pattern in other environments. A more extensive study (Seidel and Free 2001) examines the contrast in surface and free-air equivalent temperatures solely using the radiosonde Comprehensive Aerological Reference Data Set (CARDS). Comparing trends for pairs of sites (high elevation surface versus free-air above adjacent low elevation station) showed contrasting patterns, with a tendency towards increased warming at high elevation surface sites, more commonly in the tropics.

The advantage of Seidel and Free's study (2001) is that the results are based on one high quality dataset, which reduces inter dataset compatibility problems. It is, however, debatable as to how well the temperature changes represent changes at "high elevation" because many of the sites were at relatively low elevations (for example, Mexico City and Denver) or in suburban airport locations in valley bottoms, rather than in true montane locations.

This paper compares surface temperature trends from SNOW-Telemetry (SnoTel) sites in the western U.S. to simultaneous free-air trends interpolated from the NCEP/NCAR reanalysis dataset (Kalnay and others 1996; Kistler and others 2001) for 1982-2001. The reanalysis is a combination of radiosonde and satellite data with model output. The interpolation acknowledges that the free atmosphere is less complex than the Earth's surface and that the free-air temperature field is less variable (lower rates of change) and more regular.

Data and Method

Daily SNOTEL data for the western U.S. were used to represent the surface temperature field. Although there are problems with this data set (Serreze and others 1999), extensive quality control was performed. Free-air equivalent temperatures (AETs) were interpolated both vertically and horizontally for each SNOTEL site from the NCEP/NCAR reanalysis.

There are 600+ SNOTEL sites in the western U.S., concentrated in the high elevation areas that have extensive winter snowpack. The network began in the early 1980s. In 1984 there were 76 stations reporting, but by 1987 this had increased to 208. A minimum length of 18 years of record was chosen for this study, giving 76 possible stations. Thirteen of these were deemed to have inhomogeneities and were discarded. The remaining 63 sites range from 991 to 3,536 m above sea-level, and cover all states of the west except New Mexico (Figure 1). California has extensive gaps in the network, but has its own snowcourse data (not used).

For the selected stations daily maximum and minimum temperatures were screened for errors. All values were subject to a standard deviation test, and values more than three standard deviations away from the mean (calculated on a monthly basis) were flagged. This is a similar (but stricter) criterion to that employed by Serreze and others (1999). The temperature sensors have a tendency to get stuck so all repeated values (ignoring day 1) were flagged. Such procedures removed about 10% of the data.

The NCEP/NCAR reanalysis data is recorded on a 2.5 degree latitude/longitude grid, twice daily (0 and 12 Z) at pressure levels 500, 700, 850, 925, and 1,000 mb. A twice daily air equivalent temperature (AET) was created for each SNOTEL site by interpolating between pressure levels for a given time-step. The vertical interpolation was done first based on a linear lapse rate between the two nearest pressure levels. This ignores the possibility of subsidence inversions in the free-air, but normally this is not a significant problem. Because SNOTEL sites are invariably not at a 2.5-degree intersection of the NCEP/NCAR grid, horizontal interpolation from the four nearest grid points is also necessary. This was done after the vertical interpolation (See Figure 2a). On the scale of 2.5 degree grid boxes most SNOTEL sites are on higher land than the surface elevation at the four grid points used for the interpolation, so it is free-air interpolation rather than sub-surface (Figure 2b). The later would be inadvisable.

No quality control was performed on the NCEP/NCAR reanalysis beyond that already carried out. The main problems occur in 1957 (due to a time change of observations) and 1979 (due to the introduction of satellite data), both of which occur before the period of this study. The temperature observations are regarded as of high quality in the reanalysis and the model output is strongly biased towards the raw observations.

A new variable was created representing the difference between the free-air equivalent and surface temperatures, to be referred to as the Free-Air/Surface Temperature Difference or FASTDIF. A daytime FASTDIF (XFASTDIF) was derived through a comparison of the daily surface maximum temperature with the 0Z free-air grid (4 pm PST or 5 pm MST), and a nighttime FASTDIF (NFASTDIF) comparing the daily surface minimum temperature with the 12Z free-air grid (4 am PST or 5 am MST). The daytime errors in FASTDIF due to inexact timing may be important, especially on clear days in winter and to the east of the region, but those at night are expected to be small. However, the diurnal range of free-air temperatures is extremely small (typically an order of magnitude less than at the surface). The overall error due to the timing error in the NCEP/NCAR reanalysis is thus small, and most importantly is not expected to change over time, making analysis of temporal trends in FASTDIF possible.

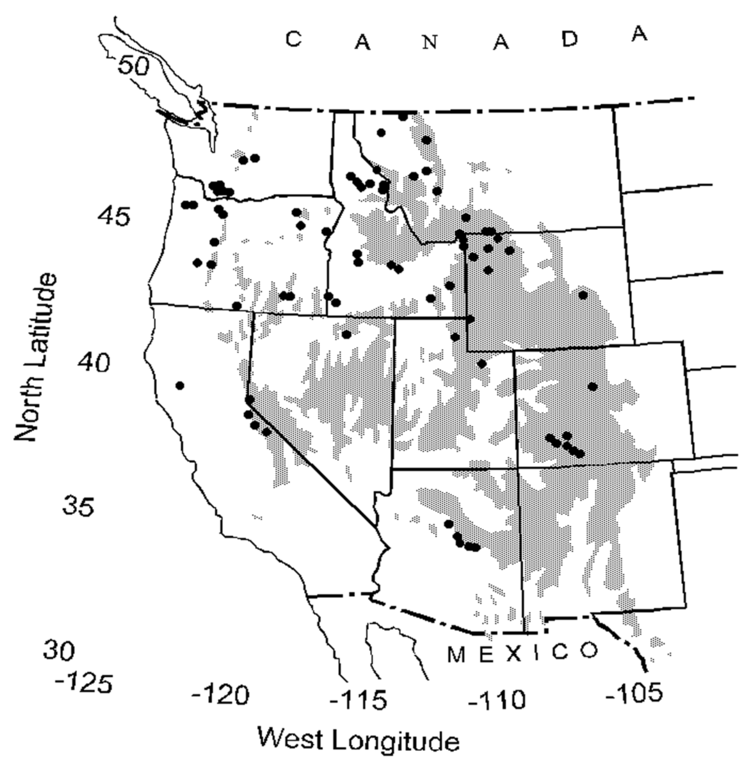

Figure 1 Map of SNOTEL sites used in this analysis

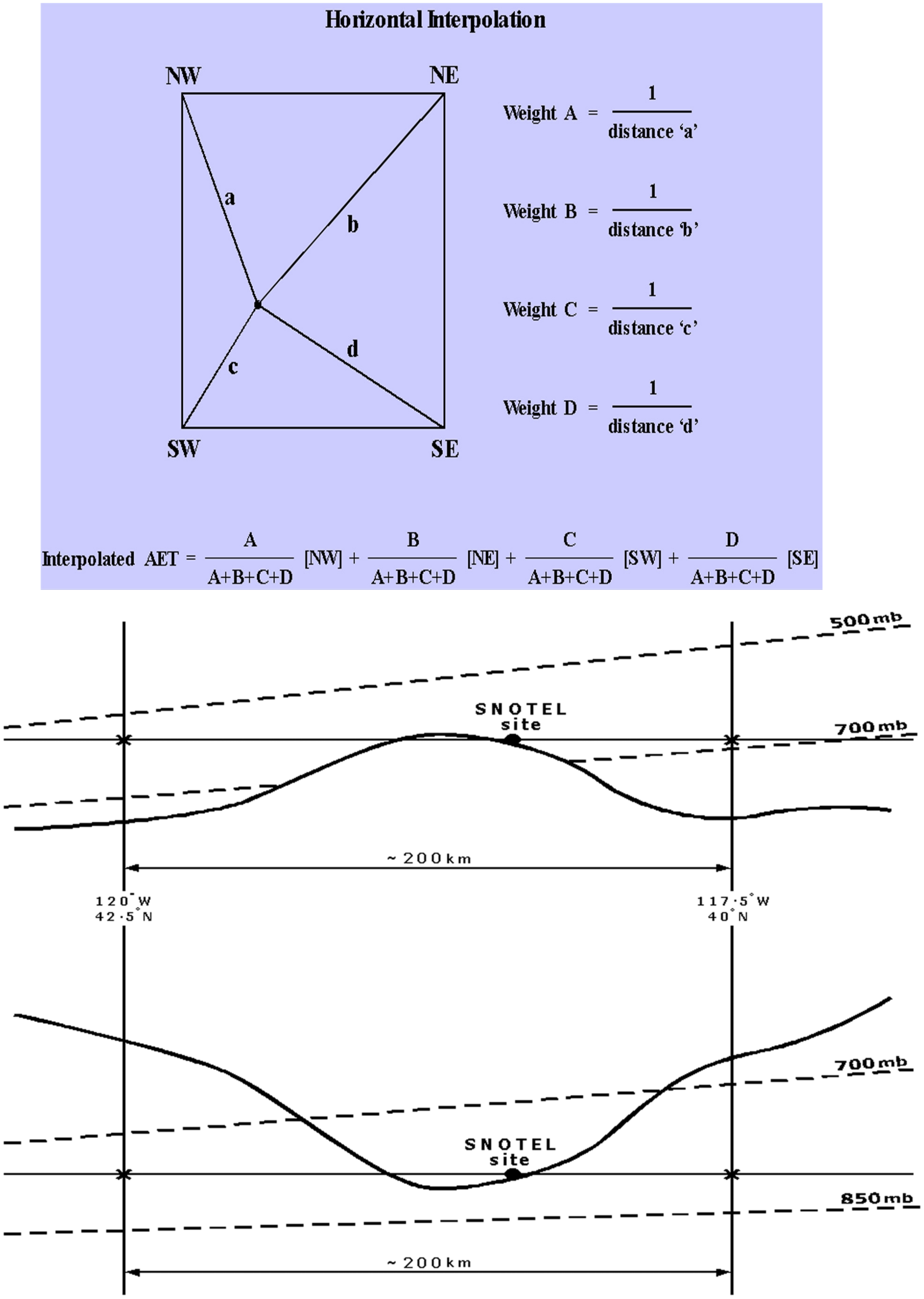

Figure 2a and 2b Interpolation method for creation of air equivalent temperatures (AETs) from NCEP/NCAR reanalysis. (a) Horizontal interpolation from four nearest grid points. (b) Schematic representation of interpolation viewed as a cross-section, illustrating free-air interpolation (top) rather than sub-surface (bottom)

Data Evaluation

Before comparing temperature trends in surface and free-air equivalent temps, both the surface SNOTEL and interpolated AETs were evaluated using simple techniques. The correlation between 0Z AET and surface maxima was calculated at each site (Figure 3a). Values are consistently high as expected. The correlation between 12 Z AET and surface minima (Figure 3b) is considerably more variable and weaker on average, illustrating the influence of cold-air ponding at night and the decoupling of surface minima from free-air equivalents under certain synoptic conditions.

Mean values of XFASTDIF are positive (Figure 4a) showing the warming of the surface above free-air by the positive radiation balance. An increase from north to south and from west to east reflects the trend toward higher solar input in the latter areas. NFASTDIF shows high local variability and is topographically controlled (Figure 4b). All values are negative as expected. Both XFASTDIF and NFASTDIF show correlations with elevation, on an annual basis and in all seasons, (Figure 5) although there is much scatter, especially at night. This reflects the enhanced diurnal radiative cycle at high elevations in the mostly cloud-free western U.S., although the tendency towards more negative NFASTDIF at high elevations is offset somewhat by local cold-air ponding at lower elevations.

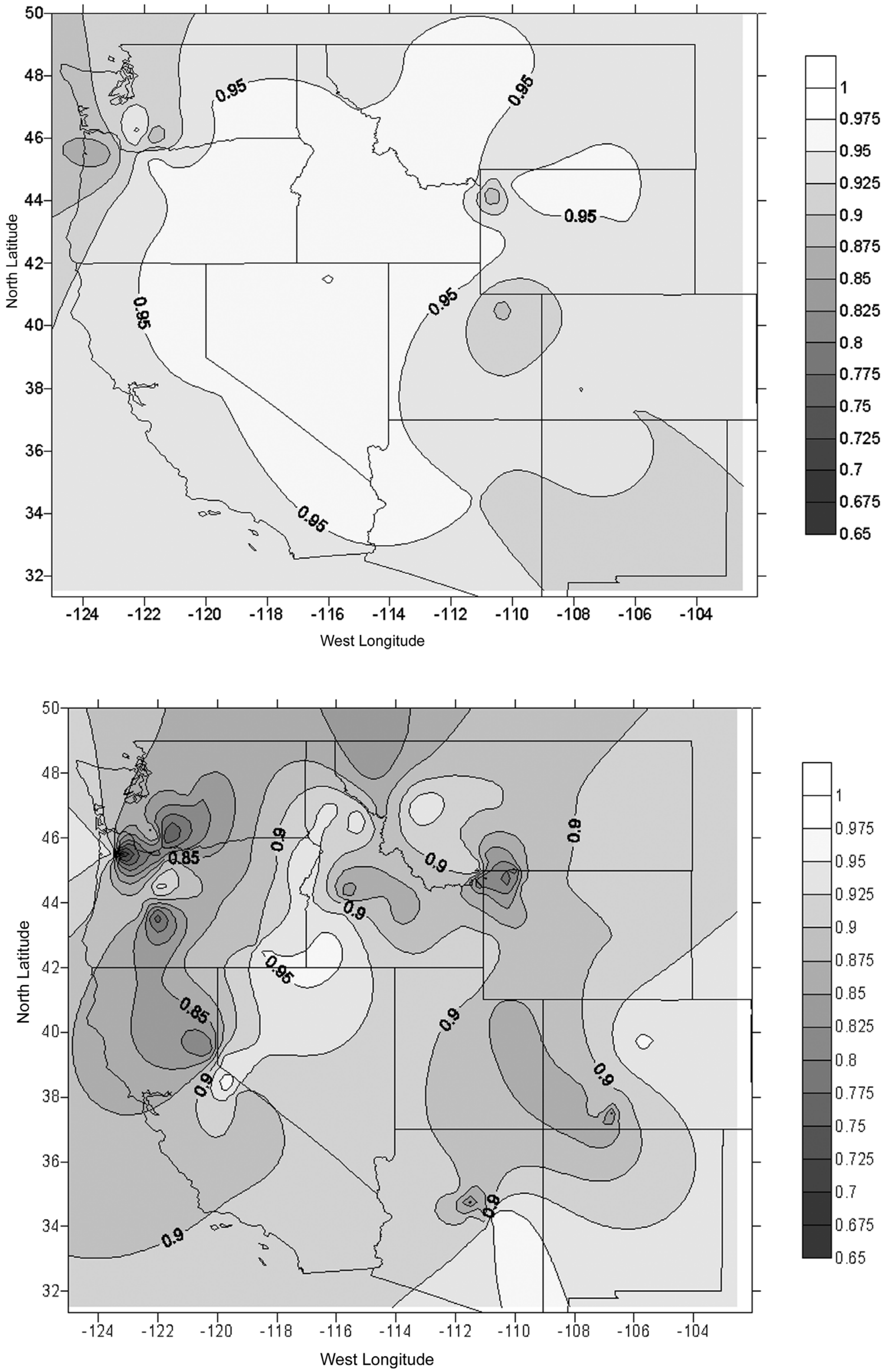

Figure 3a and 3b (a) Map of the correlation between OZ air equivalent temperatures (AET) and surface maxima (b) Map of the correlation between 12 Z AET and surface minima

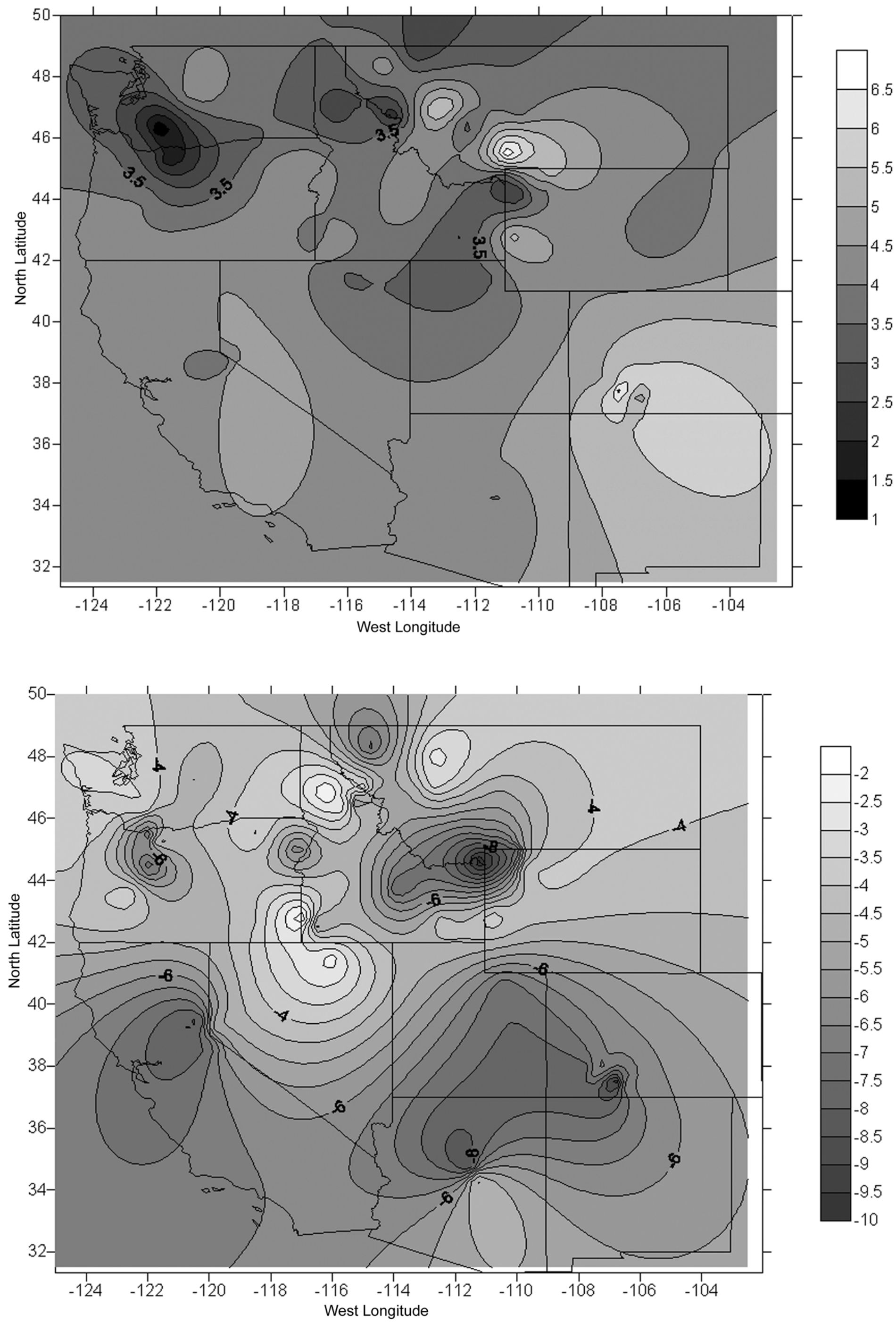

Figure 4a and 4b (a) Mean annual values of XFASTDIF (b) Mean annual values of NFASTDIF

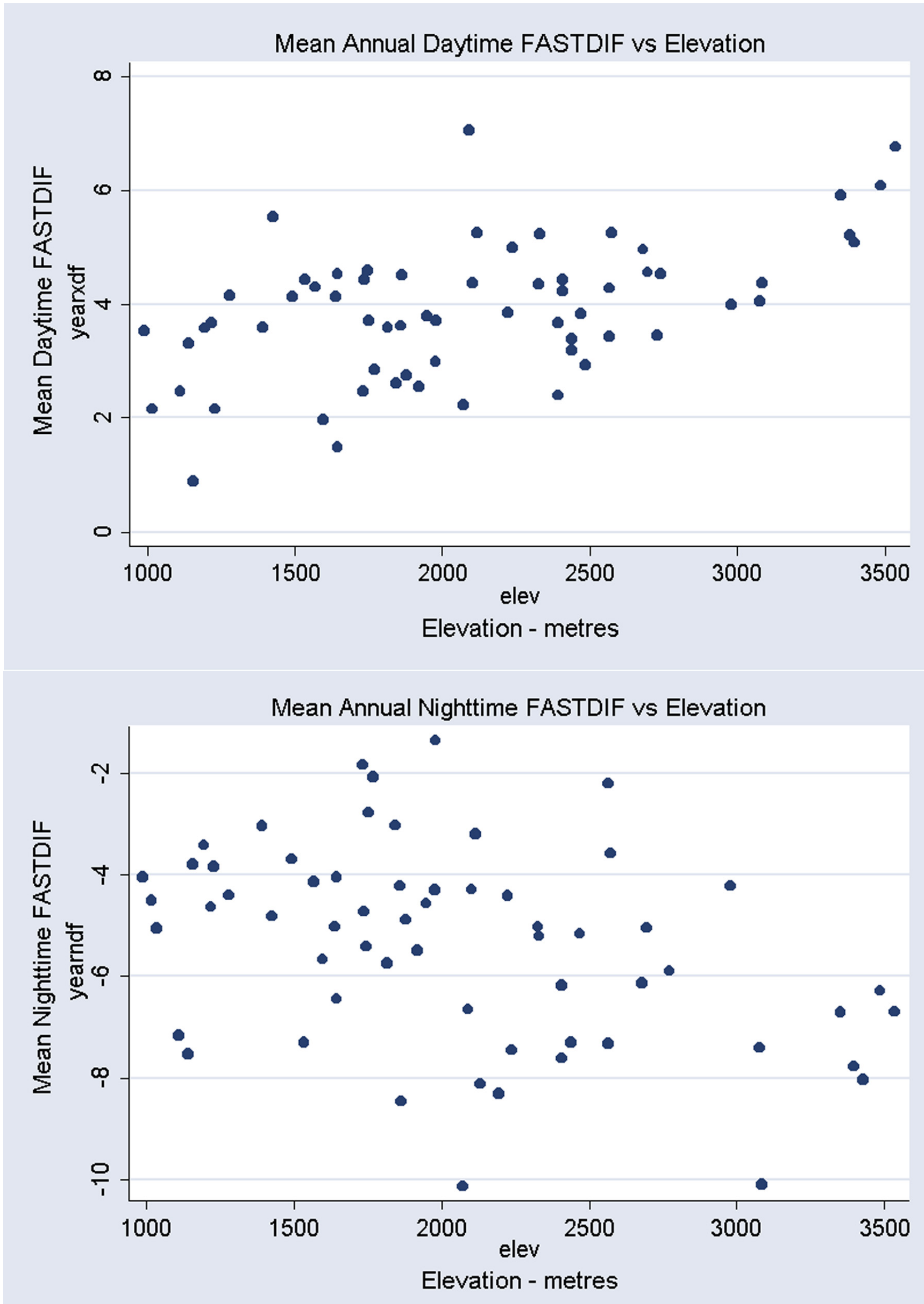

Correlations DJF -0.47 MAM -0.44 JJA -0.23 SON -0.33 Annual -0.38

Figure 5a and 5b Correlations between (a) XFASTDIF and elevation, (b) NFASTDIF and elevation

Seasonal cycles of FASTDIF were examined. At each station mean monthly FASTDIFs (day and night separately) were compared with the annual FASTDIF value to create monthly XFASTDIF and NFASTDIF anomalies. K-means cluster analysis on the 12 anomalies was performed to separate sites with differing seasonal FASTDIF regimes. Four main groups of XFASTDIF regime were identified

(Table 1), the most frequent being Type 2 (late-spring peak and winter minimum), common in the Great Basin, and Type 4 (the double spring and fall peak pattern). A similar cluster analysis for NFASTDIF also identified four main regimes, the most frequent being Type 3 (strong summer trough). The fact that similar seasonal trends could be identified at numerous sites, often in close proximity, increases confidence in the SNOTEL data, since all sites are independent data sources (unlike the NCEP/NCAR reanalysis).

Temporal Trends in FASTDIF

Monthly FASTDIF anomalies were calculated independently for day and night. Temporal trends for which $p<0.05$ were deemed significant. A map of daytime trends, expressed in deg C/yr (Figure 6a) shows positive trends (surface warming relative to free-air) of up to 0.25 deg C/yr in Utah, Idaho and Washington, while the majority of the far west and the northern states show negative trends. A plot of the trend magnitude versus elevation shows no strong relationship in this dataset, despite the findings of other authors concerning increased warming at high elevations (Beniston and others 1997). Significant negative trends are more common than positive ones, occurring at 32 stations (more than half the sample). A chi-squared analysis ($p<0.01$) supports a definite bias to negative trends. Most are not strong, weaker than -0.1 deg C/yr. The map of nighttime trends (Figure 6b) shows positive trends to be concentrated in the northern states, particularly Montana, with negative trends concentrated in Oregon, southern Idaho, Utah, and Arizona. There is no strong similarity with the daytime pattern discussed earlier. Again there was no correlation between trend magnitude and elevation, and there was no strong tendency toward one sign of trend, with almost equal numbers of significant decreases and increases. No relationship between regime type and the sign of XFASTDIF or NFASTDIF trends was found.

Table 1 Different annual regime types for XFASTDIF and NFASTDIF

Type	*Peak (most +ve)*	*Trough (most –ve)*	*n. of stations*	*Common location(s)*
X1	Mar., Apr.	Dec., Jan.	11	N. Rockies
X2	Apr., May, Jun.	Dec., Jan.	21	Great Basin
X3	Jul., Aug.	Dec., Jan.	5	Coastal W
X4	**Spring** and Fall	Jul., Aug.	26	S. Rockies
N1	May	**Dec., Jan.** & Jul., Aug.	7	ID and OR
N2	Unclear	Dec., Jan.	13	S. Rockies
N3	Nov, Dec., Jan.	Jul., Aug.	20	Northern Tier
N4	Spring and Fall	Dec., Jan. & **Jul., Aug.**	21	**Scattered**

X1 etc. refer to XFASTDIF regimes and N1 etc. refer to NFASTDIF regimes
When there are two periods in the year with strongly positive or negative values, the bold period is the most extreme.

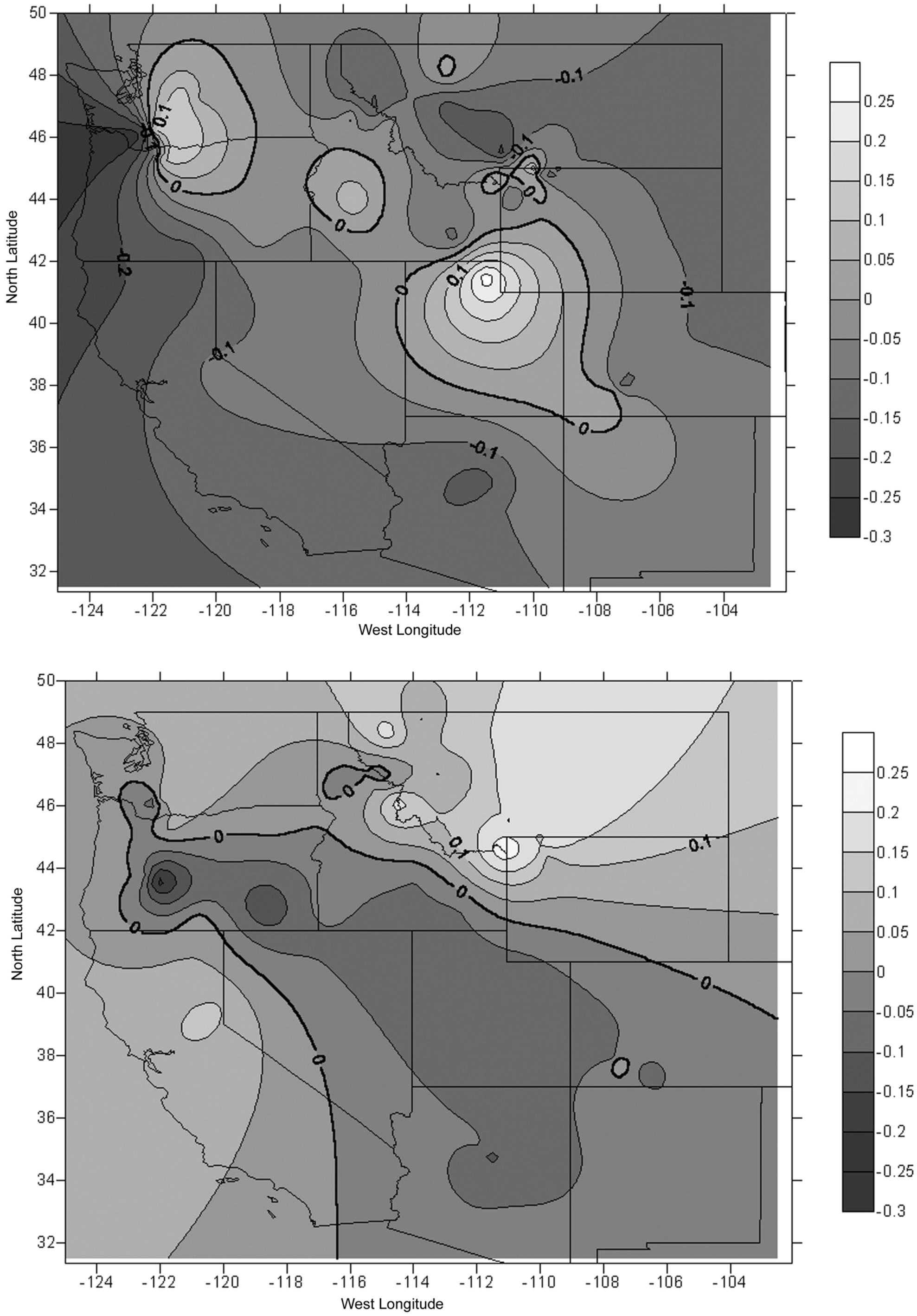

Figure 6a and 6b (a) Map of temporal trends in XFASTDIF (deg C/yr) (b) Map of temporal trends in NFASTDIF (deg C/yr)

Discussion

Despite the rather limited dataset and time period, many sites showed significant temporal trends in the free-air/surface temperature difference, meaning a systematic change in the energy balance of the surface over the western U.S. since 1984. This should inform the ongoing debate about the discrepancies between long-term measurements of surface temperature and lower and middle tropospheric indicators such as satellite data. Unless many of the trends in FASTDIF are caused by long-term instrumental drift at the SNOTEL sites, the highly local nature of the FASTDIF trends makes it difficult to make sweeping statements about data comparison on a global scale. In some areas the surface is warming faster than the free-air, but at others the opposite is true. In addition it must be remembered that looking at FASTDIF trends alone tells us little about the sign of absolute changes in surface and free-air temperatures.

More research needs to be undertaken to examine:

a. A comparison of free-air vs. surface temperature trends, both absolute and relative changes, on a global scale and over longer time periods.

b. The causes of trends in FASTDIF at individual sites.

Because the main control of FASTDIF is the energy balance of the surface, the net radiation budget, cloud cover, the presence or absence of snow cover, and the strength of the airflow at the surface are the physical controls. A more detailed examination of how these factors vary in their influence over time and space may help throw light on the patterns of change identified in Figure 6. It could be that persistent circulation anomalies lead to distinctive spatial signatures in FASTDIF, thus explaining some of the apparent spatial complexity of the trends identified in this paper.

Conclusions

The significant changes in FASTDIF outlined in this paper illustrate a decoupling of the Earth's surface from the free-air in terms of response to radiative forcing over the last two decades. Although the NCEP/NCAR interpolated free-air temperatures are highly dependent on the raw radiosonde and satellite data upon which they are based, there is an element of modeling in the NCEP/NCAR output. It may be beneficial to separate the free-air data sources by using radiosonde and satellite data separately in future analyses. Further analysis of the many SNOTEL sites rejected in this paper because of possible inhomogeneities, along with high elevation National Weather Service stations and other independent mountain sites, could greatly expand the number of surface/ free-air comparisons.

References

Barry, R.G. 1990. Changes in mountain climate and glacio-hydrological responses. *Mountain Research and Development* 10: 161-170.

Becker, A., and H. Bugmann. 2001. *Global Change and Mountain Regions*. The Mountain Research Initiative, IGBP Report 49, 86 pp.

Beniston, M., H.F. Diaz, and R.S. Bradley. 1997. Climatic change at high elevation sites: An overview. *Climatic Change* 36: 233-252.

Giorgi, F., J.W. Hurrell, M.R. Marinucci, and M. Beniston. 1997. Elevation dependency of the surface climate signal: A model study. *Journal of Climate* 10: 288-296.

HIGHEST II, *Workshop on Climate Change at High Elevation Sites: Emerging Impacts*, Davos, Switzerland, 25-28 June 2001.

Houghton, J. and others. 2001. editors Climate Change 2001: The Scientific Basis. IPCC, Cambridge University Press, Cambridge, U.K., 881 pp.

Kalnay, E. and others 1996. The NCEP/NCAR 40-year reanalysis project. *Bulletin of the American Meteorological Society* 77: 437-471.

Kistler, R. and others. 2001. The NCEP/NCAR 50-year reanalysis. *Bulletin of the American Meteorological Society* 82: 247-268.

Pepin, N.C., and M.L. Losleben. 2001. Long term changes in surface screen and free-air equivalent temperatures in continental and maritime mid-latitude mountain ranges. *2nd International Workshop on Climate Change at High Elevation Sites: Emerging Impacts*. Davos, Switzerland, 25-28 June 2001.

Pepin, N.C., and M.L. Losleben. 2002. Climate change in the Colorado Rocky Mountains: Free-Air versus surface temperature trends. *International Journal of Climatology* 22: 311-329.

Seidel, D.J, and M. Free. 2001. Comparison of lower-tropospheric temperatures at low and high elevation radiosonde sites. *2nd International Workshop on Climate Change at High Elevation Sites: Emerging Impacts*. Davos, Switzerland, 25-28 June 2001.

Serreze, M., M.P. Clark, R.L. Armstrong, D.A. McGinnis, and R.S. Pulwarty. 1999. Characteristics of the western United States snowpack from snowpack telemetry (SNOTEL) data. *Water Resources Research* 35(7): 2145-2160.

Thompson, L.G. 2000. Ice core evidence for climate change in the tropics: Implications for our future. *Quaternary Science Review* 19: 19-35.

Air Temperature and Snowmelt Discharge Characteristics, Merced River at Happy Isles, Yosemite National Park, Central Sierra Nevada

David Peterson, Richard Smith, Stephen Hager, Daniel Cayan, and Michael Dettinger

Abstract

Although snowmelt discharge (SMD) is a function of many variables, only snowpack, river discharge, and air temperature have long-term records, which are the focus of this study. Solar insolation, an important variable, covaries with air temperature and, presumably, much of the air temperature-snowmelt discharge correlation includes solar insolation effects. Two features of the seasonal SMD cycle are the spring pulse, which defines the start of the rise in SMD, and the peak SMD, which defines the start of the decline in SMD. Air temperature leads SMD, throughout the snowmelt season, from zero to a few days. Apparently the lead/lag variations depend on the rates and durations of rising and falling air temperatures. On average, however, the lead time between air temperature variations and the SMD response is longer near the start of the snowmelt season and decreases as snowmelt progresses towards the peak SMD. This pattern is most likely caused by the seasonal increase in air temperature driven response as SMD progresses. Initially, the SMD response is slow as the snowpack takes time to ripen. Another, but likely smaller, contributing factor is the seasonal change in the air temperature variation which begins to decrease near day 150 (note: the range in maximum discharge extends beyond day 150 to 182). Further, the timing of the start of the SMD season (the spring pulse) depends more on air temperature (cool or warm) than winter snowpack (wet or dry). However, as the SMD season progresses towards maximum discharge, this pattern changes and the importance of differences in winter snowpack on SMD timing increases while the importance of differences in air temperature decreases.

Introduction

The stream gaging station on the Merced River at Happy Isles, Yosemite National Park, is an excellent location for expanding the effort to link large-scale atmospheric circulation to snowmelt discharge (SMD) and river chemistry. Although the advantages of this location are too numerous to list here, a few examples include: (1) the alpine river discharge record is long (1916 to present) and largely undisturbed, (2) the air temperature variations are large scale and strongly covary with SMD, and (3) more than 85% of the annual Merced River flow at Happy Isles is SMD. For all these reasons (and more), knowing the hydrologic response of this region to climate variability and change is important to scientists and park and water managers.

Variations of SMD correlate among many western watersheds because the correlation between air temperature and SMD is strong, and the air temperature variations are large-scale (Peterson and others 2000). The present paper focuses on characteristics of this air temperature-SMD linkage using daily Merced River discharges at Happy Isles and a regional average of daily air temperatures in the central Sierra Nevada. The SMD response to air temperature is increasingly important because air temperatures in central California have increased and are likely to continue to increase (Dettinger and others 2002).

Data and Methods

Data

The air temperature series used here is an average of air temperature from four long-term weather stations in the central Sierra Nevada (Cayan and others 1993), from 1931 to 1999 and a valley floor station from 1916 to 1999 (prior to 1931, only the valley air temperatures are available). The river discharge series is from the Merced River USGS gage at Happy Isles, Yosemite National Park (USGS site 11264500; Slack and Landwehr 1992), from 1916 to 1999.

Methods

The series were filtered with a box-car filter (backwards and forwards to preserve phase) (Matlab 1996) with a 25-day filter for air temperature and a 15-day filter for river discharge. Fewer filter days are needed for river discharge because air temperature-driven SMD is filtered by snowpack but air temperature is not. Two time-series modeling approaches were used: An instrumental variable method (Ljung 1988, 1989, function 'iv4') and an extended Kalman filter method (Ljung 1988, 1989, function 'rarx'). The annual date of the onset of major snowmelt, the spring pulse date (Cayan and others 1999), was defined by the objective method described in Cayan and others (2001).

Results and Discussion

A brief description of air temperature and SMD climatology is presented before discussing the SMD response characteristics to daily variations in air temperature.

Hydroclimatology

The mean annual cycles of air temperature and river discharge are estimated from the filtered 1916 to 1999 daily mean observations (Figure 1a), showing that the river discharge typically peaks during the springtime warming period from April through June, in response to the rapid snowmelt during that period. Thus, air temperature peaks almost two months (20.9 °C, day 209) after river discharge peaks (40.5 cubic meters per second [CMS], day 150). Standard deviations from those annual cycles differ substantially between air temperature (Figure 1b) and river discharge (Figure 1c). When air temperature is a maximum, the standard deviation of air temperature is a minimum; whereas when river discharge is a maximum, the standard deviation of river discharge is a maximum.

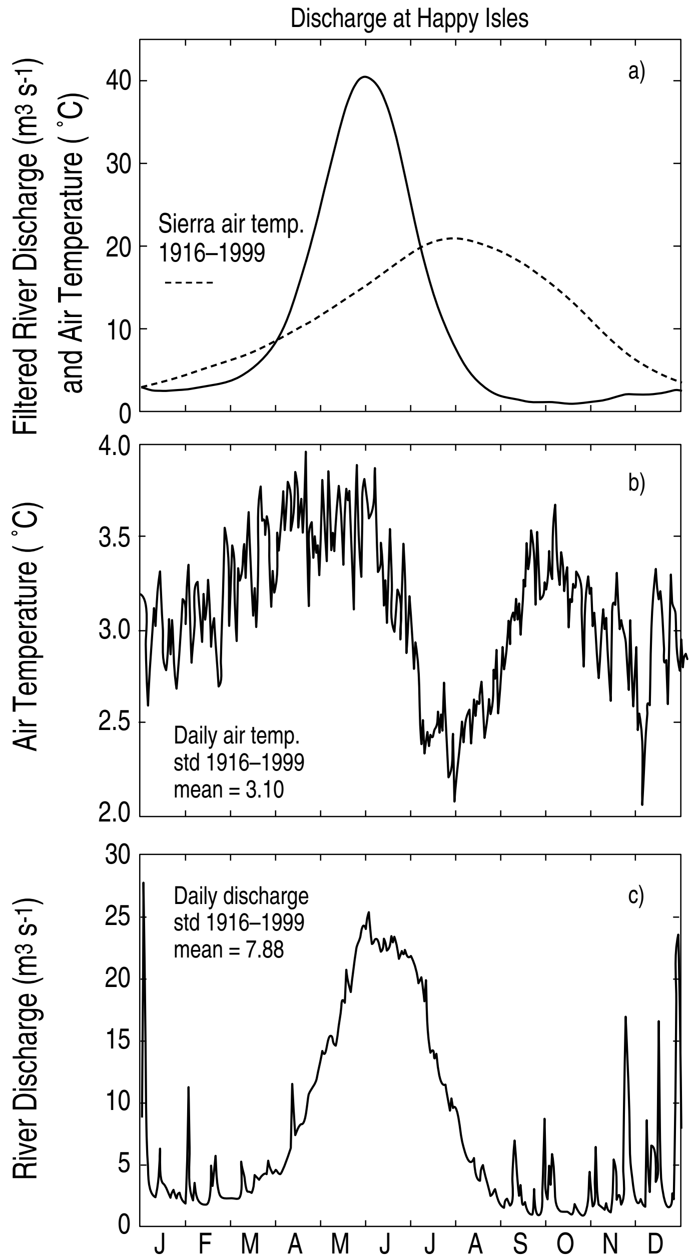

Figure 1 (a) Mean annual cycles of air temperature and river discharge; (b) Standard deviations of daily air temperature annual cycle from climatology; (c) Standard deviations of river discharge from climatology.

Snowmelt Discharge: Air Temperature Response

Snowmelt discharge (SMD) varies during the rise in the annual temperature cycle in response to the combination of temperature variation and the amount of water held in the evolving snowpack. The focus here is on the period of rising river discharge when SMD responds most strongly to air temperature. This interval is approximately bounded by the spring-pulse date and the time of SMD maximum (Figure 2a).

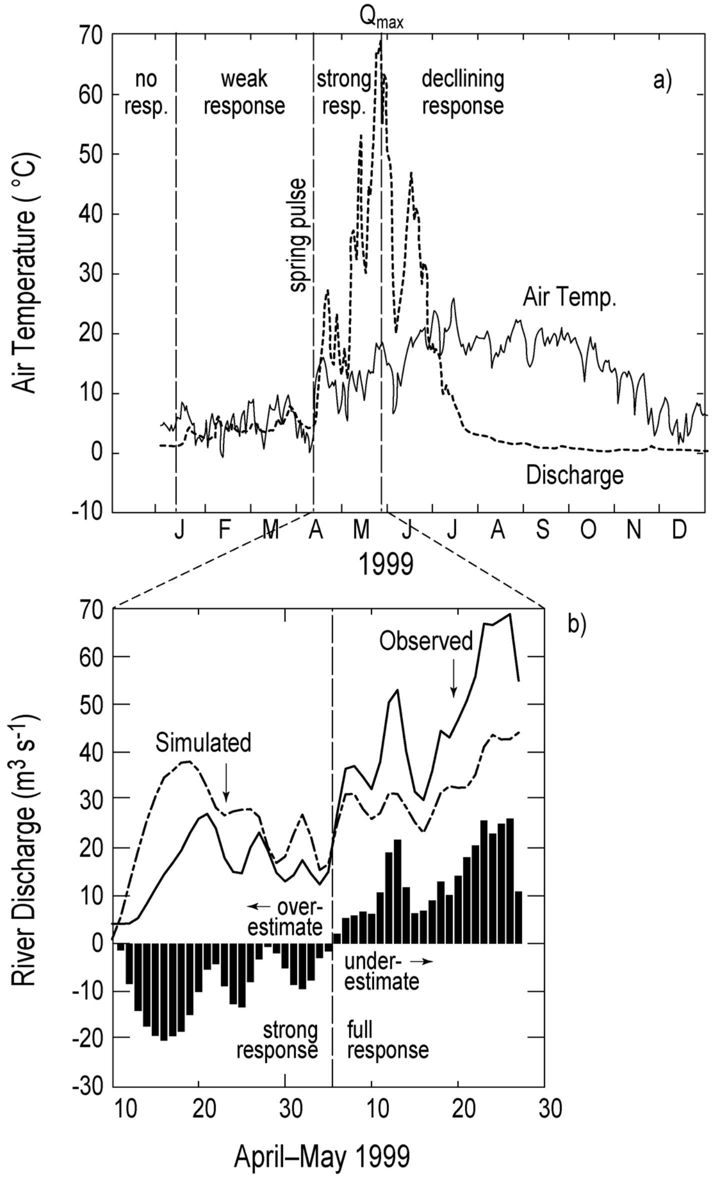

Figure 2 (a) Daily air temperature and river discharge during 1999; (b) Observed and simulated snowmelt discharge, 1999, from the spring-pulse date to the date of maximum in snowmelt discharge based on a constant parameter (iv4) model.

SMD responses to air temperature are not instantaneous. In 1999, for example, air temperature led SMD during the spring pulse (early April, Figure 2a). When air temperature leads SMD, we infer that it takes more than today's air temperature to produce today's river discharge. Snowpack, then, apparently has a memory of air temperature longer than one day. Notably, SMD responses to diurnal temperature fluctuations, which represent about 10% of daily mean SMD, are different. Diurnal air temperature fluctuations led diurnal SMD by many hours, but not by days (Lundquist and Cayan 2002; Lundquist and Dettinger 2003).

The multiple-day influence of temperatures on SMD is captured in a very simple model:
$Q_o = b_o T_o + b_{-1} T_{-1} + b_{-2} T_{-2}$(1)

Where three days of air temperature, T_o (today), T_{-1} (yesterday), and T_{-2} (the day before) contribute to today's river discharge, Q_o. How strongly the different air temperatures contribute to Q_o is estimated by fitting the weights of the response coefficients b_o, b_{-1}, and b_{-2} (instrumental variable method, Matlab function iv4, Ljung 1988, 1989). For example, past air temperature is more important to today's SMD than today's air temperature if b_o is less than b_{-1} or b_{-2}.

In the 1999 example (Figure 2c), when a single set of parameters is fitted for the entire rising limb of the SMD season, $b_o = 0.916 \pm 0.30$, $b_{-1} = 1.338 \pm 0.20$ and $b_{-2} = 0.1869 \pm 0.30$. In this example, yesterday's air temperature, on average, is more heavily weighted than today's (b_o) or the day before (b_{-2}). Also, the resulting simulated discharge is overestimated at first and underestimated later.

Fitting time-dependent response coefficients to the data, using the extended Kalman Filter (EKF) can eliminate this tendency toward over- and underestimation. The EKF not only estimates river discharge and response coefficients during the springtime SMD (Figure 3a) but throughout the annual cycle, even when the discharge is not air temperature driven because of its prediction-correction scheme. During the springtime SMD variations, the daily sum of the three response coefficients in this example ranges from about 1 to 4 CMS/ºC (Figure 3c).

The 3-day EKF model closely simulates SMD and appears to be simply "curve fitting." For this reason, the results of a more widely used and straightforward correlation method are presented first. The mean daily correlation coefficient between today's SMD and today's, yesterday's, and the day before yesterday's air temperature were calculated individually. On average, yesterday's air temperature correlated most strongly with SMD over the period of interest (Figure 4a). Further, the day before yesterday's influence was generally stronger than today's, as shown by the difference between their associated correlations with discharge (Figure 4b).

In the EKF method, the response coefficient weights were estimated each day from 1931 to 1999. The maximum response coefficient was identified for each day of the 69 years and an indicator series was constructed depending on which coefficient was largest on each day, with the indicator set equal to 1 if today's coefficient was largest, 2 if yesterday's, and 3 if the day before yesterday's. Then, the indicator series was averaged by day of year. In the result, a mean value of 2 for a particular calendar day indicates that, on average, yesterday's air temperature elicited the strongest discharge response. In general (Figure 4c), discharge responds most to yesterday's temperatures in early April, or around the time of the spring pulse. After early April, the influence of yesterday's and the prior day's temperatures tend to decrease (relative to that of today's temperature) as SMD progresses and as the overall snowmelt response to air temperature (Figure 3c) increases. This seasonal pattern of the "memory" of temperatures in SMD variations largely parallels that found by the simple correlation analysis (Figure 4b). In essence, the EKF estimator of variable response parameters appears useful in defining the air temperature lead characteristics in the SMD process and therefore may also be useful in defining the response to differences in air temperatures and initial snowpack over the course of increasing temperature and SMD.

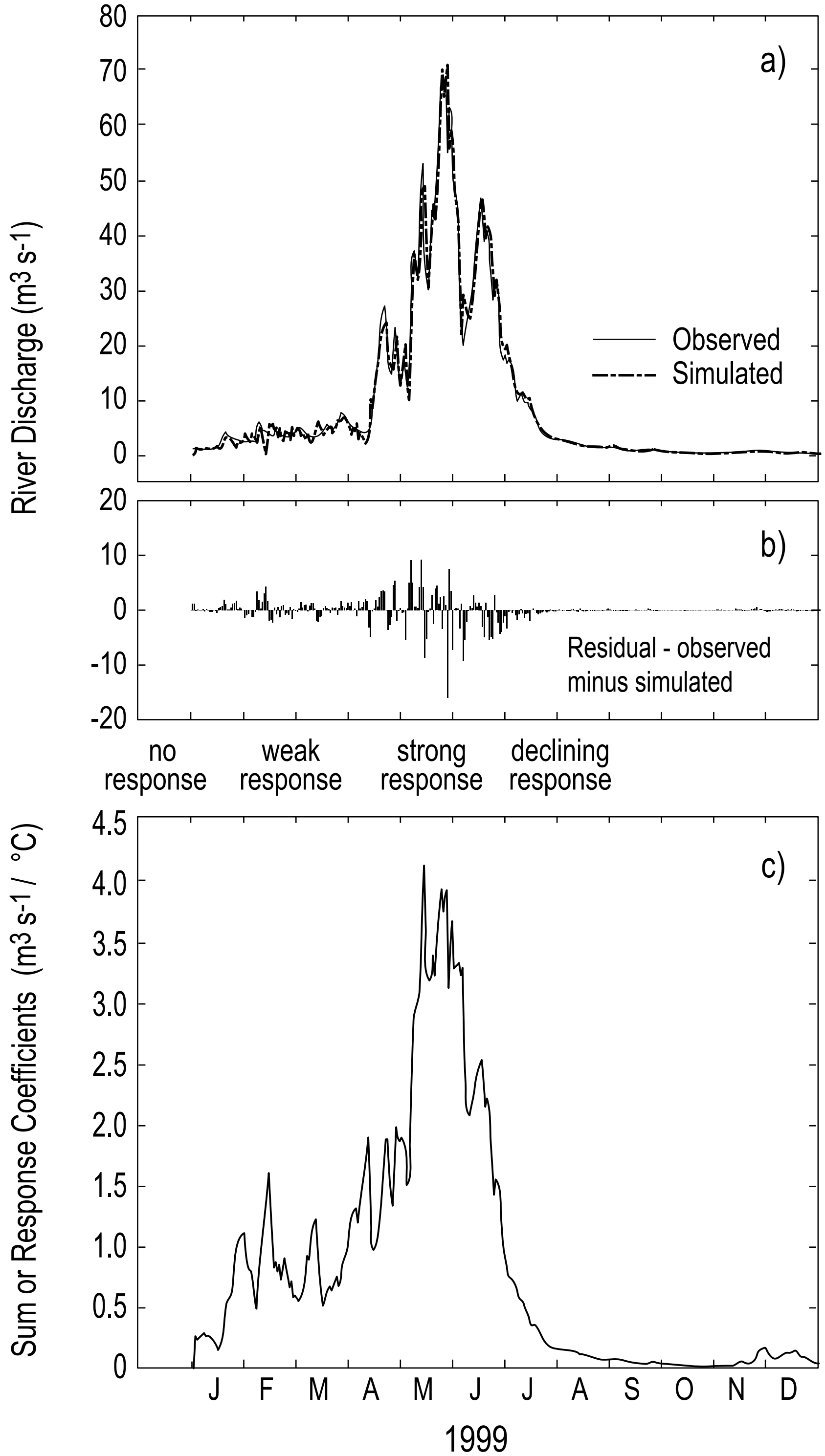

Figure 3 (a) Observed and simulated snowmelt discharge, 1999, based on a variable parameter model; (b) Sum of response coefficients.

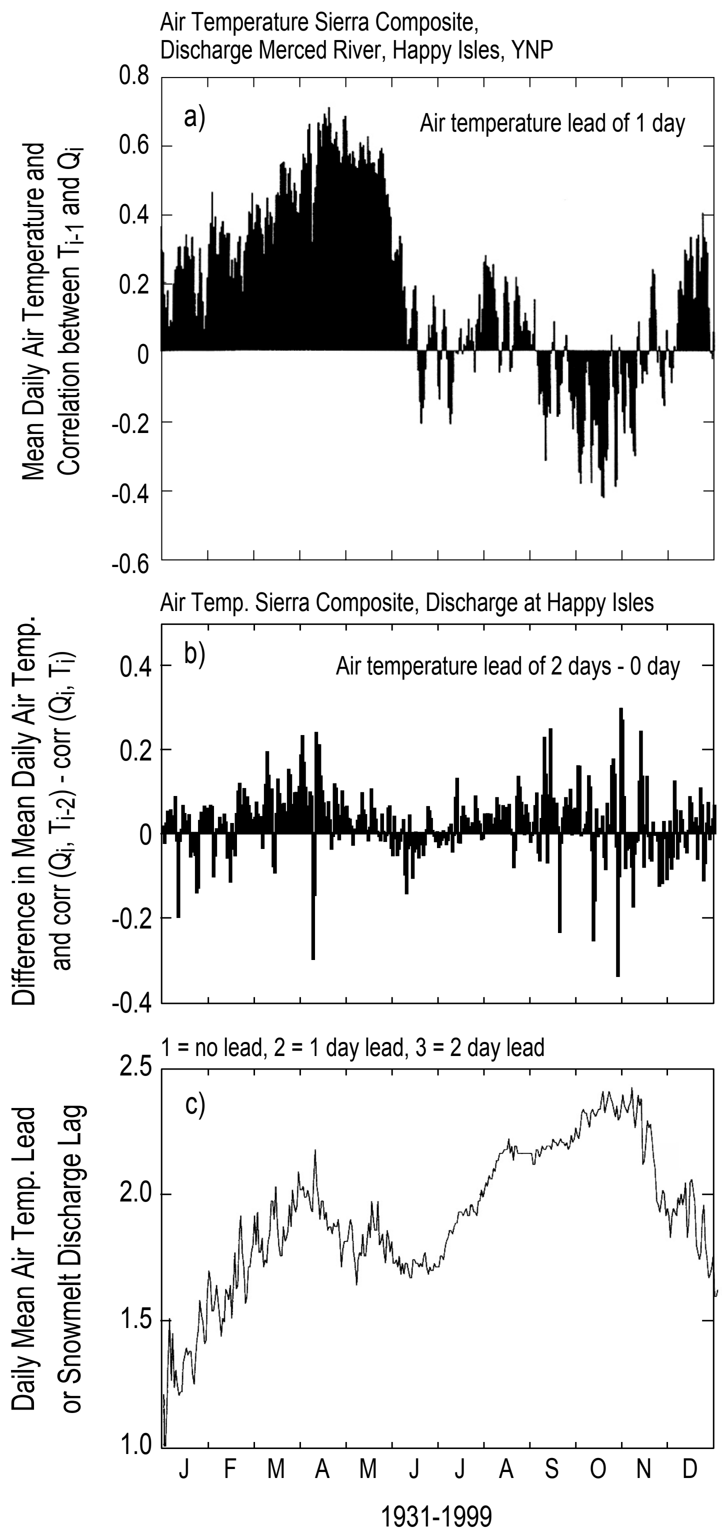

Figure 4 (a) Mean correlation between yesterday's daily air temperature and today's river discharge; (b) Mean correlation between discharge and temperatures at a two-day lead minus the correlation at a zero-day lead; (c) Mean of maximum weighted air temperature response for today, yesterday, or the day before yesterday.

The overall influences of air temperatures (at the full combination of lead times) on SMD clearly vary through the seasons (Figure 4a) in ways that reflect the seasonal temperature cycle that the day-to-day temperature variations deviate from. For example, atmospheric warming across much of western United States is causing a decrease in snow relative to rain at intermediate but not high elevations. At high elevations, the winter to early spring air temperature is too cold, even with the warming, to influence winter snowpack much (Dettinger and Cayan 1995). That is, high elevation air temperature in winter ranges from cold to less cold. Generally, though, when SMD starts, air temperatures are rising from cool to warm, whereas by the time that SMD peaks, air temperatures are already warm (ranging only from warm to very warm). At warm to very warm air temperatures, the variations in temperature should be less important to SMD, because widespread snowmelt occurs at both temperatures. When air temperatures range from cool to warm, larger snowmelt gradients are expected within the basin and thus larger SMD fluctuations result. Furthermore, because air temperature continues to rise well after SMD peaks, the timing of the SMD maximum may be more sensitive to initial snow water equivalent than air temperature history (c.f. Peterson and others 2000). Is the timing of the start of the spring SMD pulse more sensitive to air temperature while the timing of maximum SMD is more sensitive to initial snowpack depth?

Composites of the time-varying EKF response coefficients provide a way to study the likely differences in SMD response characteristics between wet and dry years, and cool and warm years. Eleven-year composites were computed for the response coefficients from the wettest, driest, coolest, and warmest years (based on the mean air temperature and river discharge over days 81 to 150) to characterize the seasonal cycles of temperature responses and daily ranges of timing of the spring pulse under these extreme conditions (Table 1). The greatest differences between the timing of largest coefficients in the composites were between the cool and warm composites, even though the wet composite peaked at higher coefficient values and the dry composite at lower values (Figure 5a). These greater differences in coefficient amplitudes favor a greater difference in SMD timing.

Table 1 Years contributing to the four climate composites based on mean air temperature and river discharge over days 81 to 150

Cool	*Warm*	*Wet*	*Dry*
1917	1926	1936	1924
1921	1931	1938	1931
1929	1934	1940	1936
1933	1939	1946	1934
1942	1947	1952	1953
1948	1966	1969	1961
1953	1976	1973	1964
1963	1978	1982	1976
1967	1990	1986	1977
1995	1992	1993	1990
1998	1997	1997	1991

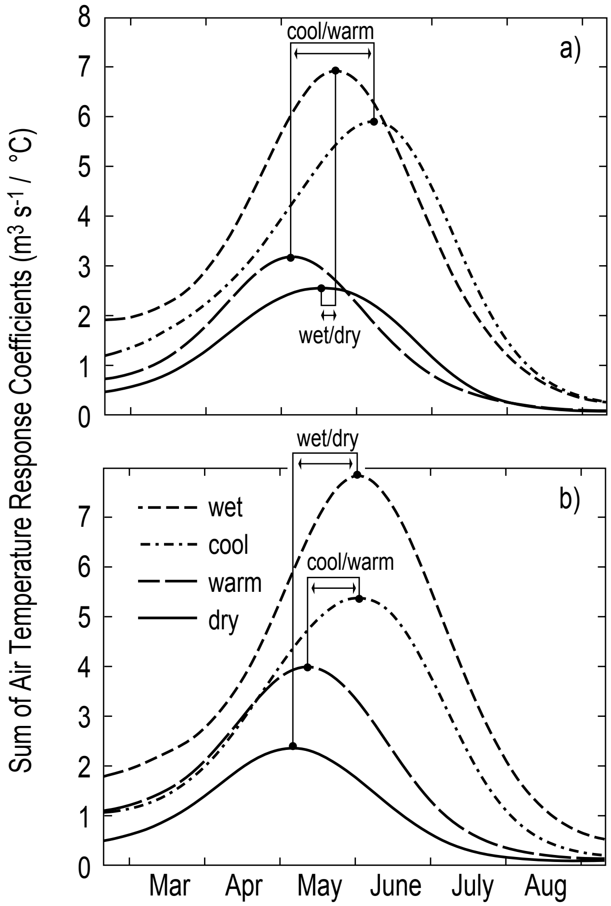

Figure 5 (a) Filtered composites of cool-, warm-, wet-, and dry-year snowmelt discharge response to air temperature. The spring composites were based on the air temperatures and discharge during days 81 to 150; (b) Same as above but for the discharge maximum composites, during days 111 to 181.

Repeating the experiment for the SMD maximum (composites based on mean temperature and discharge values over days 111 to 182), instead of the spring pulse show a relation opposite of the spring pulse (Figure 5, right panel) where the peak wet and dry response patterns extend over a greater length of time than the cool and warm response patterns. However, in this case the significance is less clear, because the wet pattern amplitude exceeds the cool pattern maximum in magnitude. Similarly, the dry pattern amplitude is less than the warm pattern, and the timing of the cool and wet peaks are the same.

To summarize, several lines of evidence indicate that, at the start of SMD, air temperature is the dominant control on the timing of the spring pulse (Cayan and others 2001). Similarly, but less clearly, as the peak SMD is approached, the importance of initial snow water content on SMD timing increases (Figure 6).

Table 2 Years contributing to the four climate composites based on mean air temperature and river discharge over days 111 to 181

Cool	*Warm*	*Wet*	*Dry*
1916	1926	1922	1923
1923	1940	1938	1931
1933	1966	1952	1934
1942	1972	1956	1939
1944	1976	1958	1961
1948	1981	1969	1976
1953	1985	1978	1977
1964	1986	1983	1987
1971	1987	1986	1988
1980	1992	1993	1990
1998	1997	1995	1994

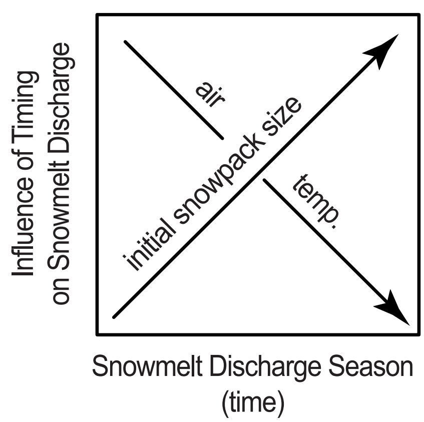

Figure 6 Simplified schematic of variation in timing response to air temperature and initial snowpack.

Summary and Conclusion

The linkage between air temperatures and SMD variations show subtle lead-lag relations such that the importance of "older" temperatures (e.g., yesterday's or the day before's) is, on average, greater near the timing of the spring pulse and less as snowmelt progresses. An explanation of these phenomena is that the system is more sluggish in response to air temperature—due to larger spatial gradients in the readiness of snowpacks at various elevations to contribute snowmelt—at the start of SMD than later in the annual cycle.

The difference in amplitude and timing of the SMD response to air temperature between cool and warm years was greater near the time of the spring pulse than later in the SMD season. This pattern of sensitivities reversed when wet and dry years were contrasted. The early vs. the later distinction is more clearly illustrated near the spring pulse; the difference in cool vs. warm was greater than wet vs. dry even though the difference in amplitudes were greater for the wet and dry composites (which would favor a greater difference in timing). This was not the case for later responses. The implication is that the spring pulse is more sensitive to air temperatures than is the timing of maximum SMD.

Acknowledgements

Many thanks for the helpful reviews provided by Noah Knowles and Jessica Lundquist.

References

Cayan, D.R., S.A. Kammerdiener, M.D. Dettinger, J.M. Caprio, and D.H. Peterson. 2001. Changes in the onset of spring in the western United States: Bulletin of the American Meteorological Society, 82, 399-415.

Cayan, D.R., D.H. Peterson, L. Riddle, M.D. Dettinger, and R. Smith. 1999. The Spring Runoff Pulse from the Sierra Nevada. 14th Conference on Hydrology American Meteorology Society, pp. 77-79.

Cayan, D.R., L.G. Riddle, and E. Aguado. 1993. The Influence of Precipitation and Temperature on Seasonal Stream flow in California. Water Resources Research 29(4): 1127-1140.

Dettinger, M.D. and D.R. Cayan. 1995. Large-scale atmospheric forcing of recent trends toward early snow-melt runoff in California, Journal of Climate, 8, 606-623.

Dettinger, M.D., D.R. Cayan, N. Knowles, A. Westerling, and M.K. Tyree. 2002. Recent projections of 21st century climate change and watershed responses in the Sierra Nevada, California, Sierra Nevada 2002: Science for Management and Conservation, 6 pp.

Ljung, L. 1988 System Identification Toolbox User's Guide for Use with Matlab. The Mathworks, Inc., 21 Eliot St., South Natick, Massachusetts, 59 pp.

Ljung, L. 1989 System Identification: Theory for the User. Prentice-Hall, Inc., Inglewood Cliffs, New Jersey, 515 pp.

Lundquist, J.D., and M.D. Dettinger. 2003, Linking diurnal cycles in river flow to interannual variations in climate: American Meteorological Society, 83rd Annual Meeting, 17th Conference on Hydrology, Long Beach, CA, J2.4-1 to J2.4-5.

Lundquist, J., and D. Cayan, 2002. Seasonal and spatial patterns in diurnal cycles in streamflow in the Western United States. J. Hydromet., 3, 591-603.

Peterson, D.H., D.R. Cayan, R.E. Smith, M.D. Dettinger, and L. Riddle. 2001, An experimental forecast of maximum daily snowmelt discharge for the year 2001: Scripps Institution of Oceanography (CAP) California Applications Program (on-line publication).

Peterson, D.H., R.E. Smith, M.D. Dettinger, D.R. Cayan, and L. Riddle. 2000. An organized signal in snow-melt runoff over the west: Journal of the American Water Resources Association, 36, 421-432

Slack, J.R., and J.M. Landwehr. 1992. Hydroclimatic Data Network (HCDN): A USGS Streamflow Data Set for the United States for the Study of Climate Variations, 1874-1988. USGS Open-File Report 92-129. 193 p.

A Late Pleistocene-Holocene Pollen Record of Vegetation Change from Little Willow Lake, Lassen Volcanic National Park, California

G. James West

Abstract

A 6.3-m sediment core from Little Willow Lake provides a 13,500-year pollen record of vegetation history for Lassen Volcanic National Park. Located 1,829 m above sea level within a mixed red fir forest, Little Willow Lake covers approximately 2.5 hectares. The pollen profile provides a sequence of local and regional vegetation for the southernmost Cascade Range.

The vegetation succession covers the transition from the late glacial climates of the Pleistocene to the post-glacial climates of the Holocene—initially a sagebrush steppe prior to 12,500 ^{14}C yr BP, then a pine-dominated forest from 12,500-3,100 ^{14}C yr BP, and finally the red fir forest of today. Abrupt transitions from sagebrush steppe to pine forest and the shift to the red fir forest took place in <500 years in response to millennial scale climate change. Between 13,500-12,500 ^{14}C yr BP the climate was more seasonal, analogous to the climates of high elevations within the Great Basin today. Conditions were warmer than today between 9,000-3,100 ^{14}C yr BP, with the warmest period between ca. 9,000-7,500 ^{14}C yr. BP. The expansion of fir beginning ca. 3,100 ^{14}C yr BP appears to be congruent with that observed in the central and southern Sierra Nevada and eastern Klamath ranges, indicating that the climate cooled and moisture levels increased, particularly winter snow depths.

Introduction

It has long been understood that vegetation has changed at different spatial and temporal scales in response to climate change. It is also known that the distribution and density of plant species reflects their differential responses to climate, edaphic factors, land use, and biotic interactions such as competition. For many climatic regions, particularly the southernmost Cascade Range, little is known of the specific direct and indirect response of plants to such climatic fluctuations. Presented here is the pollen and sediment analysis of Little Willow Lake, a record that spans the last 13,500 ^{14}C yr BP from Lassen Volcanic National Park (LVNP).

Description and Location

Lassen Volcanic National Park, just north of the Sierra Nevada, contains the southernmost Cascade volcano field, one of a chain of volcanic eruptive areas that extends northward into Canada. Lassen Peak, a glaciated volcanic dome 10,457 ft. (3,187 m) high, is the largest and most prominent feature on the north flank of the Lassen Volcanic center (Turrin and others 1998). Major glaciation of the Lassen region occurred during Oxygen Isotope Stage 2, and three smaller Holocene phases of ice advance have been recognized on the flanks of Lassen Peak (Turrin and others 1998). Little Willow Lake is located some 10 miles (16 km) to the southeast of Lassen Peak.

Little Willow Lake is mostly a marsh that covers approximately 6 acres (2.5 hectares) within a circular, crater-like, volcanic basin at the southernmost margins of LVNP (40°24’40”N; 121°23’16”W). Located at about 6,000 ft. (1,829 m) elevation on the southeastern slope of Sifford Mountain (7,409 ft. [2,258 m]) at the headwaters of one of the west forks of Willow Creek, its only overflow is into Willow Lake through a narrow intermittent drainage. Spills into Willow Lake can occur only at water levels significantly greater (ca. 1 m) than occurred in 2000, the year the fieldwork was completed.

Climate

The climate at LVNP is characterized by cold wet winters (>80% of the precipitation) and warm dry summers. Most of the precipitation in the park occurs in winter as snow, with occasional rain, primarily from convectional storms, in the summer. Depth of April snowpack commonly exceeds 16 ft. (5 m) in the upper montane (>7,900 ft. [>2,400 m]) zone (Taylor 2000). Records from Manzanita Lake (elevation 5,880 ft. [1,792 m]), approximately 15 miles (24 km) to the northwest of Little Willow Lake, show a mean annual precipitation of 42.06 in. (1,068 mm). The mean daily temperature ranges from 30.5 °F (-1.1 °C) in January to 62.7 °F (17 °C) in July. Climate at Little Willow Lake is probably similar to that at Manzanita Lake, although temperatures are likely a bit cooler at Little Willow Lake because of slightly higher elevation, different exposure, and cold air drainage.

Vegetation

The region’s landscape-scale patterns of vegetation are a composite of species response to environmental gradients of temperature (elevation); topographically controlled patterns of soil moisture; substrate; and spatial and temporal patterns of natural and human caused disturbances such as fire, windstorms, and insect attacks. However, fire regimes and insect attack may not be independent of environmental gradients or vegetation patterns (Taylor 2000; Bekker and Taylor 2001).

The landscape-scale vegetation patterns of the High Cascade Range (generally above 1,640 ft. [500 m]) is characterized by ponderosa pine, montane fir/pine, and lodgepole pine forests, with treeless alpine communities on Mount Shasta and Lassen Peak. The interface between the southern Cascades and the Sierra Nevada is defined geologically and topographically but there is no vegetational break; rather, the forests of the Cascade-Sierran axis change gradually with latitude (Hickman 1993). However, for non-arboreal taxa, approximately 24 Sierran species are at the northern limit of their range and 14 Cascadian species are at the southern end of their range.

Montane and subalpine forests are the dominant plant associations in LVNP. Yellow pine forest occurs primarily in xeric sites below 6,500 ft. (1,981 m) and is dominated by incense cedar (*Calocedrus decurrens*), Pacific ponderosa pine (*Pinus ponderosa*), Jeffrey pine (*P. jeffreyi*), sugar pine (*P. lambertiana*), and white fir (*Abies concolor*). The red fir forest is the most widespread plant community in the park and generally occurs between 6,500 and 8,000 ft. (1,981 and 2,438 m) elevation (Gillett and others 1961). California red fir (*A. magnifica*), lodgepole pine (*P. contorta* spp. *murrayana*), and western white pine (*P. monticola*) are the dominant trees of this community. Jeffrey pine is also associated with the red fir forest. The subalpine forest is primarily mountain hemlock (*Tsuga mertensiana*) and whitebark pine (*P. albiculis*), the latter forming krummholz as high as 10,000 ft.

(3,048 m). Above the subalpine forest, alpine vegetation is characterized by low, spreading, mat-like growth.

Montane shrub associations are found at elevational ranges similar to those of yellow pine and red fir forests. Members of Rhamnaceae, Ericaceae, and bush chinquapin are generally associated with the yellow pine forest. Shrub species characteristic of the Great Basin—sagebrush (*Artemisia tridentata, A. arbuscula*) and Bloomer's goldenbush (*Ericameria bloomeri*), and all members of the Asteraceae—are found in the yellow pine forest in the eastern part of the park.

The forest surrounding Little Willow Lake is composed of a dense red fir forest, with lodgepole pine and mountain hemlock. The forest is too dense for much of an understory to develop but dead wood is abundant. Montane shrub covers portions of the basin's northwest slope. Ponderosa and Jeffrey pine occur on the drier, more exposed slopes.

Western blueberry (*Vaccinium uliginosum* ssp. *occidentale*) and meadow-rue (*Thalictrum sparsiflorum*) occur on the margins of the lake (Gillett and others 1961). Copses of willow (*Salix* spp.) grow near the southwest and northeast shoreline areas. The marsh surface supports sphagnum moss, rushes (*Juncus* spp.), bur-reed (*Sparganium natans*), sedges (Cyperaceae), buck-bean (*Menyanthes trifoliata*) and, in open water areas, yellow pond lily (*Nuphar lutea* ssp. *polysepala*) and pondweed (*Potamogeton natans* and *P. gramineus*).

Anthropogenic Effects

Native Americans and early European settlers may have influenced the region's vegetation through fire and, for Europeans, the introduction of grazing (Taylor 1990; Bekker and Taylor 2001). The Maidu in the Lassen area are known to have used fire for several purposes including the driving of game and management of plant populations for food and fiber (Dixon 1905; Kroeber 1925), but their effect on landscape-scale tree species distribution and abundance is unknown. Prehistoric archeological sites present within the Little Willow Lake basin are lithic scatters from temporary seasonal camps or workshops. Significant numbers of Europeans began entering the region after 1850 and parts of the LVNP were heavily grazed by sheep and cattle between 1870 and 1905 (Taylor 1990; Bekker and Taylor 2001 citing Strong 1973). As part of the establishment of national forests, a policy of suppressing fire was implemented in 1905 and grazing controls were initiated. Lassen Volcanic National Park was established in 1916. Past grazing and logging (fences, tree stumps) is evident in the Little Willow Lake basin and still occurs on adjacent Forest Service lands.

Methods

Organic deposits are present at Little Willow Lake and the marsh and catchment are the ideal size for such studies (Faegri and Iversen 1989). Sediment sampling was done with a modified Livingston piston corer from the marsh surface. Two cores were recovered within 10 m of one another some 55 m from the southeast shore of the marsh. The upper 20-cm block at the Core 2 locality, some 10 m north of the Core 1 locality, was saved, sampled, and used for pollen analysis.

Core 1 and the peat and root mass block of Core 2 were logged and samples (1.5 cm^3 each) were taken at 3-cm intervals except where the sampling interval occurred at an observable stratigraphic contact. At the stratigraphic contacts, samples were taken on either side of the contact. Tephra samples were recovered at two levels, but have not been identified.

One-hundred twenty samples were processed by standard palynological techniques (Faegri and Iversen 1989). Four tablets (Batch #414831), each containing about 12,100 exotic *Lycopodium* spores, were added to each sample to determine absolute pollen abundance by volume (Stockmarr 1971). Counting of pollen grains was done under bright field and phase contrast using a Nikon Labophot microscope with a 40X objective and 10X eyepieces. Individual pollen grains were identified to the lowest possible taxonomic level based on type slides made from herbarium collections and on illustrations and keys in standard pollen texts. Plant and pollen nomenclature follows Hickman (1993), Gillett and others (1961), Adam (1967), and Faegri and Iversen (1989). For most samples a minimum of 250 pollen grains or *Lycopodium* spores were counted. The algae *Pediastrum* and *Botryococcus* colonies were counted but excluded from the pollen sum. The relative pollen diagrams were created using TILIA, a computer program developed by Eric Grimm, Illinois State Museum.

Five samples for radiocarbon dating using the AMS method were cut from Core 1. Each sample was cleaned, dried, and weighed. These bulk sediment radiocarbon samples were selected where changes were noted in the pollen spectra and the deepest organic mud.

Results

Sediment Description

A detailed sediment description is available in West (n.d.). Sediment recovery was approximately 92%, although some compression during extrusion may have occurred and recovery was more likely >95%. Gaps in recovery occur between 60-100 cm, 170-200 cm, 293-300 cm, and 597-600 cm.

For the most part, sediments consist of clay, soft and course peat, and organic mud. Pebbly layers at 106 cm and isolated angular pebbles near the base of the section were observed. The sub-rounded pebble layer at 106 cm most likely represents a single high-energy storm event, while the pebbles near the base are near bedrock. The coarser peats are composed of *Sphagnum* moss whereas the fine peats and muds appear to be organic lake deposits. The upper 500 cm are primarily peat or organic lake muds; below 500 cm organic mud and mud and clays are dominant. Most of the contacts are gradational except for two (possibly three) tephra layers, some *Sphagnum* layers, and laminations below 621 cm.

Charcoal

Small charcoal fragments were observed in 50% of the samples counted, but they were not quantified. Their diachronic distribution does not appear to indicate any pattern of occurrence, but their presence does indicate that fires did occur prehistorically.

Age Determination

Five AMS radiocarbon dates of the sediments are:

Sample #	*Description*	*Results*
LWL130-134-3 (Beta 168352)	Peat (130-134 cm)	3,120±40 ^{14}C yr BP (3,400 to 3,250 cal yr BP)
LWLC1 (Beta 151142)	Peat (213-217 cm)	4,460±40 ^{14}C yr BP (5,290-4,950 cal yr BP and 4,930-4,880 cal yr BP)
LWL440-445-1 (Beta 168350)	Peat (453-457 cm)	9,240±50 ^{14}C yr BP (10,550-10,240 cal yr BP)
LWLC2 (Beta 151143)	Organic mud (548-554.5 cm)	12,230±70 ^{14}C yr BP (15,330-14,620 cal yr BP; 14,380-14,070 cal yr BP; 13,920-13,850 cal yr BP)
LWL610-615-2 (Beta 168351)	Organic mud (610-615 cm)	13,410±60 ^{14}C yr BP (16,530-15,780 cal yr BP)

When the five radiocarbon ages are plotted against depth the result is lineal (R^2=0.99), suggesting that sedimentation at Little Willow Lake has been uniform through time and there are no major depositional hiatuses. Because of this relationship temporal constraints have been applied directly to the interpretation of the pollen profile. Measured conventional radiocarbon ages are presented as ^{14}C yr BP and calibrated radiocarbon before present ages as cal yr BP.

Pollen Samples

Pollen preservation varies from excellent in the upper organic sediments above 560 cm to poor in samples near the base of the section that have a high mineral content. Thirty-six pollen types were identified, as well as spores from peat moss (*Sphagnum*) and dung fungus (*Sporormiella*). Two alga taxa were also identified. Pollen concentration values (absolute abundance) also vary with values ranging from 8,083 to 279,829 grains/cm^3, and a mean of 83,060 grains/cm^3.

Arboreal pollen grains, primarily pine, are the dominant type above 570 cm, while non-arboreal (shrubs and herbs) and aquatic-emergent types are generally present at <15% of the total. Below 570 cm, pollen grains from shrubs and herbs are the dominant types (Figure 1). Some layers below 350 cm have abundant *Sphagnum* spores. Unknowns/undifferentiated are generally <5% of the pollen sum but range between 10% to 16% in the four lowermost samples. Sixty-six samples have been counted and the major contributors are plotted on the relative pollen diagrams (Figures 1 and 2).

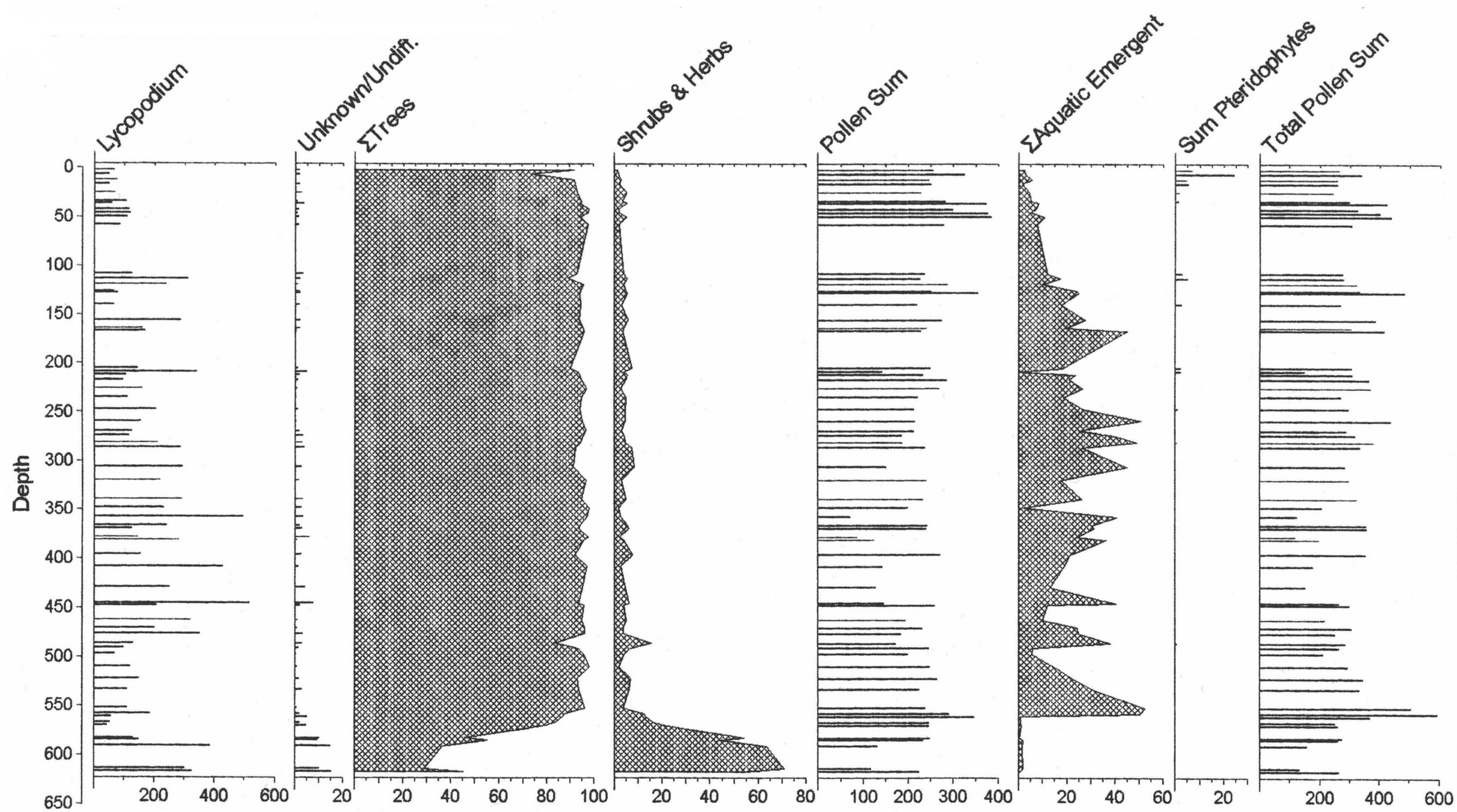

Figure 1 Pollen and *Lycopodium* sums, including relative sums for trees, shrubs and herbs, and aquatic-emergent taxa.

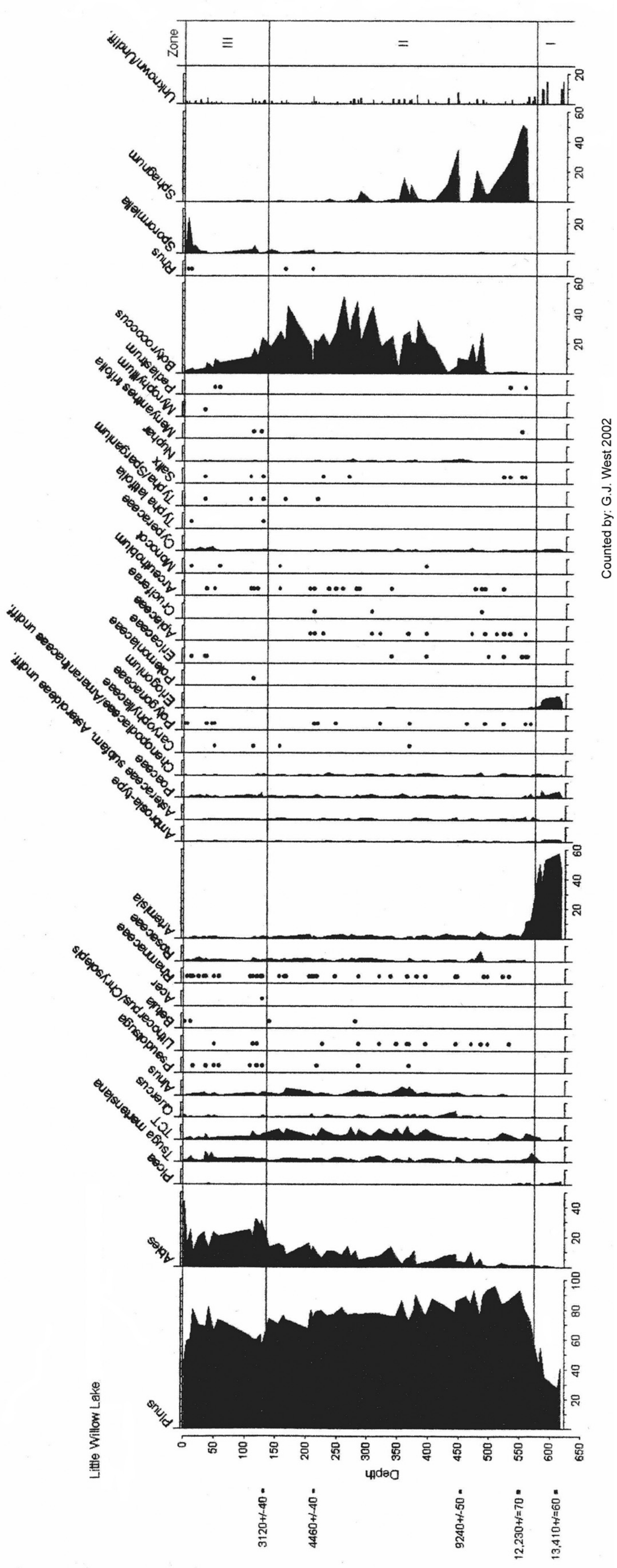

Figure 2 Relative pollen values for major types and presence for taxa at <2%.

Pollen Types

Pinus (Pine) grains are the most abundant pollen type above 565 cm. The grains were counted as wholes and thirds. The sum from thirds generally ranged from 25% to 50% of the pine total. While eight species of pine grow in the region, no effort was made to distinguish individual species or classes of pine because of significant overlap in size and morphological characteristics and the large fraction of the pine count based on thirds sums. With the exception of sugar pine (*P. lambertiana*), whitebark pine (*P. albicaulis*), and western white pine (*P. monticola*), all the pines are in the subgenus *Diploxylon*. Ponderosa (*P. ponderosa*), sugar, and Jeffrey pines (*P. jeffreyi*) ssp. murryana are the most common pine in the regional forest; however, lodgepole (*P. contorta*) is most abundant in the higher elevations around Little Willow Lake and commonly occurs in pure stands within the red fir and sub-alpine forests. Many pine pollen grains present at 510 cm (ca. 10,500 ^{14}C yr BP), 561 cm and below (>12,000 ^{14}C yr BP) are small in size and are likely derived from lodgepole pine.

Abies (Fir) grains are continuously present above 585 cm, although one grain is present in the sample at 591-592 cm. Relative fir pollen values gradually increase above 585 cm with a major incremental jump above 140 cm at about 3,100 ^{14}C yr BP. Seven species of fir occur in California: two species are restricted to coastal areas (*A. bracteata* and *A. grandis*), two species (*A. lasiocarpa* and *A. amabilis*) occur in isolated stands in western Siskiyou County, and the three remaining species (White, *A. concolor*; California red, *A. magnifica;* and Noble-*A. procera*) are widely distributed in higher-elevation forests. There are no sharp geographic boundaries between white, red, and noble firs, although red and noble are found in the upper part of the montane fir forests. Noble fir may intergrade into the Shasta form of red fir (*A. magnifica* var. *shastensis*) and no distinct boundary can be dawn between the two species (Griffen and Critchfield 1976). The most likely candidates in the Little Willow Lake fossil record are red and white fir.

Small numbers of spruce (*Picea* spp.) grains, possibly derived from Engelmann spruce (*P. Engelmannii*), are present sporadically below 546 cm (>12,000 ^{14}C yr BP) with the exception of 1 grain at 42 cm. Today the nearest spruce to Little Willow Lake is Englemann spruce found as an isolated stand along the upper reaches of Clark Creek, a tributary to Lake Britton and the Pit River in northeastern Shasta County (Griffen and Critchfield 1972). Two other species are present in California: Brewer spruce (*P. breweriana*) and Sitka spruce (*P. sitchensis*). Sitka spruce is found along a narrow coastal strip seldom extending more than 30 miles inland discontinuously northward from Mendocino County and is an unlikely candidate. Brewer spruce is found in the Klamath and Siskiyou mountains as far eastward as Castle Crags in the upper Sacramento River drainage some 110 miles (177 km) northwest of Little Willow Lake.

Mountain hemlock (*Tsuga mertensiana*) is common in the Lassen Peak region between 7,500 and 9,200 ft. (2,286-2,804 m) in elevation (Gillett and others 1961) and is mixed into the forest surrounding Little Willow Lake. The highest value observed in the profile is about 8% and it is not present below 585 cm.

Taxodiaceae, Cupressaceae, and Taxaceae (TCT) pollen grains are combined together because of the difficulty in distinguishing the various taxa. Incense cedar (*Calocedrus decurrens*) is probably the main contributor, but other possible contributors are the yews, California nutmeg (*Torreya californica*), and Pacific yew (*Taxus brevifolia*). TCT pollen grains are discontinuously present through the profile, but are most abundant between 400 and 120 cm, approximately 8,000 to 3,000 ^{14}C yr BP.

Oak *(Quercus* spp.) pollen grains are likely representative of more than one species. Five species are found in the region and two, black oak (*Q. kelloggii*) and huckleberry oak (*Q. vaccinifolia*), are present within LVNP boundaries. Black oak is common in the lower elevations surrounding the park and huckleberry oak is common on dry rocky slopes. Huckleberry oak pollen grains have a smoother tectum than that found in most other oaks, but it was not distinguished in this analysis because of its relatively low abundance.

Alder (*Alnus* spp.)-Mountain alder (*A. incana* ssp. *tenuifolia*) is the most likely contributor of the majority of alder pollen grains. It is the only alder found in LVNP and is common and widespread, forming dense thickets on meadow borders, along lakes and streams, and on springs (Gillett and others 1961).

Other arboreal taxa, but not major contributors, include Douglas fir (*Pseudotsuga menziesii* var. *menziesii*) grains in samples above 370 cm (ca. 6,500 ^{14}C yr BP) and chinquapin/tanoak (*Chrysolepis*/*Lithocarpus*) pollen (grains cannot be readily separated from each another), which is discontinuously present in small numbers throughout the profile above 547 cm (ca. 12,000 ^{14}C yr BP). Maple (*Acer*) was noted in one sample and Birch (*Betula*) was noted in four samples.

Non-arboreal taxa, with the exception of sagebrush (*Artemisia* spp.), are minor contributors to the pollen spectra. There is a number of *Artemisia* species present in the region and they have a wide spatial and elevational distribution. Three species are found within LVNP boundaries—dwarf sagebrush (*A. arbuscula* ssp. *arbuscula*), mugwort (*A. douglasiana*), and big sagebrush (*A. tridentata* ssp. *tridentata*)—but in the past other species also may have been present. Pollen identification can only be made to the genera level in sagebrush. While present throughout the profile, sagebrush is important only >12,500 ^{14}C yr BP, reaching values of more than 55%.

Other members of the sunflower family (Asteraceae), the *Ambrosia*-type and Asterodiaceae undifferentiated (high-spine type), are far less prominent than sagebrush. *Ambrosia*-type pollen has a small increase in value co-occurring with high sagebrush values.

Polygonaceae (Buckwheat Family) grains were sorted to Polygonaceae and *Eriogonum*. Polygonaceae is discontinuously present above 560 cm. On the other hand, *Eriogonum* pollen grains are discontinuously present in the profile but reach their greatest relative values below 560 cm at the same time as the high values for *Artemisia* occur. Most of the region's *Eriogonum* are found on dry sandy or rocky soil in meadows or in open bushy or wooded places. Some of the Polygonaceae grains may have been derived from aquatic-emergent Polygonaceae.

Grass (Poaceae) pollen grains are present in low values throughout the profile but are most prominent prior to 12,500 ^{14}C yr BP. Because of their limited morphological variation and low numbers, no attempt was made to divide the grass grains into sub-types.

Chenopodiaceae/Amaranthaceae (goosefoot/amaranth) pollen grains, with the exception of *Sarcobatus* (greasewood), cannot be separated with a light microscope. They are discontinuously present in small numbers throughout the profile. The occasional pollen grains of greasewood (not plotted), a shrub that grows on alkaline soils in the Great Basin, are likely the result of long-distance wind transport.

Rhamnaceae (Buckthorn Family) pollen grains are from shrubs and small trees. Species in LVNP include mountain whitethorn (*Ceanothus cordulatus*), mahala mat (*C. postratus*), tobacco brush (*C.*

velutinus var. *velutinus*), and Sierra coffeeberry (*Rhamnus rubra*). Most are associated with the dry soils of open woods and rocky slopes. The grains are present in small numbers above 550 cm.

Rosaceae (Rose Family) pollen grains are from a large family of herbs, shrubs, and small trees. There are 29 species that occur in the park. Their pollen grains occur above 560 cm at values of less than 4%, except one sample at 6%.

Sphagnum (peat moss) spores have five prominent, but diminishing, peaks in the early Holocene, suggesting its rapid expansion and contraction with varying water levels. There are about 17 species of *Sphagnum* in the Sierra Nevada and most occupy similar habitats (wetlands and areas with high moisture levels).

Other non-arboreal pollen types include members of Polemoniaceae (cf. *Gilia*), Caryophyllaceae (Pink family), Ericaceae (Heath family), Crucifereae (Mustard family), *Arceuthobium* (conifer mistletoe), *Rhus* (cf. skunkbrush), and an unidentified monocot. All are present in small numbers and are discontinuously present above ca. 560 cm.

Aquatic-Emergent pollen types noted included willows (*Salix*), water lilies (*Nuphar*), sedges (Cyperaceae), buck-bean (*Menyanthes*), Apiaceae (cf. *Sium suave*, water hemlock), water-milfoil (*Myriophyllum*), cattail (*Typha latifolia*), and bur-reed/cattail monads (*Sparganium/Typha*). All are discontinuously present and none is abundant.

Unknown/undifferentiated grains consist of those pollen grains that either could not be keyed out or were so weathered as to be indistinguishable. The majority of unknown/undifferentiated grains appear to be from non-arboreal taxa. The number of unknown/undifferentiated grains co-vary with the high values for sagebrush and reach a value of more than 15% of the pollen sum.

Colonies of the algae *Botryococcus* are most important during the middle Holocene and early late Holocene between 500-50 cm. The presence of *Botryococcus* is likely reflecting water levels and productivity (Whiteside 1965). With the exception of one sample at 522-523 cm, the algae *Pediastrum* are quite rare, being observed in only three other samples.

Sporormiella spores from dung fungus are present above 230 cm, increasing to more than 25% at 5 cm. Davis (1987) has pointed out the significance of dung fungus spores in Pleistocene and historic sediments in the Sierra Nevada. *Sporormiella* species are common on the dung of domestic herbivores such as cattle and horses and on the dung of deer and elk.

Pollen Biozones

Three pollen biozones are identified on the basis of their relative pollen values. Zones II and III have been further subdivided into subzones based on the presence of individual or groups of additional pollen types. The zones are interpreted to reflect a succession of landscape-scale vegetation patterns at Little Willow Lake. They are defined as follows:

Zone I –Sagebrush/Buckwheat/Grass/Pine (13,500-12,500 ^{14}C yr BP)

This pollen assemblage is representative of an open sagebrush community. Intermixed with the sagebrush were grasses, members of the buckwheat family (*Eriogonum*), and the sunflower (Asteraceae) family. Groundwater levels were low although laminated sediments indicate that some ponding within the basin did occur. Isolated or widely-spaced pines may have been present on the basin's slopes and possibly extended on to the basin's floor, but pine pollen values are low enough to be considered background (Adam 1967; Anderson and Davis 1988). Many of the pine grains are small, suggesting that they have been derived from lodgepole pine. Small numbers of spruce may have grown nearby in isolated cool shaded protected areas. Sagebrush Steppe was rapidly displaced as a forest of pines, hemlock, and TCT invaded the Little Willow Lake basin, giving rise to the pine zone. Mean pollen concentration value for this zone is 36,000 grains/cm^3.

Zone II –Pine (12,500-3,100 ^{14}C yr BP)

Pine forest has covered the basin during this time. Species diversity expanded significantly as six new taxa became contributors to the pollen rain. Hemlock and TCT become part of the forest. Fir values increase slowly and pine values decline. *Artemisia* percentages drop to background values. Mean pollen concentration value for this zone is 69,000 grains/cm^3.

Zone II a –Pine/TCT/Sphagnum (12,500-11,500 ^{14}C yr BP)

The basin is covered by a pine and TCT forest. Hemlock is present in the region. Sphagnum moss expanded rapidly on the basin's floor as groundwater levels rose. While the values of *Sphagnum* spores have four more peaks in the profile, the peaks diminish through time, suggesting a fluctuating water table. There appears to be an inverse relationship with the algae *Botryococcus* as the presence of *Botryococcus* colonies indicates open water, whereas *Sphagnum* indicates saturated ground. High pollen concentration values may indicate a dense forest.

Zone II b –Pine/Fir/TCT (11,500-3,100 ^{14}C yr BP)

A pine, fir, and TCT forest with hemlock covered the basin. The presence of large amounts of the algae *Botryococcus* indicates Little Willow Lake was an open, though productive, body of water. Alder is now present, almost certainly growing on the margins of the lake. Oak pollen, while not ever abundant in the profile, reaches its highest values between 9,000-3,100 ^{14}C yr BP. The expansion of the oaks was probably not so much within the Little Willow Lake basin but regionally at lower elevations. Fir values gradually increase through this zone.

Zone III –Fir /Pine/Hemlock (3,100 to present ^{14}C yr BP)

Fir values show a sharp increase in this zone, whereas pine and TCT values decline. Oak and alder values are low; the latter probably because higher lake levels submerged alder habitat, causing it to die back. Mean pollen concentration value for this zone is 129,000 grains/cm^3. Tree density of the surrounding forest is highest for this zone.

Zone III a –Fir/Pine/Hemlock (3,100 ^{14}C yr BP-~AD 1,870)

The red fir forest expands displacing pines while mountain hemlock holds its own. *Botryococcus* declines as the lake becomes smaller and the marsh expands reducing the amount of open water. *Sporormiella* is present but not abundant.

Zone III b –Fir/Pine/Hemlock with abundant *Sporormiella* (~AD 1,870 to present)

This is the historic red fir forest that has had significant grazing by domesticated animals, possibly even out on to the marsh surface. The abundance of *Sporormiella* spores is consistent with the intense grazing of the late 19th and early 20th centuries.

Discussion

The vegetation history at Little Willow Lake outlines the development of a southern Cascades forest. The landscape-scale vegetation succession covers the transition from late glacial climates of the Pleistocene to the post-glacial climates of the Holocene—from a sagebrush steppe to a pine dominated forest, which lasted for most of the Holocene, to a late Holocene red fir forest beginning some 3,100 ^{14}C yr BP. The pollen data reflect changes in both the composition and density of the vegetation.

The initial high sagebrush pollen values of pollen Zone I reflect a very different vegetation pattern than occurs in the Little Willow Lake area today; comparable sagebrush pollen values are found only east of the Sierra Nevada crest, within the Great Basin, and the High-elevation Steppe of southeastern Oregon (Adam 1967; Anderson and Davis 1988; Minckley and Whitlock 2000). Comparable age and later early Holocene records from the western Sierra Nevada have abundant *Artemisia* pollen (Adam 1967; Davis and Moratto 1988; Anderson 1990). A further indication that sagebrush steppe was widespread during the late Pleistocene comes from a paleoenvironmental record at Medicine Lake, on the Modoc Plateau some 85 mi (137 km) north of Little Willow Lake at 6,884 ft. (2,036 m) elevation, where ca.11,000 ^{14}C yr ago *Artemisia* pollen values were 30%-40% of the pollen sum (Starratt and others 2002). The presence of small numbers of spruce (*Picea*) pollen grains co-occurring with the sagebrush, however, is indicative of a plant community unknown locally and possibly reflects a plant community that may have no modern analogs within the region. It is unlikely that spruce grew in the Little Willow Lake basin, but it must have been growing close enough that wind was able to transport its relatively large pollen grain into the catchment of Little Willow Lake basin.

Next, and the major shift in the profile, is the transition from the high pollen values for shrubs and herbs (primarily from sagebrush (Zone I)) to tree pollen (Zone II), which occurred about 12,500 ^{14}C yr BP. This rapid shift over a period of about 500 yr or less may reflect the rapid climatic shift that occurred at the end of the last glacial on a global scale or it may be reflecting local geomorphic changes (damming of the outlet by a debris flow which allowed water to pond to higher levels) within the basin. While the latter may have occurred, such a shift is not supported by radiocarbon dates derived from the debris flow at the outlet (Meyer 2002). It is more likely the change observed is a regional vegetation response to a significant climatic shift since the pollen values change both quantitatively and qualitatively. *Artemisia* pollen values drop to background levels and *Eriogonum* pollen virtually disappears by 12,000 ^{14}C yr BP. Another sagebrush community never reappears in the profile.

Above 550 cm (ca. 12,000 ^{14}C yr BP) diversity in the pollen taxa expands, particularly for the non-arboreal and aquatic-emergent types. Conditions in the basin shifted allowing plants to invade new niches. Soil moisture levels increased and permanent ponded water was established within the basin by about 11,500 ^{14}C yr BP, providing new environments. Many new species also joined the pine forest.

Oak, while never a major contributor to the pollen rain, is most prominent between 3,000 to 9,000 ^{14}C yr BP. The increase in oak pollen can be attributed to the expansion of lower elevation oak communities outside of the Little Willow Lake basin, as oaks were never important members of the forest within the basin. Alder pollen values are greatest at the same time as the highest oak pollen values, an increase that may be due to lower lake levels that allowed alder to expand on to the margins of the lake. While still an oligotrophic lake, as indicated by high levels of *Botryococcus* colonies present at this time, productivity was relatively high, suggesting shallow relatively warmer water conditions.

Transitions also are present in the sedimentary record with shifts of muds, peats, and lake sediments that may be related to both climate and geomorphic changes of the basin's drainage outlet (Table 1). The sediments reflect oscillations between meadows, wet meadows, and standing water conditions. This evidence primarily occurs in the lower levels (>506 cm) of the core section although such evidence occurs at higher levels with muds at 458.5-386 cm and 384-373 cm (ca. 9,000-7,500 ^{14}C yr BP) interspersed between peats and lake sediments. The shifts within the latter timeframe may reflect the driest part of the record after a permanent lake was established in the basin. Such a timeframe overlaps with the early part of the oak and alder pollen increase.

The second major shift in pollen values is the increase in fir (*Abies*) grains in pollen Zone III. This shift occurs ca. 3,100 ^{14}C yr BP and is concurrent with the shift in fir values observed at Osgood Swamp in the central Sierra Nevada (Adam 1967) and between ca. 3,700-3,000 ^{14}C yr BP further south in the Sierra Nevada (Davis and others 1985; Anderson 1990; Smith and Anderson 1992). Similar increases in fir pollen in the late Holocene have been observed in the eastern Klamath Range at Cedar Lake (West 1989) and Bluff Lake (Mohr and others 2000). Average pollen concentration values suggest that forest density (number of trees/unit area) is greatest in Zone III. The high pollen concentration values in Zone III b may be anthropogenic, the result of historic fire suppression.

Conclusions

The late Pleistocene and Holocene vegetational history from Little Willow Lake provides information on the responses of vegetation to millennial-scale changes in climate, as well as more localized shifts in the environment. The changes in vegetation vary from relatively abrupt shifts occurring in less than five centuries to more subtle changes that occur over millenniums. Several conclusions can be drawn from the study:

1. Significant vegetation change has taken place within the Little Willow Lake catchment in the last 13,500 ^{14}C yr BP. Landscape-scale vegetation patterns have been defined from diachronic pollen biozones that indicate both taxa and forest density shifts.
2. The rapid shift from an *Artemisia*-dominated shrub steppe community to a pine forest occurred in ~ 500 yr beginning ca.12,500 ^{14}C yr BP. This change most likely was in response to the shift from glacial climates at the end of the Pleistocene to the Holocene climatic regime. The age of the debris flow deposits that may have affected the basin's outlet are not congruent with this shift. Nevertheless, the shift in vegetation is so great that it appears to be a regional landscape-scale shift rather than a localized response to a local geomorphic event. The presence of a late Pleistocene and early Holocene sagebrush steppe community is consistent with that observed in records in the central and southern Sierra Nevada and Modoc Plateau.
3. The Little Willow Lake basin changed rapidly from a cold dry meadow to a moist meadow; then oscillated between a *Sphagnum* moist meadow and a small lake as water levels varied; to a lake that filled the entire basin; and finally, to a remnant lake almost entirely filled with sediments. Lake levels have varied throughout its existence but generally were lower between 9,000-3,100 ^{14}C yr BP than today.

4. The forest composition has changed through the Holocene. It initially started as a pine forest with mountain hemlock and one or more TCT species; then progressed to a pine forest with fir, mountain hemlock and TCT; and finally culminated in the fir forest of today. Oaks expanded regionally, but were not important within the immediate area of Little Willow Lake.

5. The landscape-scale changes in vegetation most likely took place in response to millennial scale climate shifts occurring within the late Pleistocene and Holocene. Between 13,500 and 12,500 ^{14}C yr BP, the climate at Little Willow Lake was more seasonal, similar to the climates of high elevations within the Great Basin today. Conditions were warmer than today between 9,000-3,100 ^{14}C yr BP, with the warmest period between ca. 9,000-7,500 ^{14}C yr BP. The expansion of fir (beginning ca. 3,100 ^{14}C yr BP; 3,400 to 3,250 ^{14}C yr BP) appears to be congruent with that observed in the central and southern Sierra Nevada and the eastern Klamath ranges, indicating that the climate cooled and moisture levels increased, particularly winter snow depths.

6. While there is no direct evidence that prehistoric populations had any landscape-scale effects on the vegetation, historic fire suppression may have enhanced the density of the current forest.

References

Adam, D.P. 1967. Late Pleistocene and Recent Palynology in the Central Sierra Nevada, California. *In* Quaternary Paleoecology, EJ Cushing, HE Wright Jr. Editors, pp. 275-301, Yale Univ. Press, New Haven

Anderson, RS. 1990. Holocene forest development and paleoclimates within the central Sierra Nevada, California. J. Ecology 78:470-489.

Anderson, R.S., and O.K. Davis. 1988. Contemporary pollen rain across the central Sierra Nevada, California: relationship to modern vegetation types. Artic and Alpine Research, 20:448-460.

Bekker, M.F., and A.H. Taylor. 2001. Gradient analysis of fire regimes in montane forests of the southern Cascade Range, Thousand Lakes Wilderness, California, USA. Plant Ecology 155:15-28.

Davis, O.K. 1987. Spores of dung fungus *Sporormiella*: Increased abundance in historic sediments and before Pleistocene megafaunal extinction. Quaternary Research 28:290-294.

Davis, O.K, and M.J. Moratto. 1988. Evidence for a warm dry early Holocene in the western Sierra Nevada of California: Pollen and plant macrofossil analysis of Dinkey and Exchequer Meadows. Madroño 35(2): 132-149.

Davis, O.K., R.S. Anderson, P.L. Fall, M.K. O'Rourke, and R.S. Thompson. 1985. Palynological evidence for early Holocene aridity in the southern Sierra Nevada, California. Quaternary Research 24:322-332.

Dixon, R.B. 1905. Maidu Myths. American Museum of Natural History. Vol. 17, Part 111.

Faegri, K., and J. Iversen. 1989. Textbook of Pollen Analysis, IV Edition by K. Faegri, P.F. Kaland and K. Krzywinski. John Wiley & Sons, Chichester.

Gillett, G.W., J.T. Howell, and H. Leschke. 1961. A Flora of Lassen Volcanic National Park, California. Wasmann Journal of Biology, Vol. 19:1-185. (Revised by VH Oswald, DW Showers, MA. Showers, reprinted by the Calif. Native Plant Society 1995)

Griffin, J.R., and W.B. Critchfield. 1972. The Distribution of Forest Trees in California. USDA Forest Service Research Paper PSW-82/1972 (Reprinted with Supplement, 1976).

Hickman, J.C., Editor. 1993. The Jepson Manual, Higher Plants of California. University of California Press, Berkeley and Los Angeles

Kroeber, A.L. 1925. Handbook of the Indians of California. Bulletin 78 of the Bureau of American Ethnology of the Smithsonian Institute. Government Printing Office, Washington.

Meyer, J. 2002. Geoarchaeological study for portions of Lassen Volcanic National Park, Lassen and Shasta counties, California. Unpub. report prepared for Anthro.Studies Center, Chico State University, Chico. CA. 24 pages.

Minckley, T., and C. Whitlock. 2000. Spatial variation of modern pollen in Oregon and southern Washington, USA. Rev. Palaeobotany and Palynology 112:97-123.

Mohr, J.A., C. Whitlock, and C.N. Skinner. 2000. Postglacial vegetation and fire history, eastern Klamath Mountains, California, USA. Holocene 10(4): 587-601.

Smith, S.J., and R.S. Anderson. 1992. Late Wisconsin paleoecologic record from Swamp Lake, Yosemite National Park, California. Quaternary Research 38:91-102.

Starratt, S.W., J.A. Barron, T. Kneeshaw, J. Lowenstern, and L. Phillips. 2002. A Holocene record from Medicine Lake, Siskiyou County, California: Preliminary diatom, pollen and sedimentological data. American Quaternary Association Abs, 17th Bienn. Meet., Anchorage, AK, August 8-11, 2002. pp.121-122.

Stockmarr, J. 1971. Tablets with Spores used in Absolute Pollen Analysis. Pollen et Spores, Vol. 13, No. 4:615-622.

Strong, D.H. 1973. These happy hunting grounds: a history of the Lassen region. Loomis Museum Associates, Red Bluff, CA. cited in Bekker and Taylor, 2001.

Taylor, A.H. 1990. Tree invasion of meadows of Lassen Volcanic National Park, California. Prof. Geographer 4:457-470.

Taylor, A.H. 2000 Fire regimes and forest changes in mid and upper montane forests of the southern Cascades, Lassen Volcanic National Park, California, USA. J. Biogeography 27:87-104.

Turrin, B.D., R.L. Christansen, M.A. Clynne, D.E. Champion, W.L. Grestel, L.J.P. Muffler, and D.A. Trimble. 1998. Age of Lassen Peak, California, and implications for the ages of late Pleistocene glaciations in the southern Cascade Range. GSA Bulletin, v. 110, no. 7, p931-945.

West, G.J. 1989. Late Pleistocene/Holocene vegetation and climate. In Basgall M, Hildebrandt W R., editors, Prehistory of the Sacramento River Canyon, Shasta County, California. Center for Archaeological Research, Davis. UC Davis, pp. 36-55.

West, G.J. n.d. A pollen record of late Pleistocene-Holocene vegetation and climate history, Lassen Volcanic National Park, California. Report prepared for Anthropological Studies Center, California State University, Chico.43 pages.

Whiteside, M.C. 1965. On the occurrence of *Pediastrum* in lake sediments. J. Arizona Academy Science 3:144-146.

Wood, M.C., and J. Kienle, Editors.1990. Volcanoes of North America: United States and Canada. Cambridge University Press. 354 p.

Abstracts[1]

Abstracts for PACLIM 2003
Asilomar Conference Grounds
Pacific Grove, California
April 6-9, 2003

Directional Positive Feedback and Pattern at an Alpine Treeline

Kathryn J. Alftine
Earth Systems Science and Policy
California State University, Monterey Bay, Seaside, CA

The spatial pattern at alpine treeline may be part of a feedback process in which wind plays a central role. The basic aspects of such a feedback are embedded in a cellular automaton. Spatial metrics of the patterns generated by this simulation and those observed at a windy treeline site are ordinated using PCA. Only the simulations that include a directionally weighted feedback fall close to the observed sites in ordination space. MANOVA indicates that the directionally weighted feedback is most important in structuring the treeline pattern, but that random hotspots for establishment and the overall steepness of the environmental gradient from forest to tundra in space also have an effect. The importance of wind in determining feedback with the spatial pattern of a canopy indicates that nonlinear reactions to climatic change are likely.

Fractional Snow Cover in the Colorado River and Rio Grande Basins, 1995-2002

Roger C. Bales
Department of Hydrology and Water Resources, University of Arizona

Estimating snow cover properties at a basin scale, particularly snow water equivalent (SWE), remains a challenge. We have used a combination of remote sensing and ground-based data to estimate SWE for portions of the Southwestern U.S. for an eight-year period. Two immediate applications for this product were: (1) to provide snowpack information for evaluating hydrologic models of snowmelt runoff and other components of the water balance, and (2) to evaluate the seasonal and interannual variability in snow cover patterns. Snow covered area (SCA) maps with a 1-km^2 grid were developed from AVHRR scenes using a three-part cloud masking procedure and spectral unmixing algorithm. A 1-km^2 SWE product was developed for the same area using interpolation of ground-based SnoTel data, followed by masking with the SCA scenes. In this way the interpolated SWE maps were adjusted on a pixel-by-pixel basis for the fraction of area actually snow covered. This fractional product gives significantly different snow coverage than do binary products, resulting in 20%-50% differences in basin-wide SWE estimates. Even larger differences result in comparing interpolated SWE from

1. In alphabetical order by lead author.

SnoTel with versus without masking using the SCA images. Areas with persistent snow cover were relatively reproducible from year to year, and they correspond to higher elevations. However, the annual maximum snow extent, or area with any snow cover during the year, exhibited significant interannual variability, and was not well correlated with maximum SWE. The current products are available on a set of CDs (see http://resac.hwr.arizona.edu/).

Tidal Cycles in Santa Barbara Basin Sediment

Wolfgang H. Berger[1], Arndt Schimmelmann[2], and Carina B. Lange[3]
[1] Scripps Institution of Oceanography, UCSD, La Jolla, CA
[2] Dept. of Geological Sciences, Indiana University, Bloomington, IN
[3] Depto. Oceanografía, Universidad de Concepción, Concepción, Chile

The sediments of the deep center of the Santa Barbara Basin, a valuable source of information about the history of the California Current, show cyclic deposition in at least three properties: varve thickness, total organic carbon (TOC) accumulation, and fish scale abundance. A surprising number of these cycles are multiples of the common tidal cycles, namely the 4.425-year perigee period (closeness of the moon), and the 18.6-year lunar nodal period. We suggest that the record of the basin is partly a result of pulsed sedimentation aligned with tides. These findings support the hypothesis that a considerable portion of sediment destined for deposition in the center of the basin goes through a phase of shallow storage on the shelf where it can be remobilized through storms and tides. The presence of tidal signals in the varve record must be taken into account when interpreting the paleoceanographic information contained in various sedimentary proxies.

Late Quaternary History of the Atacama Desert and Pacific Slope of the Central Andes

Julio L. Betancourt[1], Jay Quade[2], Claudio Latorre[3], Jason Rech[4], Christa Placzek, Camille Holmgren[2], Mathias Vuille[5], and Kate Rylander[1]
[1] U.S. Geological Survey Desert Lab, Tucson, AZ
[2] Univ. of Arizona Desert Lab, Tucson, AZ
[3] Univ. of Chile, Santiago
[4] Miami Univers., Oxford, OH
[5] Department of Geology, Univ. of Massachusetts, Amherst, MA

The hyperarid Atacama Desert extends along the Pacific Andean slope from the southern border of Peru (18 °S) to Copiapó, Chile (27 °S). The region's hyperaridity is due to the extreme rainshadow of the high Andes, which blocks the advection of tropical/subtropical moisture from the east; the blocking influence of the semi-permanent South Pacific Anticyclone, which limits the influence of winter storm tracks from the south; and the generation of a temperature inversion at ~1,000 m by the cold and north-flowing Humboldt Current, which constrains inland (upslope) penetration of Pacific moisture. The South Pacific Anticyclone has been anchored against the westward bend in the South American continent throughout the Neogene, the Andean orogeny doubled the average elevation of the central Andes during the past 10 million years, and the Humboldt Current reached its present intensity by early Pliocene. Seasonal and annual precipitation totals are determined by the number of precipitation days, as well as associated circulation anomalies during rainy and dry days. Precipitation variability in both summer and winter is modulated primarily by Pacific SST gradients and associated upper-air circulation anomalies. These anomalies promote either greater spillover of summer moisture from the Amazon and Altiplano to the east, or conversely, greater penetration of winter storms steered northward by migrating, cut-off lows.

Throughout the Quaternary, the most pervasive influence of climate variability on the Atacama Desert has been millennial-scale changes in the frequency and seasonality of the scant rainfall. During the past five years, we have mapped modern vegetation gradients and developed a number of paleoenvironmental records—including vegetation histories from fossil rodent middens, groundwater levels from wetland (spring) deposits, and lake levels from shoreline evidence—along a 1,600-km transect (16-26 °S) in the Atacama Desert. A strength of this paleoclimate transect has been the ability to apply the same methodologies across broad elevational, latitudinal, climatic, vegetation, and hydrologic gradients. The paleoclimate transect is being used to reconstruct histories of the South American tropical and extratropical rainfall belts, precisely at those elevations where average annual rainfall wanes to zero. Our results for the central Atacama (~22-24 °S) indicate maximum summer precipitation between 11.8 and 10.5 cal kyr BP, contrasting with pluvial lake highstands on the adjacent Altiplano from 16-14 cal kyr BP.

The focus of the Atacama work has been on the transition from sparse, prepuna vegetation into absolute desert, an expansive waterless terrain that extends from just above the coastal fog zone (1,000 m) to more than 3,000 m in the most arid sectors. Our research has matured and can now be used to test theories and empirical models about the influence of present and past climate on both physical and biological processes, including historical development of large-scale plant diversity gradients, constraints on rates and kinds of soil formation, and the influence of vegetation, and lack thereof, on microbial populations and processes.

Climatic Teleconnections for Influencing California Reservoir Operations

Levi D. Brekke and John A. Dracup
Dept. of Civil and Environmental Engineering, University of California, Berkeley

Despite the apparent existence of teleconnections between distant climatic precursors and Western United States hydrologic variations, there remains limited use of this information to influence water management in settings like California's Central Valley reservoir operations. This problem is related to a lack of understanding among decision-makers on how relying on climatic teleconnections would affect operational outcomes and decision-related risk.

Using Northern California reservoir inflow and Central Valley reservoir operations as the case study setting, three research phases were performed within a decision-oriented framework. The intent was to identify and assess teleconnections that might influence California water supply planning protocols (i.e., autumn stored-water carryover targeting and winter-spring allocation of stored-water). Phase One involved identifying strong teleconnections (i.e., correlation > 99% significant) between Pacific-region climatic variability and Northern California reservoir inflow variations during seasonal to annual supply-related periods. Phase Two involved evaluating the strong teleconnections from Phase One for added information value in supporting stored-water carryover targeting and water allocation

given the competing information set already supporting these decisions (i.e., climatology, snow surveys). Phase Three focused on how wet season flood control constrains the possible use of supply-related teleconnections, and involved identifying teleconnections related to seasonal flood event likelihood as a means to relax this constraint.

Results indicate a presence of strong supply-related teleconnections involving regionalized modes of mid-latitude Pacific atmospheric pressure structure variability and seasonal-to-annual Northern California reservoir inflow variations. Evaluating the use of these strong teleconnections in decision-support showed that the teleleconnections related to the autumn stored-water carryover targeting process offer an added information value (i.e., teleconnections involving water-year inflow response). However, the teleconnections related to the winter-spring water allocation offer little or no added information value because of the substantial information overlap between the teleconnections and snow survey data already conditioning this decision process. Finally, the "flood event"-related teleconnection assessment showed that summer observed climatic precursors embedded in the mid-latitude Pacific atmospheric pressure structure have potential for indicating wet season (October-Mar.) peak runoff rates. This latter result plus the existence of supply-related teleconnections related to stored-water carryover targeting indicates promise for teleconnections-based coordination of wet season flood-control and stored-water supply management strategies in California reservoir operations.

Pacific Decadal Oscillation Selectively Removes Winter Season ENSO-Precipitation Signal in the Western United States

David P. Brown and Andrew C. Comrie
Department of Geography and Regional Development, University of Arizona

Seasonal forecasts of winter precipitation in the western United States are of great importance in decisions regarding water resource use, drought mitigation, fire management, and other public and private stakeholder issues. The strength of these forecasts rests in large part on a robust El Niño-Southern Oscillation (ENSO) signal, wherein warm (cool) ENSO events during the fall season typically correspond to below (above) normal winter precipitation in the Pacific Northwest and northern Rocky Mountains, and above (below) normal winter precipitation across the Southwest. In this paper, we show that the consistency of these ENSO-precipitation relationships is modulated in a bipolar fashion by phase changes in the Pacific Decadal Oscillation (PDO). During warm PDO phases, fall ENSO-winter precipitation correlations are diminished across the Northwest, while cool PDO phases result in a weakened ENSO-precipitation relationship for the Southwest. An examination of winter precipitation variability for a sample of locations in the West during years of decreased ENSO correlation reveals that inconsistencies in the canonical ENSO-precipitation relationship are evident during both El Niño and La Niña episodes. This discovery of a bipolar, multi-decadal absence of statistically significant ENSO signals changes our understanding of winter precipitation variability in the western United States and suggests a need for restraint in making precipitation forecasts based largely or solely on ENSO behavior.

Unexpected Forest Responses to Climate Change in Mountain Regions: The Role of Landscape Heterogeneity

L.B. Brubaker[1], D. Gavin[2], J.S. McLachlan[3], W.Y. Fujikawa[1], and D.G. Sprugel[1]
[1] University of Washington, Seattle, WA
[2] University of Illinois, Urbana-Champaign, IL
[3] Dartmouth University, Durham, NC

One of the major challenges to understanding how mountain regions will respond to future climate change is the role of landscape-climate interactions in controlling tree species distributions and forest disturbance regimes. Pollen records from the Olympic Mountains and the San Juan Islands of Washington indicate that landscape factors (elevation, topography, soil) have modified vegetation responses to climate change during the Holocene and raise questions about traditional views of climatically-driven forest shifts in mountains. First, the predominant response to Holocene climate change was not elevational shifts in tree distributions or northward-southward migration of species along mountain chains. The pollen data instead suggest that tree population sizes fluctuated dramatically across elevations between times of favorable and unfavorable climate, but that species did not disappear under adverse conditions. For example, during the hot, dry climate of the early Holocene, mesic tree species appear to have persisted at favorable locations in small populations, which provided seeds for rapid colonization across an array of sites when favorable conditions re-established ca. 6,000 years ago. Second, pollen records at sites ca. 30 km apart on wet and dry sides of the Olympic Mountains indicate that a given regional climate change may cause different shifts in treeline locations, depending on site moisture conditions. For example, during the early Holocene, treeline was lower than today in the west Olympics but similar to or higher than today in the east. Third, the importance of landscape controls appears to vary over time. In both the Olympic Mountains and San Juan Islands, landscape controls are strong and cause complex patterns in vegetation under some climates, but climatic controls predominate at other times, resulting in relatively uniform forest composition across landscape types. Fire-climate-landscape interactions appear equally complex, as stand-level reconstructions of forest composition on Mount Constitution, Orcas Island, indicate that local site conditions alter the effects of climate-fire interactions on forest composition, causing shifts in the patchiness for forest composition overtime. In sum, numerous examples from paleorecords of these areas emphasize the complexity of vegetation responses to climate in mountain landscapes. Predicting forest responses to future climate changes will not be straightforward in mountain regions even if future climates are correctly known.

Cytometric Sorting of Pinaceae Pollen and Its Implications for Radiocarbon Dating and Stable Isotope Analyses

Roger Byrne[1], Jungjae Park[1], Lynn Ingram[2], and Tak Hung[3]
[1] Department of Geography, UC Berkeley, Berkeley, CA
[2] Department of Earth and Planetary Science, UC Berkeley, Berkeley, CA
[3] Union Biometrica, Somerville, MA

Several members of the Pinaceae family, for example: *Pinus, Abies*, and *Picea*, produce vast quantities of wind-dispersed pollen. So much so that in some areas of the Northern Hemisphere Pinaceae pollen

makes up a significant fraction of the sediment accumulating in lakes. Pinaceae pollen is also found in significant quantities in marine sediments and glacial ice. Most Pinaceae pollen grains are large, i.e., their longest axis is over 50 micrometers. This means that they can be easily concentrated by sieving, although other non-pollen material of the same size, e.g., microscopic charcoal fragments, is typically present in the residue. The development of radiocarbon dating by AMS has made it possible to use pollen directly as a means of dating sediment cores. However, because of the difficulties involved in extracting a pure pollen concentrate, the technique has not been widely applied. Also, there are some reports that radiocarbon ages based on pollen residues may be unexpectedly old, although whether this is due to lag effects in pollen transport or to the extraction techniques themselves is not clear. In addition to its usefulness in radiocarbon dating, Pinaceae pollen in lake and marine sediments may also provide a proxy record of climate change. For example, changes in $\delta^{13}C$ and $\delta^{18}O$ of Pinaceae pollen could theoretically provide evidence of changes in temperature and/or evaporation in the terrestrial environment.

In this paper, we show how new developments in cell cytometry have made it possible to concentrate large quantities of Pinaceae pollen from sediments in a relatively short period of time, i.e., ca. 25,000 grains/hour. Cytometric sorting of Pinaceae pollen is relatively easy because Pinaceae pollen autofluoresces at several wavelengths. We have found that excitation at 514 nm with a yellow filter (emission 545 nm) gives the best results. As a preliminary test of the potential paleoclimatic usefulness of cytometrically concentrated Pinaceae pollen, we have analyzed the stable isotopic (oxygen and carbon) composition of four samples from a sediment core taken at Lake Moran in the central Sierra Nevada. The samples date to 500, 6,000, 10,000, and 14,000 years BP. These results are compared with the stable isotopic composition of modern pine pollen samples collected at different elevations throughout the state.

Regional Climate and Environmental Change Recorded in Ice Cores from the Upper Fremont Glacier, Wyoming: Implications for Long-Term Stewardship of Buried Waste at U.S. Department of Energy Facilities

L. Dewayne Cecil[1], Mitch Plummer[2], David L. Naftz[3], Lisa J. Graumlich[4], Paul F. Schuster[5], Jaromy R. Green[1], and David D. Susong[3]
[1] U.S. Geological Survey, Idaho Falls, ID
[2] Idaho National Engineering and Environmental Laboratory, Idaho Falls, ID
[3] U.S. Geological Survey, Salt Lake City, UT
[4] Big Sky Institute, Montana State University, Bozeman, MT
[5] U.S. Geological Survey, Boulder, CO

Geochemical records preserved in the ice and snow collected from the Upper Fremont Glacier in the Wind River Range, Wyoming, include seasonal fluctuations of naturally produced isotopes such as oxygen-18 and oxygen-16, anthropogenic radioactive fallout such as plutonium, tritium, and chlorine-36 from atmospheric nuclear-weapons tests in the 1950s and 1960s, and signals from global and regional events such as volcanic eruptions, droughts, and forest fires. Organic matter entombed in the glacial ice also has provided a means to age-date sections of the core utilizing the carbon-14 inventory. Additionally, tree-ring chronologies extending back to approximately the year 1550 have been collected at or near the Upper Fremont Glacier and provide another proxy record of long-term climate variability. A chronology from a white bark pine tree near the alpine tree line adjacent to the Upper Fremont Glacier records variability in summer temperature and the tree-ring record from a Douglas fir collected at lower elevation records variability in winter precipitation.

By combining all the information gained from the analyses of these records we have concluded that, since the mid-1800s, there have been relatively rapid changes in the regional climate of southern North America that continue today. In the mid-1800s, these rapid changes are interpreted as an abrupt end of the Little Ice Age, occurring within less than 10 years, but potentially within as little as 2 to 3 years. A reconstructed temperature profile from the glacial ice samples showed that, since 1960, the average annual air temperature for the high-altitude areas in this same region has increased on the order of 1.5 ° to 3.5 °C (see Naftz and others, these proceedings).

The ice-core and tree-ring data offer the potential to characterize the seasonal climatological history archived at and near this site. For example, the high elevation summer tree-ring record supports our conclusion that there has been a general long-term rise in average annual air temperature starting in the mid-1880s. In contrast, the tree-ring record does not show as abrupt a rise in air temperature as that indicated by the ice-core data. This result is not surprising since these proxy records (the tree-ring and ice-core records) may be reflecting the climate record from different seasons. The tree-ring records are predominately a representation of the summer growing season and the ice-core records reflect an early fall to early summer snow-accumulation period.

The rapid changes in regional climate and air temperature affect water and other natural resources and, thereby, potentially affect the long-term stewardship of buried waste at U.S. Department of Energy (DOE) facilities across the nation. This is particularly true with respect to changes in amounts and timing of precipitation that could affect short- and long-term storage of buried mixed chemical and nuclear waste. The historical isotopic and geochemical information gained from studying the Upper Fremont Glacier has been used to refine our conceptual models of groundwater flow in, and recharge to, the eastern Snake River Plain aquifer in southeastern Idaho. This information also is being used to evaluate the level of risk to humans from environmental contaminants at and near the DOE's Idaho National Engineering and Environmental Laboratory (INEEL). The INEEL is located at the same latitude and approximately 350 kilometers west of the Upper Fremont Glacier.

Regional Timing of Neoglaciation in the Western Cordillera: Constraints from Glacial and Lacustrine Records

Douglas H. Clark
Geology Department, Western Washington University, Bellingham, WA

Studies that integrate detailed moraine mapping with analysis of sediment cores from downstream lakes suggest regionally coherent onset and maximum extents of Neoglaciation in the mountains of the western Cordillera. Climate reconstructions based on these records indicate that glaciers in many western mountains began to form and grow by ~4,000-3,500 cal yr BP, but did not reach Holocene maxima until 200-300 yr ago, during the culmination of the Little Ice Age. The record remains incomplete, however, and future studies will test this emerging pattern and provide a more complete record.

Alpine glacial deposits and lake sediments provide unique records of regional climate patterns in alpine regions. Whereas moraines alone provide constraints of climate extremes (maximum glacial climates), alpine lake sediments preserve continuous sedimentologic, geochemical, and ecological records of past climate change changes. Variations in moisture delivery and temperature affect the size (and consequent sediment output) of adjacent glaciers, the rates of soil formation and erosion, and the vegetation communities existing in these alpine settings. New dating and correlation tools for these records may help establish high-resolution linkages with other records in the region, and perhaps with some global records.

Clastic sediments in alpine lake cores from below modern glaciers in the Sierra Nevada and the North Cascades suggest that the coastal ranges were dominated by warm, non-glacial conditions throughout the early and middle Holocene, after the Pleistocene glaciers had retreated or disappeared. Starting about 3,600-3,200 ^{14}C yr BP (~3,900-3,400 cal. yr BP), increases in fine clastic silt indicate onset of glacier growth. Glaciers appear to have advanced episodically for the remainder of the Holocene. Lichen constraints and the absence of evidence for pre-Little Ice Age (LIA) moraines in most western mountains, combined with evidence of two severe droughts before ~600 cal yr BP (Stine 1994), suggest that most glaciers did not reach their Holocene maxima until the late Little Ice Age (i.e., last 200-300 yrs). Some sites in the Rocky Mountains suggest local Holocene maxima may have occurred earlier than LIA, but the data are equivocal. Future coring studies should yield more robust and higher-resolution records of Holocene glacial variations in western North America.

The regional coincidence of both the onset and maximum of Neoglaciation in the western Cordillera suggests that the primary cause was a decrease in regional temperature rather than an increase in precipitation. Comparison of reconstructed and modern Holocene equilibrium line altitudes in several ranges suggests that conditions throughout the west at the height of the LIA were ~0.5-1.0 °C cooler than present. Although nearly all are now in retreat, many glaciers remain larger than they were for most of the Holocene; this suggests that modern alpine climates have not yet reached those characteristic of the early and middle Holocene.

WestMap: The Western Climate Mapping Initiative

Andrew C. Comrie[1], Kelly Redmond[2], and Christopher Daly[3]
[1] Dept. of Geography, University of Arizona, Tucson, AZ
[2] Western Regional Climate Center/Desert Research Institute, Reno, NV
[3] Spatial Climate Service, Oregon State University, Corvallis, OR

We report on the development and future plans of the Western Climate Mapping Initiative (WestMap). WestMap aims to provide an easily accessible, comprehensive package of fine-scale, high temporal resolution climate data, error measures, associated diagnostic analysis tools, and educational resources to the highly diverse user communities of climate data stakeholders in the United States. The data envisioned are a suite of fine-scale (~1km) gridded time series (~1 month for ~100 years) that can be aggregated to user-specified domains. The scope of western stakeholder demand for this kind of climate data has been noted by the western Regional Integrated Science and Assessment projects (e.g., CLIMAS, the Climate Assessment for the Southwest). This demand is so large and the climate so complex across the western United States that the early focus of WestMap will be on a domain covering this region. The western focus is due to the myriad climate mapping challenges throughout the area, including fine scale topographic variations, extensive high elevation mountain ranges, deserts, coastal boundary regions, interior valleys, rain shadows, data availability and poor

station distribution. The WestMap initiative was conceived by a consortium that includes the University of Arizona/CLIMAS, the PRISM climate mapping group at Oregon State University, the Western Regional Climate Center/Desert Research Institute, Scripps Institute/California Applications Project, NOAA Climate Diagnostics Center, and the USDA Natural Resource Conservation Service. The WestMap consortium is currently seeking feedback and support from the western climate research and data communities, as well as exploring the possibilities for multi-agency funding for the WestMap initiative.

Integration of Fire-Climate Information Into a Decision Support System: The Walter Project

Michael A. Crimmins[1], Susan M. Taunton[1], Stephen R. Yool[1], Andrew C. Comrie[1], and Barbara J. Morehouse[2]
[1] Dept. of Geography and Regional Development, University of Arizona, Tucson, AZ
[2] Institute for the Study of Planet Earth, University of Arizona, Tucson, AZ

It is well understood that wildfire dynamics are critically linked to the immediate weather conditions under which they persist. often overlooked, though, are the longer-term antecedent conditions prior to wildfire events that are governed by local and regional climate variability. Wildfire dynamics are a product of climate variability at a continuum of temporal scales from longer-term antecedent conditions (governing fuel production) to the immediate fire weather conditions at the time of the wildfire event. It is important to understand the critical climate pathways across temporal scales that contribute to environmental conditions for large fire events.

The University of Arizona WALTER project is developing a decision support system called FCS-1 that will facilitate in the dissemination of integrated wildfire, urban-wild land interface, and climate spatial data for several test venues in the southwest United States. This system will help the public visualize the critical overlaps between wildfire, climate, and social interactions with the natural environment. This presentation will outline the framework for integrating regional fire-climate relationships that capture changes in fuel production with remote sensing techniques that capture shorter-term fuel moisture conditions. These methods together provide insight into the important sequences of fuel production and conditioning moderated by climate.

Climate Mapping Challenges in the Western United States

Christopher Daly
Spatial Climate Analysis Service, Oregon State University, Corvallis, OR

The western United States is the one of the most climatically complex regions in the world. The presence of major topographic features and coastal effects creates a myriad of spatially complex precipitation and temperature regimes. Only a small number of these regimes are well-represented by surface observations. Therefore, producing accurate climate maps for this region is quite challenging. PRISM, a knowledge-based climate mapping system, was originally developed in 1991 to map precipitation in the West. Since then, it has been expanded and refined over time to model more climate variables and address more climatological processes. Model improvements have come primarily as a result of lessons learned through repeated applications of the model and peer-review of the results. This paper will survey some of the major climatological processes driving temperature and precipitation patterns in the West, and how PRISM accommodates these processes. These include elevational gradients, rain shadows, coastal influences, temperature inversions, and the varying orographic effectiveness of terrain features. Specific case studies will be drawn from the Oregon Cascades, Olympic Mountains, coastal California, and others. Needs for future improvements to PRISM include a more explicit characterization of susceptibility to cold air drainage.

What Happens When Pacific Climate Goes East over the Mountains?

Walter E. Dean and Joseph G. Rosenbaum
U.S. Geological Survey, MS 980 Federal Center, Denver, CO

Sediments deposited over the last 26,000 years in Bear Lake, Utah/Idaho, were recovered in three overlapping piston cores. The sediments deposited during the last glacial interval consist of carbonate- and organic-poor, red, silty clay. This red-clay deposition coincides in time with the highest level of Lake Bonneville, although the two lakes were not connected. These glacial sediments were deposited by a more active Bear River, which has its headwaters in the Uinta Mountains. The Bear River bypassed Bear Lake during late Pleistocene and most of the Holocene. As the salinity of the lake increased, carbonate began to precipitate about 16,000 years ago, first as calcite, then as aragonite. Aragonite precipitation was interrupted briefly about 9,000 years ago during a period of freshening, probably caused by re-entry of the Bear River.

Sediments deposited over the last 250,000 years in Bear Lake were recovered in two holes with a maximum length of 120 m during testing of the new Global Lake Drilling (GLAD800) platform (now officially the R/V Kerry Kelts). The dominant sediment in most of the 120-m section is calcareous, gray to black, silty clay, with calcite as the dominant carbonate mineral. The dominance of siliciclastic sediment indicates that the Bear River commonly was connected to Bear Lake, but either no red sediment was deposited or the red color was reduced to black and gray in the organic-rich sediments. XRD results indicate that two aragonitic intervals occurred prior to the Holocene aragonite interval. Preliminary volcanic-ash and U/Th dating indicate that these aragonitic intervals were deposited during the last two interglacials equivalent to Oxygen Isotope Stages 5 and 7. If so, these high carbonate, aragonitic interglacial intervals coincide with warm continental climates, warm SSTs, increased coastal upwelling under the California Current, and increased organic productivity, all recorded in piston cores and recent ODP cores along the Pacific margin. This implies that the subtropical atmospheric high-pressure system that today drives the California Current during the summer was a more permanent feature of North Pacific circulation during interstadials. During the last glacial interval and other stadials, the Aleutian low-pressure system, presently dominant during the winter, was a more permanent feature of North Pacific circulation, producing storms and precipitation that increased the levels of Lake Bonneville and Lake Lahontan, and increased the flow of Bear River. On the California margin, the California Current upwelling system was greatly reduced. Sediments deposited on the continental margin of California during stadials indicate that organic productivity there was considerably lower. These climatic patterns over the North Pacific are recorded in Bear Lake by river-borne detrital clastic sediments deposited during stadials, and carbonate sediments, dominated by aragonite, during the more arid interstadials.

The Thermal Evolution of Snowpack at Gin Flat, Yosemite National Park, Winter and Spring 2002

Michael D. Dettinger[1] and Frank Gehrke[2]
[1] U.S. Geological Survey, Scripps Institution of Oceanography, La Jolla, CA
[2] California Cooperative Snow Surveys, Department of Water Resources, Sacramento, CA

The Gin Flat automated snow-telemetry site, at 7,050 feet above sea level in Yosemite National Park, has been augmented during the past two years to measure components of the water and radiation budgets of the snowpack in addition to the precipitation, temperatures, and snow-water content (SWC) measurements typical of such sites. New measurements at Gin Flat include cosmic-ray SWC measurements, snow thickness, incoming solar radiation, and net radiation to the snow surface. Together, the measurements at Gin Flat characterize gross water and radiative-heat budgets of the winter snowpack, as well as snow density. During 2002, temperatures within the (6 ft) snowpack also were monitored at one-foot vertical intervals, as indicators of the time and depth varying thermodynamics of the snowpack. The measurements at Gin Flat, taken together, illustrate multi-day downwelling of cold into the Sierra Nevada snowpack during two prolonged cold snaps, but, otherwise, the snowpack and soil hovered near freezing until melt began. Additional instrumentation such as that operated at Gin Flat is proving robust to the elements and is providing new insights into the workings of the Sierra Nevada snowpack. Augmentations have now been included at several more sites, including Tuolumne Meadows and Dana Flat in Yosemite National Park. Updates from the current (2003) season will be available for comparison with spring 2002.

Climate Linkages Between Uplands and Lowlands

Henry F. Diaz and Jon K. Eischeid
NOAA-CIRES Climate Diagnostics Center, Boulder CO 80305

A conceptual view has emerged among scientists of the connectedness between natural ecosystems and the larger environment within which it operates. To that view of the natural workings of natural living systems, must now be added the impact of human activities, which affect the operation of these natural ecosystems on a variety of space and time scales. The western portions of the United States have experienced tremendous demographic growth, which is changing the fabric of the urban and rural landscapes across the region. The physical chord that connects the entire palimpsest of western history to the present time is water—its scarcity on the landscape and the riparian corridors that connect upland and lowland environments like a gaunt "vascular system" pumping the lifeblood of the region. In the last 30 years changes in the climate of the region have brought about measurable changes in plant phenology, in the seasonal cycle of snowmelt and streamflow, in the rate of growth of high elevation forest conifers, and in the drought cycles that are an integral part of the growth dynamics of grasslands and open woodlands in the West. Here we consider the implications of changes in climate for selected western U.S. regions by examining the recent climatic history uplands—the higher elevations of the West, and the lower border grasslands and riverine systems that connect them to the regions where most of the people live. We also consider possible implications of future changes in water resources systems due to changes in the hydroclimatology of the West.

Global Environmental Effects on Mountain Ecosystems: A Case Study from Glacier National Park

Daniel B. Fagre
U.S. Geological Survey, Glacier National Park

The glaciers of Glacier National Park, Montana are disappearing. At the end of the Little Ice Age (ca. 1850) there were an estimated 150 glaciers within current park boundaries. Today, fewer than 37 are deemed viable or large enough to be classified as glaciers. Glacier recession is the most visible sign of global climate change but the entire mountain ecosystem has also responded. Upper treelines have advanced, tree growth rates have increased, subalpine meadows have been invaded by conifers and snow patterns have been altered. What are the consequences for Glacier Park of disappearing glaciers and the climate change that drives glacial melt? The results from a variety of studies aimed at answering this question suggest some profound future changes. Computer models applied to the Glacier Park ecosystem suggest that all glaciers will be gone by 2030 at current warming rates in the Northern Rocky Mountains. Snowpacks are projected to persist for 2 months less despite modest increases in future precipitation. Net primary productivity will likely increase on the western sides of the mountains but reduced net primary productivity and biodiversity can be expected in the drier, east-side forest ecosystems. These profound changes to a treasured mountain landscape will challenge park managers and alter visitors' experiences.

Subregional Climatology Affects Area Burned by Wildfire in the U.S. Pacific Northwest

Ze'ev Gedalof [1,2], David L. Peterson[3], and Nathan J. Mantua[1]
[1] Climate Impacts Group, Joint Institute for the Study of the Atmosphere and Oceans, University of Washington
[2] University of Victoria Tree-Ring Laboratory
[3] USDA Forest Service, Pacific Northwest Research Station, Seattle, WA

Empirical Orthogonal Function (EOF) analysis is used to determine the coherence (or patterns) in area burned by wildfire in the Pacific Northwest. Anomaly fields of 500 hPa height were regressed onto the resulting principal component time series to determine the patterns in atmospheric circulation that are associated with variability in area burned by wildfire. Additionally, cross correlation functions were calculated for the Palmer drought severity index (PDSI) over the year preceding the wildfire season. A second analysis was undertaken using the same fire and climatic data sets, but based on superposed epoch analysis rather than linear regressions. This analysis focused only on the extreme fire years (both large and small), and does not require the association between fire and climate to be linear in nature. Extreme wildfire years are forced in part by antecedent drought and summertime blocking in the 500 hPa height field. However the response to these events is modulated by the ecology of the underlying forest. At more mesic forest types antecedent drought preconditions forests to burn, but is not a good predictor of area burned due to the rarity of subsequent ignition. At especially dry locations, blocking events alone can lead to increases in area burned even in the absence of antecedent drought. Summertime cyclones can also lead to increased area burned, probably due to dry lightning storms that bring ignition and strong winds but little precipitation. The patterns

identified in this analysis were quite similar to those observed during the August-October 2002 Biscuit Fire in southwest Oregon. In the context of these findings we believe that management paradigms that rely on fuel treatments alone to eliminate large, intense fires are unlikely to be successful.

Columbia River Flow Since AD 1750 Reconstructed from Tree Rings

Ze'ev Gedalof[1,2], David L. Peterson[3], and Nathan J. Mantua[1]
[1] Climate Impacts Group, Joint Institute for the Study of the Atmosphere and Oceans, University of Washington
[2] University of Victoria Tree-Ring Laboratory
[3] USDA Forest Service, Pacific Northwest Research Station, Seattle, WA

A network of drought sensitive tree-ring chronologies is used to reconstruct flow on the Columbia River at The Dalles, Oregon, since 1750. The reconstruction explains 30% of the variability in mean water-year flow, with a substantial fraction of unexplained variance caused by underestimates of the most severe low-flow events. Residual statistics from the tree-ring reconstruction, as well as an identically specified instrumental reconstruction, exhibit positive trends over time. This finding suggests that the relationship between drought and streamflow has changed over time, supporting results from hydrologic models, which suggest that changes in land cover over the 20th century have had measurable impacts on runoff production. Lowpass filtering the flow record suggests that persistent low flows during the 1840s were probably the most severe of the past 250 years, but that flows during the 1930s were nearly as extreme. The period from 1950 to 1987 is anomalous in the context of this record for having no notable multiyear drought events. A comparison of the flow reconstruction to paleoproxy records of the Pacific Decadal Oscillation (PDO) and El Niño/Southern Oscillation (ENSO) supports a strong 20th century link between large-scale circulation and streamflow, but suggests that this link is very weak prior to 1900.

Proxy Reconstruction of the Entire Pacific Sea Surface Temperature Field

Alexander Gershunov[1], Michael Evans[2], and Malcolm Hughes[2]
[1] Climate Research Division, Scripps Institution of Oceanography
[2] Laboratory of Tree-Ring Research, University of Arizona

Tree-ring reconstructions of Pacific climate typically use regional chronologies and focus on specific indices such as the Southern Oscillation (SOI) or the North Pacific Oscillation (NPO). Trees integrate seasonal-annual climatic effects, but since individual climate modes don't act in isolation, there is no physical or biological reason why trees, especially those trees growing in the midlatitudes, should respond to specific indices while the climate in which they grow is affected by a complex cornucopia of patterns all shifting, changing and vacillating either in unison or in opposition with each other. We use proxy data from around the Pacific rim (mostly tree ring records, but other proxies as well), to reconstruct patterns of sea surface temperature (SST) in the entire Pacific basin. This is done by the application of Canonical Correlation Analysis, a pattern-to-pattern matching technique, to first relate observed tropical and extratropical Pacific SST patterns to patterns in a network of tree-ring chronologies spanning the west coast of north and south America as well as proxies from around

the Pacific rim. The statistical model is optimized in terms of the number of patterns and relationships required to capture the co-variability in the SST and proxy records. The optimization is based on a cross-validation scheme that maximizes the SST variance explained by the proxy network. An optimized statistical model developed on the observational period is then used to reconstruct the SST field back several centuries. ENSO and NPO indices derived from the reconstructed SST patterns will be compared with other available reconstructions. Observed Pacific space-time SST variability during the last century will be discussed in the context of the longer reconstructed perspective. This is a contribution to the work of the "past PDO group", several of whose members made available important data not yet in the public domain.

Tree-Ring Based Reconstructions of Precipitation Variability in Northeastern Utah

Stephen T. Gray[1], Stephen T. Jackson[1], and Julio L. Betancourt[2]
[1] Department of Botany, University of Wyoming, Laramie, WY
[2] University of Arizona and U.S. Geological Survey Desert Laboratory, Tucson, AZ

Like much of the West, the economy of the Uinta Basin Watershed (UBW) in northeastern Utah depends almost entirely on agriculture, timber production, and outdoor recreation. Furthermore, this area contributes some 1.4 million acre-feet of runoff to the Colorado River each year. In turn, characterizing precipitation variability in the UBW is one of the most desirable goals for local resource managers and downstream water-users alike. However, the short duration of instrumental climate records greatly hinders such efforts. Therefore, we developed a new tree-ring based reconstruction of annual (June-June) precipitation in the UBW over the AD 1226-2001 period. Based on samples taken from 144 piñon pines (*Pinus edulis*) at four at sites, the full reconstruction reveals significant precipitation variability at interannual to decadal scales. In general, both single-year and decadal-scale dry events were longer and more severe prior to the instrumental record. In particular, dry events in the late 13th, 16th and 18th centuries surpass both the magnitude and duration of any droughts after 1900. On the other hand, the end of the 20th century represents one of the wettest periods in the reconstruction. Overall, evidence from the proxy record demonstrates that the climate of the instrumental period is not representative of the full range of precipitation variability the UBW has experienced in the past. In addition, estimates of future water availability in the UBW and forecasts for exports to the Colorado River are likely too high as they were calculated during anomalously wet periods. Finally, comparisons of our UBW precipitation reconstruction with those from surrounding areas point to a regional synchronization of climate during severe drought events with important implications for land management and water resources.

Hourly Measurements of Concentrations of Nitrate Plus Nitrite and Dissolved Silica in the Merced River

Stephen W. Hager, Richard E. Smith, and David H. Peterson
U.S. Geological Survey, Menlo Park, CA

As part of a broad program linking variations in large-scale atmospheric circulation (climate) to variations in river chemistry, it is useful to be able to monitor chemical variations at rates comparable to those of the hydroclimate variables. We are now making hourly measurements of nitrate plus nitrite (N+N) and dissolved silica (DSi) in the waters of the Merced River at the Hydrologic Benchmark Network station at Happy Isles Bridge in Yosemite National Park. We are deploying instruments (NAS-2E and AutoLAB; W.S.Envirotech, U.K.) that can be programmed to perform standard colorimetric analyses on discrete samples. The major challenge for N+N has been to develop a freshwater routine accurate and sensitive enough to observe the small variations occurring in snowmelt. Our versions of the analytical routines analyze a standard, a turbidity blank, a distilled water blank, and a reagent blank in addition to the sample. Precision (two standard deviations on the standard) is now typically better than 0.1 micromoles per liter for N+N. Precision for DSi is about 0.8 micromoles per liter.

Although the NAS-2E is submergible, we deploy the analyzers in an enclosure on the bank of the river, with the water pumped to them. This setup allows elaborate analytical routines, larger reagent quantities, and use of renewable (solar) power, while ensuring the lowest possible chance of contamination of the river. Successful deployments of 12 weeks have been made possible with the N+N analyzer by improvements in the reductor that converts nitrate to nitrite. Length of deployment of the DSi analyzer is currently limited to about 4 weeks by the instability of the molybdate reagent.

Data sets obtained so far demonstrate the utility of hourly sampling toward understanding the pathways the snowmelt water goes through on its way to the gage and toward elucidating the response of the watershed to episodic, flow-generating events. Concentrations of N+N undergo regular diel cycles during snowmelt. For a surprisingly long period at the beginning of the 2002 snowmelt season, transport of N+N increased more rapidly than flows did. We will be able to look at this flushing of the winter accumulation of nitrate from the watershed in some detail. Later in 2002, thunderstorms following a period of dry weather produced large, short-duration spikes in concentration. Comparison with hourly conductivity measurements using data from June 2000 reveals the likelihood of at least two pathways, possibly those of the groundwater and shallow soil water. Concentrations of DSi also display a regular diel cycle, but they show a progressive decrease through the spring. Possible explanations include depletion of dissolved silica in soils, the seasonal change from lower to higher elevation source areas, and biological uptake.

Sources of Hydrologic Predictability in the Columbia River Basin: A Comparison of the Role of Hydrologic State Variables and Winter Climate Forecasts

Alan F. Hamlet and Dennis P. Lettenmaier
JISAO CSES Climate Impacts Group, and
Dept. of Civil and Environmental Engineering, University of Washington

In the Columbia River Basin (CRB) skillful forecasts of winter precipitation and temperature based on the El Niño Southern Oscillation (ENSO) and Pacific Decadal Oscillation (PDO) can be made with lead times of up to about six months (i.e., on about June 1). Using a hydrologic model and near real time estimates of hydrologic state variables such as soil moisture and snowpack, we produce probabilistic forecasts of streamflow at various locations throughout the CRB starting in June and proceeding through the subsequent fall and winter snow accumulation season. A useful standard of comparison for these experimental forecasts is a January 1 extended streamflow prediction (ESP) forecast, which essentially exploits hydrologic initial conditions (snow and soil moisture), but

represents the full historical climatic range of future (precipitation and temperature) conditions. ESP forecasts represent the current state of the art for operational water management throughout much of the western U.S. In order to understand the role of the various sources of hydrologic predictability, we generate probabilistic streamflow forecasts using a simple categorical PDO/ENSO climate forecast based on predictions of evolving SST on the forecast date, and estimates of hydrologic state variables available on October 1, November 1, and December 1. These are compared, using a quantitative skill metric, to January 1 ESP forecasts based solely on hydrologic state variables. On October 1, the skill of the streamflow forecasts is primarily attributable to skill in the winter climate forecasts, with a relatively small contribution from the estimated initial soil moisture state. As snow accumulates in the basin in the fall and early winter, however, the forecasts on November 1 and December 1 are increasingly influenced by the persistence of the hydrologic state, and the forecasts become progressively more skillful and less sensitive to uncertainties in the climate forecasts. These experiments show that October 1 forecasts based on PDO/ENSO forecasts, while frequently better than climatology, are generally not as skillful as January 1 ESP forecasts, and that the error characteristics of the October 1 forecasts are also generally less desirable than those of the January 1 ESP forecasts. Preliminary results for the November 1 and December 1 forecasts, however, suggest that by about November 1, the skill of the PDO/ENSO forecasts are frequently comparable to the January 1 ESP forecasts and by December 1, the skill of the PDO/ENSO forecasts exceeds the skill of the unconditional January 1 ESP forecasts in most years. Very long-range forecasts made on June 1, which estimate fall soil moisture based on current hydrologic conditions, are also shown to be nearly as skillful as the October 1 forecasts, although increased likelihood of misclassification of PDO/ ENSO state with increased lead time adds some uncertainty to the forecasts.

Effects of Climate Change on the Pacific Northwest Ski Industry

Alan F. Hamlet[1,2], Philip Mote[1], Amy K. Snover[1], and Dennis P. Lettenmaier[1,2]
[1] JISAO CSES Climate Impacts Group, University of Washington
[2] Dept. of Civil and Environmental Engineering, University of Washington

In the western U.S., loss of snowpack is expected to be one of the most prominent impacts associated with global warming. Changes in snow accumulation and melt in the mountain west, for example, have been shown to have serious implications for water management due to related streamflow timing shifts, particularly in moderate elevation river basins where mid-winter temperatures are close to freezing and the seasonal streamflow peak would, on average, occur substantially earlier. Changes in winter snow accumulation, however, would also have direct impacts on winter recreation both in managed ski resorts and in back country areas. Using the Variable Infiltration Capacity (VIC) energy balance snow model and topographically corrected gridded climate data from 1949-1999, we examine the potential effects of four global warming scenarios on managed ski areas in the Pacific Northwest, as well as a several unmanaged areas used by the public for snow-related winter recreation activities. As in previous studies that have examined climate change effects on snow, the modeling results show that moderate elevation areas in the western Cascades would be most greatly impacted, whereas impacts to high elevation sites or areas with colder winters would be more strongly associated with less certain changes in precipitation. At Alpental Ski Area near Snoqualmie Pass in the western Cascades (elevation ~900m), for example, the probability of accumulating sufficient snow depth to be able to open the ski area on December 1 declines from about 42% for the current climate (1950-

1999) to about 20% by the 2020s, and the average number of days that the ski area would be open each year declines from about 118 days to 85 days. By comparison, Schweitzer Mountain Ski Area, which is on the east side of the Cascades at higher elevation (~1,200 m), would be able to open about 50% of the time on Dec. 1 for the current climate, and about 45% for the two 2020s scenarios, and the number of days open would decline only slightly from 117 to 112 days per year on average. Higher elevation areas such as those at Mount Bachelor and Mount Baker are the least sensitive to warming, and are primarily affected by relatively uncertain changes in precipitation variability in the scenarios. Other impacts, such as changes in the number of days with rain when the ski area is open, generally follow the patterns of the date of opening and average length of season statistics.

A High Elevation Tropical Climate Reference Network

Douglas R. Hardy and Raymond S. Bradley
Department of Geosciences and Climate System Research Center,
University of Massachusetts, Amherst MA

There is a dearth of climatological data from high elevations, especially in the Tropics. Environmental changes in the Tropics are of vital importance, as it is in this region that future population growth and environmental pressures will be greatest. Furthermore, many tropical lowland regions rely on water resources from adjacent upland areas, so environmental changes in mountain regions are critical to the well being of millions of people, and to healthy, diverse natural systems. The recession and even disappearance of tropical glaciers and ice caps has highlighted the need to monitor climatic changes in these regions. Looking toward the future, model simulations with 2xCO_2 suggest that warming will be considerable in the mid-troposphere, at elevations corresponding to the mean annual freezing level height. Currently, we do not have a reliable network, employing precise measurements, to track these anticipated long-term changes.

High elevation sites offer pristine environments, above lower tropospheric temperature inversions and pollutants, where long-term observations can be made without the inevitable uncertainties imposed by air quality degradation at lower elevations. Solar power is often abundant. In some locations (e.g., astronomical observatories, ski areas), very high elevation sites are easily accessible, and power and other infrastructure exists that could provide support for climate reference stations. In some extratropical locations, high elevation observatories were established in the late 19th or early 20th centuries (e.g., Pic du Midi, Sonnblick, Jungfraujoch), providing long-term data against which modern observations can be compared.

Establishing a network of high elevation climate stations is advocated, following the U.S. Climate Reference Network (USCRN) concept. Such a network would extend along a transect through the western mountains of the Americas, with supplemental stations at sites close to low latitude ice caps where paleoclimate records exist (e.g., Kilimanjaro, Quelccaya), and at selected high elevation observatories with existing long-term records. Successful operation of several observing stations since 1996 demonstrates the feasibility of such a network.

Low-Frequency Climatic Variations in the 20th Century in the Upper Colorado River Basin: Teleconnections With the North Pacific?

Hugo G. Hidalgo-Leon
Department of Civil and Environmental Engineering, UC Berkeley
(now at Scripps Institution of Oceanography, La Jolla, CA)

Historical records and paleoclimatic information obtained from tree-ring data were used to characterize multidecadal to centennial oscillations in the Upper Colorado River Basin (UCRB).

The analysis showed that the Pacific Decadal Oscillation (PDO) and UCRB's streamflow present a strong ~20 year cycle from 1660 to approximately the last third of the 19th century, and a tendency towards lower frequencies (multidecadal to centennial) during the 20th century.

We also identified a period dominated by low-frequency variations that occurred around 1550 to 1650. This period contains the most severe drought in terms of water allocation in the UCRB identified through tree-ring reconstructions. At this moment it is uncertain if the two epochs of low-frequency streamflow variations respond (even partially) to similar climatic forcing mechanisms, or if the UCRB variations have a corresponding period of low-frequency PDO variability. The role of anthropogenic influences in these variations is also not clear at this moment and requires more research, but the lower PDO frequencies observed in the more recent epoch of low frequency variations, seem to have moderate spectral power at the end of the 19th century and throughout the 20th century, suggesting that part of this mechanism is related to natural climate variability.

The tendency towards lower frequency streamflow variations in the basin in the 200 suggests an increase in the risk of severe and sustained droughts compared to the previous 200 years, especially if some of the climatic forcing mechanisms responsible for the late 1500 drought are a reflection of a natural mode of variation of the ocean-atmosphere system.

Paleoclimate in San Francisco Bay and Its Watershed: What Do We Know and What Do We Need to Know?

B. Lynn Ingram[1,2], Frances Malamud-Roam[1], Malcolm Hughes[3], and Joan Florsheim[4]
[1] Department of Geography, U.C. Berkeley
[2] Department of Earth and Planetary Sciences
[3] Laboratory of Tree-Ring Research University of Arizona
[4] Geology Department, U.C. Davis

The San Francisco Bay and its Watershed is a focus for paleo-climate research because it contains sedimentary and tree ring evidence of past climate conditions spanning much of the Holocene, and because this evidence reflects climate over a large portion of the state of California. Investigation of paleo-climate in San Francisco Bay and its watershed provides a means of extending relatively short historical records documenting climate variability and change. Initial comparison of paleo-climate proxy records from the Sierra through the Central Valley lowland rivers to the Bay Delta and Estuary illustrate effects of climate changes that influence upstream watershed hydrology as well as downstream sea level and estuarine salinity. We review of paleo-climate records from the Bay Estuary, lowland floodplain rivers in the Central Valley, and from the Sierra that illustrate our approach to developing a time-line of climate variability and change in the San Francisco Bay Delta Watershed. Examples include: (1) three cores collected from the open bay, multiple cores collected from seven marshes spanning the salinity gradient of the northern reaches of the Estuary, and archeological reports from prehistoric shellmound middens. Bay records indicate that, while sea level rise over the Holocene has produced a gradual increase in salinity moving eastward in the Estuary, this trend has been punctuated by periods of higher and lower salinity that are attributable to changes in regional precipitation. Marsh records reveal how changes in water salinity in the Estuary affected vegetation patterns, linking the physical and the biological systems. These records are compiled and compared with paleo-climate records from the larger San Francisco Bay-Delta watershed and from sites outside the watershed such as: (2) sediment records illustrating geomorphic variability in lowland floodplain rivers in the Central Valley; (3) Sierran lake records; (4) tree-ring derived records of past flow rates of the Sacramento River and (5) selected coastal sedimentary records (e.g., Santa Barbara Basin). This comparison reveals that the range of natural variability in California climate has included periods of prolonged drought, as well as wetter periods. However, while evidence for such droughts or floods is present in some records, it is absent or asynchronous in other records.

Determining Long-Term Water Quality Change in the Presence of Climate Variability: Lake Tahoe (USA)

Alan D. Jassby
Dept. Environmental Science and Policy, University of California, Davis, CA

Water transparency (measured as Secchi depth) is still occasionally over 40 m at Lake Tahoe, but average annual transparency has declined nearly 10 m since 1967, prompting a large-scale restoration program. Year-to-year variability is extremely high, however, obscuring restoration actions and compliance with water quality standards. We developed a time series model of water clarity for Lake Tahoe that incorporated a mechanistic understanding of interannual variability with sufficient simplicity to allow data-based parameter estimation. The model focused on Secchi depth during summer, when the lake is least transparent and most heavily used. Interannual variability for the summer season is driven almost entirely by precipitation differences. The model offers a means for determining compliance with water quality standards when precipitation anomalies may persist for years. As demonstrated by an *ex post* forecast, increasing Secchi depths during 1999-2001 were simply climate-driven and do not represent a recovery of the lake. The long-term trend for summer is most likely due to the accumulation of allochthonous mineral suspensoids.

A Mesoscale Modeling and Assimilation Study of the Role of Snowpack on Climate Variability in the Sierra Nevada Region

Jiming Jin and Norman L. Miller
Lawrence Berkeley National Laboratory, Berkeley, California

The Penn Sate-National Center for Atmospheric Research fifth-generation Mesoscale Model (MM5) driven by a 6-hourly reanalysis dataset from the National Centers for Environmental Prediction has been used to study the impact of snowpack on climate variability and the mechanisms of snowmelt

over the Sierra Nevada region. The analyses of a one way nested 48 km to 12 km model run during the 1998 snowmelt season (April-June) showed that the underestimated snowpack resulted when there was stronger precipitation and higher temperature. An observed daily snowpack dataset collected from the automated Snowpack Telemetry system was assimilated in the model to improve its performance. The results showed that the assimilation processes greatly reduced the warm bias because the energy used to increase the temperature in the original model run was consumed by snowmelt. The cooled surface led to a more stable simulated atmospheric structure, reduced the intensity of spring storms, and therefore, suppressed the exaggerated precipitation. In the meantime, both atmospheric and land-surface conditions affected the snowmelt rate in the region studied. The faster snowmelt positively correlated with high pressure, which resulted in stronger downward solar radiation due to fewer clouds and brought warm air from the tropical Pacific Ocean to the region. The variation of vegetation fraction also strongly affected the snowmelt because it modified surface albedo and changed the radiative forcings on the snow surface. However, the exaggerated snowmelt was produced by the land-surface model in the version of MM5 used in this study because of the lower simulated surface albedo and the neglect of the effects of vegetation fraction on snowmelt. Thus, a realistic physically based land-surface scheme in a meso-scale model is crucial to predictions of snowmelt, which is essential to the climate variability and water resources in the Sierra Nevada region.

Elevational Dependence of Hydrologic Response to Projected Sierra-Nevada Warming

Noah Knowles
U.S. Geological Survey, Menlo Park

California's primary hydrologic system, the San Francisco estuary and its upstream watershed, is vulnerable to the regional hydrologic consequences of projected global climate change. Previous work has shown that a projected warming would result in a reduction of snowpack storage leading to higher winter and lower spring-summer streamflows and increased spring-summer salinities in the estuary. The present work shows that these hydrologic changes exhibit a strong dependence on elevation, with the greatest loss of snowpack volume in the 1,300-2,700 m elevation range. Exploiting hydrologic and estuarine modeling capabilities to trace water as it moves through the system reveals that the shift of water in mid-elevations of the Sacramento river basin from snowmelt to rainfall runoff is the dominant cause of projected changes in estuarine inflows and salinity. Additionally, although spring-summer losses of estuarine inflows are balanced by winter gains, the losses have a stronger influence on salinity since longer spring-summer residence times allow the inflow changes to accumulate in the estuary. The changes in inflows sourced in the Sacramento River basin in approximately the 1,300-2,200 m elevation range thereby lead to a net increase in estuarine salinity under the projected warming. Such changes would impact ecosystems throughout the watershed and threaten to contaminate much of California's freshwater supply.

Effects of Pacific Decadal Oscillation on Streamflow In the Feather River Basin, California

Kathryn Koczot and Michael Dettinger
U.S. Geological Survey, San Diego, CA

The timing of maximum monthly streamflow for the Feather River in northern California has come earlier in the year in recent decades (since the 1950s), as have timings in most rivers throughout California and the western United States. Much of the timing shift in the Feather River basin appears to coincide with interdecadal changes in the North Pacific climate regime. The coincident timing changes are seen as a shift in the month of maximum streamflow from April-May during the cooler Pacific Decadal Oscillation (PDO) phase to March-April during the warmer phase. Specifically, reconstructed "natural" streamflow in Lake Oroville at the foot of the river basin has peaked earlier on average during the recent warm (1977-1998) phase of PDO, whereas during the preceding cooler (1949-1976) PDO phase, flows peaked later. In an earlier warm PDO phase, from about 1925 to 1947, Feather River flows also peaked earlier on average. The earlier peak flows are consistent with warmer winters and springs during the warm PDO phase, which yielded more precipitation as rain and earlier snowmelts, and the later peak flows are consistent with less rain and later snowmelts during the cool PDO phase.

The change in streamflow timing in the Feather River basin became an issue during the construction of watershed models, when the performance of the watershed models degraded in simulations of maximum monthly flows during the most recent years (1998-2001). The model calibration period (1971-1997) was dominated by the warmer (1977-1998) PDO phase. More recent simulations, representing the 1998-2002 period, include years in a newly re-established cool PDO phase, which began in late 1998. Simulations of flows during this most recent period have failed to reproduce streamflow timing as well as during the earlier calibration period, probably reflecting some unaccounted shifts in the balance between rainfall and snowfall on this middle-elevation basin. Overall model performance for recent years could be improved by calibrating a second set of models to the cooler PDO phase.

Hydrologic Changes of Salton Sea During the Late Holocene: Evidence from Radiocarbon Dated Isotopic Records

Hong-Chun Li[1], Teh-Lung Ku[1], H. Paul Buchheim[2], and Xiaomei Xu[3]
[1] Department of Earth Sciences, University of Southern California, LA, CA
[2] Department of Natural Sciences, Loma Linda University, Loma Linda, CA
[3] Department of Earth System Science, University of California, Irvine, CA

We have obtained 135 pairs of $\delta^{18}O$ and $\delta^{13}C$ analyses on a 26-cm long pipe core collected from the depocenter of Salton Sea, California. The core represents a sedimentation spanning the past ~110 years as estimated from fallout ^{137}Cs and other criteria. Sedimentary and isotopic features show four readily distinguishable intervals of varied hydrological history of the lake. Between the depths of 26 and 20 cm, the sediments are laminated, and their carbonates show large and positively correlated changes in $\delta^{18}O$ and $\delta^{13}C$. The $\delta^{18}O$ ranges from -2.34 to -6.42‰ (PDB) and the $\delta^{13}C$ from -1.67 to 1.76‰, indicating the existence of a relatively small closed lake under natural conditions. Between

20 and 14 cm, the sediments are fine-grained and uniform in texture, with average $\delta^{18}O$ and $\delta^{13}C$ values of -5.04±0.28‰ and 0.68±0.35‰, respectively. The light and relatively constant isotopic values as well as the homogenous nature of the sediments suggest deposition during the AD 1905-1907 flood years when the Colorado River drained into Salton Sea. From 14 to 9 cm depths, the $\delta^{18}O$ increased from ca. -5.6 to -2.6‰ corresponding to a decline of the lake level as the Colorado River returned to its earlier course after the flooding. Within this interval, the $\delta^{13}C$ shows an opposite trend to that of the $\delta^{18}O$, and its values decrease by about 2‰ perhaps reflecting the result of agricultural irrigation. The well-laminated top 9-cm part of the core shows average $\delta^{18}O$ and $\delta^{13}C$ of -2.95±0.39‰ (PDB) and -1.68±0.30‰, respectively. The heavy and relatively constant $\delta^{18}O$ values infer a high salinity of the lake whereas the light and constant $\delta^{13}C$ values reflect the impact of human activities. A comparison of the $\delta^{18}O$ record with the measured lake-level record strongly suggests that the $\delta^{18}O$ in lake deposits can be used as an indicator for hydrological changes in Salton Sea.

A carbonate shell sample collected from massive barnacle shell deposits on modern shoreline of Salton Sea (ca. 1940-50) has an AMS ^{14}C age of 210 yr BP, and $\delta^{18}O$ and $\delta^{13}C$ values of -1.8 and -0.57‰, respectively, which are close to the isotopic values of modern sediments in Salton Sea. The age of the sample indicates that the reservoir effect on the radiocarbon date is of minor magnitude even under the saline condition of the modern lake water. Three gastropod samples from tufa deposits collected from the highest shoreline of Lake Cahuilla (ancient Salton Sea) at Travertine Rock in the Salton Trough were dated at 1,505 to 1,720 ^{14}C yr BP. The $\delta^{18}O$ of these gastropods ranges from -6.72 to -8.13‰, and the $\delta^{13}C$ varies from -3.89 to 0.25‰. These results indicate the presence of a large, overflowing lake in the Salton Trough about 1,500 ^{14}C yr ago. Whether the formation of this large lake was due to a change in climate or to a tectonic disturbance in the Colorado River drainage basin remains to be studied.

Pacific Teleconnections and Fire in the Western United States: 1700-1900

Jeremy S. Littell[1] and David L. Peterson[2]
[1] College of Forest Resources, University of Washington, Seattle, WA
[2] USDA Forest Service, Pacific Northwest Research Station, Seattle, WA

Fire regime in forest ecosystems in the U.S. Mountain West has been widely described. However, the relationship between pre-settlement fire regimes and ocean/atmosphere controls of drought in the western U.S. has been documented only for the Southwest. We present an analysis of two aggregate fire history databases: one from the Pacific Northwest (PNW) and Northern Rockies (NR) and one from the Southwest (SW) United States. Both databases cover the period 1700-1900 AD and are based primarily on fire histories derived from fire-scarred trees. We used superposed epoch analysis (SEA) to relate large fire years to known Pacific drivers of climatic variability in the western U.S. The 5% largest fire years (those years recorded most frequently in the fire scar record) in the SW are clearly related to the Southern Oscillation (SO), but the relationship between drought and fire in the PNW and NR is more complex. The 5% largest fire years in the PNW and NR are related to the SO, the Pacific Decadal Oscillation, or both. We employed evolutive multi-taper time series analysis to examine tree-ring estimates of precipitation or Palmer Drought Severity Index (PDSI) from both regions. Our results suggest that regional differences in fire regime between the SW and the PNW/NR are at least partially a function of differences in temporal concentration of variability in the climatic mechanisms that drive precipitation in these regions. Given the regional differences in the

frequency of drivers of drought, expected fire return intervals in the PNW/NR are likely to be longer and more variable than those in the SW.

Soil Moisture in the Alpine and Sub-Alpine, Niwot Ridge, Colorado

Mark Losleben[1], Kurt Chowanski[1], and Timothy Bardsley[2]
[1] Mountain Research Station, University of Colorado, Nederland, CO
[2] National Resources Conservation Service Snow Survey, Salt Lake City, UT

Soil moisture conditions are important to most aspects of life in the western United States, and wherever moisture is a limiting factor. It impacts, and is impacted by, snowmelt, run-off, streamflow, reservoir storage, vegetation type and cover, forest fire frequency and intensity to name a few. We present daily field soil moisture data for two and one half years, and coincident soil temperature and precipitation events, at three locations on Niwot Ridge, Front Range, Colorado; two in the alpine tundra, and one in the sub-alpine forest below.

The principle of operation for the volumetric soil moisture sensors is to detect change in the relative permittivity of water, the main variant in soil. The permittivity between liquid and solid water varies by a factor of about 18, resulting in great apparent contrasts in both absolute value and variability between frozen and unfrozen soil states. To create a homogeneous data set across seasons, we investigate two standardization schemes, and present lab test results comparing frozen and liquid states. This is important in part, because it has been reported by others that frozen soil moisture conditions are far from invariant.

Results include a time series of soil moisture conditions generally high during spring snow melt, a gradual drying throughout the summer, punctuated by precipitation events, and lower variability in the winter at all three locations. The contrast between the drier year 2002 soil moisture conditions and the wetter year 2001 is more apparent at the lower elevation site than in the alpine tundra. Intra-seasonal variability is also clear and variable from year to year.

Spatial and Temporal Variability in Snowpack Controls: Two Decades of SnoTel Data from the Western United States

Mark Losleben[1] and Nicholas Pepin[2]
[1] Mountain Research Station, University of Colorado, Nederland, CO
[2] Dept. of Geography, University of Portsmouth, Portsmouth, UK

Snowpack is a crucial, and often primary, water resource in much of the western U.S. Thus, its variability and sensitivity to changes in climate are important issues. We attempt to describe characteristics of snowpack development related to these issues. Toward this end, two indices are developed for this study. First, a snowpack index (SI) to evaluate the role of non-precipitation factors in snowpack development. The SI is derived from the percent of average SWE and cumulative precipitation on April 1. The second index, FASTDIF, is the difference between surface and derived elevationally equivalent free air temperatures for the same locations as the SnoTel sites. The snowpack index eliminates the variability in snowpack development related to precipitation, and the FASTDIF

suggests changes in surface to free air feedback processes (radiation balance and related factors, for example).

The spatial scope of this study is the mountainous western U.S., reported both as a whole unit and also eight separate mountain sub-regions. We will present April 1 SWE (snow water equivalent), cumulative winter precipitation, and maximum and minimum October 1- April 1 temperatures using SnoTel data from several hundred sites for 1979-99.

Our presented results include trends in snowpack, precipitation, the SI, FASTDIF, and temperature. Results showing variability over time and by elevation of these parameters, and absolute values of SWE and precipitation are also presented. These results show:

- All SI trends are negative (95% sig. level), meaning an increase in factors detrimental to snowpack development under conditions of constant precipitation. These negative trends are greatest in the Arizona mountains followed by northern NM/southern Colorado, Oregon/Washington and Utah (tied), the western U.S. as a whole, and Colorado.
- Trends in minimum October 1-April 1 temperature (95% sig. level) are increasing in the mountains of northern NM/southern CO, Idaho/Montana, Utah, and the west as a whole.
- Maximum temperatures are also increasing in mountainous California, northern NM/southern CO, and Utah, and decreasing in Oregon/Washington
- Variability in SWE and cumulative winter precipitation are greatest near the Pacific coast (California, Oregon, Washington most variable), and least inland (Wyoming, Colorado, eastern Montana least variable).
- SI varies more by elevation in Colorado, and at the higher elevations of California and Wyoming, and more over time in mountainous Arizona, northern New Mexico/southern Colorado, Oregon/Washington, and the lower elevations of California and Wyoming.
- Less distinct patterns of variability are seen in the Utah and Idaho/Montana mountains.

These results may identify mountain snowpacks vulnerable to non-precipitation changes in climate and surface/free air feedback mechanisms. In this regard, the more vulnerable snowpacks appear to be in the mountains of Arizona/southern NM and Oregon/Washington, whereas the less vulnerable snowpacks are in the mountains of Wyoming and northern Colorado.

Meteorology and Hydrology in Yosemite National Park: A Sensor Network

Jessica D. Lundquist[1], Daniel R. Cayan[1,2], and Michael Dettinger[2]
[1] Scripps Institution of Oceanography, La Jolla, CA
[2] U.S. Geological Survey, Scripps Institution of Oceanography, La Jolla, CA

More than half of California's water supply comes from high elevations in the snowmelt-dominated Sierra Nevada. Natural climate fluctuations, global warming, and the growing needs of water consumers demand intelligent management of this water resource.This requires a comprehensive monitoring system within and across the Sierra Nevada. Unfortunately, because of severe terrain and limited access, few measurements exist. Thus, meteorological and hydrologic processes are not well understood at high altitudes. However, new sensor and wireless communication technologies are beginning to provide sensor packages designed for low maintenance operation, low power consumption, and unobtrusive footprints. A prototype network of meteorological and hydrological sensors has been deployed in Yosemite National Park, traversing elevation zones from 1,200 to 3,700 m. Communication techniques must be tailored to suit each location, resulting in a hybrid network of radio, cell-phone, land-line, and satellite transmissions. Results are showing how, in some years, snowmelt may occur quite uniformly over the Sierra, while in others it varies with elevation.

Is Sierra Nevada Snowmelt Independent of Elevation?

Jessica D. Lundquist[1], Michael D. Dettinger[2], and Daniel R. Cayan[1,2]
[1] Scripps Institution of Oceanography (SIO), UCSD, La Jolla, CA
[2] U.S. Geological Survey, La Jolla, CA

Recent studies have shown that USGS-monitored rivers draining the Sierra Nevada and Rocky Mountains rise and fall with great simultaneity each spring, suggesting an organized signal of snowmelt initiation and runoff across the region. These are all large basins (over 100 km^2), spanning broad ranges of aspect and elevation. Recent data from subbasins of the Tuolumne and Merced Rivers in Yosemite National Park, from small lake basins throughout the Sierra Nevada Mountains, and from California Department of Water Resources (DWR) snow pillows throughout the central Sierra Nevada suggest that, in many years, this simultaneity extends to subbasins within the range. For example, in 2002, streams from even small high-altitude glacial cirques rose at the same time as much larger basins gauged at lower altitudes, and streams from north- and south-facing cirques rose and fell together.

Elevation and aspect exert strong influences on air temperature and solar radiation, but often the influence of synoptic weather systems is stronger. Synchronous snowmelt initiation, so named when 90% of DWR snow pillows across the central Sierra Nevada recorded maximum snow accumulation and melt initiation within five days of each other, occurred in four out of eleven springs between 1992 and 2002. These springs are characterized by strong, cold winter storms that persist into March or April. When the storms finally cleared, rapid temperature rises averaging more than +10 °C, combined with dry, easterly winds, marked clear transitions between winter and spring in basins throughout the range. In the other, non-synchronous years, periods of little or no storm activity preceded the onset of spring snowmelt, allowing elevation and aspect to play a role as spring arrives gradually.

700-Hectopascal Atmospheric Circulation Patterns Associated With Winter Precipitation in the Yellowstone Region

David L. McGinnis[1], Gregory J. McCabe[2], and Heather K. Conley[3]
[1] Department of Geosciences, Idaho State University, Pocatello, ID
[2] U.S. Geological Survey, Water Resources Discipline, Denver, CO
[3] Department of Geography, University of Iowa, Iowa City, IA

The northern Rocky Mountains, and in particular, the Greater Yellowstone Area (GYA), is an important headwater area for many western rivers. Streamflow in this region is highly dependent on winter precipitation and resultant snowpack accumulations. The magnitude and extent of snowpack accumulations in this region are controlled by the sequence and variability of regional atmospheric circulation patterns. This research uses Kohonen Self-Organizing Maps (SOMs), a neural-network based pattern classification methodology, to create a synoptic climatology of 700-hectoPascal (700hPa) patterns for the western United States. The resulting climatology of 700hPa patterns is used to explain temporal and spatial variability in winter precipitation in the GYA. The temporal frequencies of 700hPa patterns as well as variability in winter precipitation are related to variability in climate indices (teleconnections) and changes in storm track locations.

Extracting Seasonal Precipitation Signal from Tree-Ring Width

David M. Meko and Christopher H. Baisan
Laboratory of Tree-Ring Research, University of Arizona, Tucson, AZ

Marker features within the annual rings of some tree species allow the portions of annual growth to be approximately assigned to different parts of the calendar year. For conifers in the semiarid parts of Mexico and the southwestern United States, “earlywood” and “latewood” width components are significantly correlated with precipitation in the cool season and warm season preceding the end of the growth year. Analysis of daily precipitation data and tree-ring indices of Douglas-fir shows that seasonal precipitation in southeastern Arizona can be reconstructed much more accurately from partial-width indices than from total-width index. The gain in accuracy is considerable for cool-season precipitation (R^2=0.50 vs R^2=0.64), but is remarkable for the warm season (R^2=0.02 vs R^2=0.53). Moreover, partial-width chronologies offer the advantage of circumventing the probable confounding effects of a marked age trend observed in the proportion of earlywood in the annual ring. The age trend is described for a data set of merged new and previous collections from the Santa Rita Mountains, southern Arizona.

A 7,000-Yr Record of Climate Change Reconstructed from Pyramid Lake, Nevada

Scott A. Mensing
Dept. of Geography, University of Nevada, Reno, NV

Closed basin lakes along the eastern Sierra Nevada Range, including Pyramid Lake, preserve a record of lake level fluctuations associated with wet and dry climatic episodes. Whereas Pleistocene Lake levels are recorded in wave-cut terraces and lake deposited tufas above the modern shoreline, the Holocene climate record is preserved exclusively in the sedimentary record. Pyramid Lake is the only large closed basin lake in the western Great Basin to have not dessicated during the Holocene. For this reason, it is an ideal site to reconstruct Holocene climate change.

Three sediment cores spanning the last 7,500 calendar years (cal yr BP) were analyzed for pollen at decadal to century-scale resolution. Climatically dry periods were interpreted from the ratio of Chenopodiaceae (saltbush) pollen in relation to *Artemisia* (sagebrush). This ratio suggests that the mid-Holocene (7,500-6,300 cal yr BP) was the warmest and driest portion of the record. Beginning about 6,300, there is a gradual but erratic increase in precipitation that continues as a generally wetter climate through 3,500 cal yr BP. A return to very dry conditions is seen between 2,500-1,800 years

ago. The last 1,800 years have seen repeated dry episodes, however none as extensive as the earlier periods. The Pyramid Lake record supports the evidence for prolonged droughts centered at ~800 and ~600 cal yr BP identified from submerged stumps at Mono Lake and Fallen Leaf Lake. These results are compared with the $\delta^{18}O$ and magnetic susceptibility records from Pyramid Lake, the tree-stump record of Lake Tahoe, and packrat midden data from the central Great Basin.

Responses of High-Elevation Pines in the Eastern Sierra Nevada and Western Great Basin to Late Holocene Decadal- and Century-Scale Climate Variability

Constance I. Millar[1], Robert D.Westfall[1], Diane L. Delany[1], John C. King[2], and Harry Alden[3]
[1] USDA Forest Service, PSW Research Station, Albany, CA
[2] Lone Pine Research, Bozeman, MT
[3] The Smithsonian Institution, Suitland, MD

We present results from a series of ongoing studies of high-elevation pine ecosystems in the eastern Sierra Nevada and western Great Basin ranges that demonstrate forest response to past climate changes at decadal- and century scales. Using standard tree-ring and ecological analysis methods, we document 20th century growth responses in krummholz *Pinus albicaulis* at treeline and invasion of meadows and formerly persistent snowfields by *P. albicaulis*, *P. contorta*, and *P. monticola* that correlate with climate. Responses range from progressive trends throughout the century to episodic and reversible responses that appear triggered by threshold conditions. These responses correlate complexly with decadal trends in minimum temperature, PDO indices, and precipitation. Century- to millennial-scale growth variability of *P. flexilis* forests over the past 3,500 years correlates with major temperature and precipitation patterns derived from various proxies. Repeating extirpation and recolonization events at the watershed scale in *P. flexilis* correlate with neoglacial, medieval, little ice age, and 20th century periods, with periods of extirpation during extended droughts. Implications of climate variability to vegetation dynamics has not been integrated into conservation analysis and planning, and as a result, misdiagnoses of ecological condition and misapplication of management treatments have occurred.

Development and Limitations of Transfer Functions Used to Reconstruct Air Temperatures from Ice Cores, Wind River Range, Wyoming

David L. Naftz[1], David D. Susong[1], Paul F. Schuster[2], L. Dewayne Cecil[3], and Michael D. Dettinger[4]
[1] U.S. Geological Survey, Salt Lake City, UT
[2] U.S. Geological Survey, Boulder, CO
[3] U.S. Geological Survey, Idaho Falls, ID
[4] U.S. Geological Survey, San Diego, CA

Continuous ice cores exceeding 160 meters (m) in length were collected at altitudes greater than 4,000 meters from Upper Fremont Glacier (UFG) in northwestern Wyoming. Detailed chemical and isotopic analyses of these cores have resulted in a unique record of environmental change in the western United States since the early 1700s. Site-specific transfer functions relating delta oxygen-18

($\delta^{18}O$) values in snow to the average air temperature (T_A) during storms on UFG were determined using data collected from four seasonal snowpacks (1989-90, 1997-98, 1998-99, and 1999-00). The timing and amount of precipitation from each storm was measured at an automated snowpack telemetry (SnoTel) site in proximity to UFG. Statistically significant and positive correlations between $\delta^{18}O$ values in the snow and T_A were consistently observed in three of the four seasonal snowpacks. The snowpack with the poor correlation ($R^2 = 0.11$, $p = 0.14499$) was deposited during the 1997-1998 El Niño Southern Oscillation (ENSO), indicating that the $\delta^{18}O$ values in snowfall may also be sensitive to major shifts in moisture sources. An ultrasonic snow-depth sensor installed on UFG provided a continuous record of snow accumulation and removal from September 1999 through April 2000. For the same time period, the transfer function (relating $\delta^{18}O$ to T_A) derived from the snow depth sensor record was different than the transfer function (relating $\delta^{18}O$ to T_A) developed from the SnoTel data. Differences between the transfer functions were caused by early season wind-removal of snow, resulting in a seasonally biased snowpack. Transfer functions derived from seasonal snow cover on UFG are used to reconstruct T_As from $\delta^{18}O$ values determined from two ice cores containing continuous precipitation records that accumulated during the last 300 years.

Assessment of Environmental Influences on California Commercial Fish and Invertebrate Landings

Jerrold G. Norton and Janet E. Mason
Pacific Fisheries Environmental Laboratory, SWFSC, NMFS

Records of the commercial harvest of fish and invertebrates landed in California ports, compiled by the State of California Department of Fish and Game from 1928 to 2001, have been converted from printed documents to computer accessible formats (CACom) at the Pacific Fisheries Environmental Laboratory (PFEL/SWFSC). These data were examined for fluctuations indicating environmental influence on the catch composition. CACom data series for 1930-2000 were standardized to give species and species groups similar weighting in Empirical Orthogonal Function (EOF)-analysis. The CACom data have considerable persistence (autocorrelation). Environmental indices which show persistence in ocean processes were developed from published data sets by accumulating anomalies from long-term means. Correlation coefficients larger than 0.6 between CACom EOFs and environmental series, strongly suggest linkages between variables. Distinct changes in species composition, occurred during the 1958-1961 warm interval and in the period since the mid-1970s. CACom species composition was also altered in response to the 1982 and 1997 El Niño events. Treatment of landings series as ensembles of species and species groups in EOF-analysis reduces the effects of inconsistent species designation. Shorter-termed harvest events may be smoothed by market factors and the longevity of harvested species, but larger-scale, longer lasting environmental events are clearly evident in the relative species composition. Although not adjusted for fishing effort, overall there has been net decline in the pounds of finfish landed, and invertebrates have made up an increasing percentage of the total pounds landed since the mid-1970s.

A Comparison of Free-Air and Surface Temperature Trends at High Elevations in the Mountainous West of the U.S.

Nicholas C. Pepin[1], Mark Losleben[2], and Mike Hartman[3]
[1] Department of Geography, University of Portsmouth, U.K.
[2] Mountain Research Station, University of Colorado
[3] Cooperative Institute for Research in Environmental Sciences, Boulder, CO

Reconciling differences between past surface and free-air (satellite and radiosonde) temperature trends concerns the international scientific community. There is an apparent discrepancy between glacier melting at high elevations and the lack of strong warming in the upper troposphere, especially in the tropics. Free-air temperature changes may not be the same as on high elevation mountain surfaces. This research examines the difference between temporal trends in surface temperature observations at high elevation based on SnoTel (snow telemetry) data and simultaneous free-air equivalent temperatures, interpolated vertically and horizontally from NCEP/NCAR reanalyses. Daily comparisons are examined from 1982 to 2000 using a database of 76 stations in the western states of the U.S. Trends in the free-air/surface temperature difference (FASTDIF) are examined as well as surface and free-air temperatures separately. Systematic annual and monthly changes in FASTDIF are revealed, but the sign and magnitude of change depends on location. Trends are mapped and compared with terrain factors such as exposure, aspect, continentality and elevation. Such changes in the free-air/surface temperature difference over the 20-year period are indicative of changes in the energy balance of high mountain areas, relating to trends in snow cover, amongst other variables. Thus free-air changes are not always good indicators of change experienced at the Earth's surface.

Central Sierra Air Temperature, Snowmelt Discharge and River Chemistry—Monitoring, Modeling and Prediction

David H. Peterson, Richard Smith, Stephen Hager, Daniel Cayan and Michael Dettinger
U.S. Geological Survey, Menlo Park and La Jolla, CA

Merced River at Happy Isles, Yosemite National Park is an excellent location for an expanding effort linking large-scale atmospheric circulation to snowmelt discharge (SMD) and river chemistry. Although the advantages of this location are too numerous to list, a few examples are: (1) the alpine river discharge record is long, 1916 to present; (2) the air temperature variations are large scale and strongly covary with SMD; and (3) the SMD-driven variations in river chemistry are large. Further, knowing the hydrologic response of this region to climate variability and change is important to scientists and managers.

More than 85% of the annual Merced River flow at Happy Isles is SMD. Although SMD is a function of many variables, only snowpack and air temerature have long-term records, the focus of this study. Solar insolation, an important variable covarys with air temperature and, presumably, much of the air temperature—SMD correlation includes solar insolation effects. Two features of the seasonal SMD cycle are the spring pulse, which defines the start of the rise in SMD, and the maximum or peak SMD, which defines the start of the decline in SMD. The timing of the start of the SMD season (the spring pulse) depends more on air temperature (cool or warm) than winter snowpack (wet or dry). This pattern reverses as the SMD season progresses towards the day of

maximum discharge. All of the variations in air temperature leads (or SMD lags), from zero to a few days, appear throughout the snowmelt season. Apparently the lead/lag variations depend on the rates and durations of rising and falling air temperatures. On average, however, the lead-time between air temperature variations and the SMD response is longer near the start of the snowmelt season and fades as snowmelt progresses towards the peak SMD. This pattern is most likely caused by the seasonal increase in air temperature driven response as SMD progresses (SMD is sluggish at first). Another, but likely smaller contributing factor, is the seasonal change in the air temperature variation which begins to decrease near day 150 and the timing of maximum discharge ranges from day 111 to 182.

The results indicate many directions for future research. Perhaps the most important is that a persistent rise in air temperature before the start of the spring pulse provides an opportunity to forecast the timing of the spring pulse using forecasted air temperature out to seven days.

High Resolution Analysis of Subfossil Midges: Indicators of Fish Introduction and Climate Change in the Sierra Nevada of California

David F. Porinchu[1], Glen M. Macdonald[1,2], and Aaron P. Potito[1]
[1] Department of Geography, UCLA, Los Angeles, CA
[2] Department of Organismic Biology, Ecology and Evolution, UCLA, Los Angeles, CA

The use of subfossil chironomid remains to produce millennial to sub-centennial records of environmental change has largely focused upon the relatively rapid climatic oscillations that occurred at the close of the last glaciation and commencement of the present interglacial, e.g. Younger Dryas, Killarney Oscillation and Preboreal Oscillation. Paleolimnologists are now attempting to use chironomids to address recent environmental problems that are decadal to sub-decadal in nature. Interpreting and providing climatic estimates from subfossil chironomid records present in recently deposited lake sediments requires an understanding of the sensitivity of chironomids to both climate and more local, human induced perturbations of lake ecosystems. In the Sierra Nevada, as well as other mountainous regions in the USA, one of the largest human induced perturbations of the aquatic ecosystem involves the introduction of fish into historically fishless lakes. Many studies have documented the effects that the introduction of fish to historically fishless lakes has on aquatic ecosystem dynamics and community composition. However, there has been little work carried out using subfossil chironomid remains to assess whether the introduction of fish into historically fishless lakes compromises our ability to use subfossil chironomid remains from these lakes to develop high-resolution (decadal to sub-decadal timescale) surface-water temperature reconstructions to detect the pattern and impact of recent climatic variation.

In order to address this question, chironomid stratigraphies spanning the last 170 years from two historically fishless lakes that are located closely adjacent to each other in King's Canyon National Park, California were developed. One of these lakes, MG-2 (unofficial name) had golden trout introduced in 1963, while the other, MG-3 (unofficial name) may have had fish introduced in the late 1920s, but if fish were introduced into this lake, it is unlikely that they survived for more than a decade. Chironomid analysis reveals that there were differences in the specific chironomid taxa that were present in each lake, however, these differences existed prior to the introduction and establishment of fish in one of the lakes. Changes that occurred post-fish introduction were limited to a decrease in head capsule concentrations and a reduction in chironomid richness. Application of a chironomid-based inference model to the chironomid stratigraphies indicated that both lakes experienced similar fluctuations in surface-water temperature between AD 1830 and AD 1998. Fluctuations in the surface-water temperature of the study lakes closely tracked fluctuations in mean July air temperature in Fresno, California, during the period AD 1895 to AD 1998. The similarities in the reconstructed temperatures for both lakes, and the air temperature data from Fresno, suggest that high elevation lakes in the Sierra Nevada can be used to develop high-resolution reconstructions of recent climate change.

High Resolution Time-Series of the Younger Dryas Cold Event in the Eastern Sierra Nevada, California

Aaron P. Potito[1], Glen M. Macdonald[1,2], and David F. Porinchu[1]

[1] Department of Geography, University of California, Los Angeles, CA

[2] Organismic Biol. and Evol. Ecol., University of California, Los Angeles, CA

The Younger Dryas climate oscillation was a distinct and sudden cooling event that occurred due to massive drainage of glacial meltwater into the North Atlantic during the Pleistocene-Holocene transition (~11,000 to 10,000 yr BP). The cold freshwater input into the North Atlantic disrupted ocean circulation and caused cooling in many regions of the northern hemisphere, briefly reversing the warming trend that was prevalent at this time. There is evidence that the Younger Dryas event resulted in cooler sea surface temperatures in the eastern North Pacific, leading to a drier western North America and California. However, the timing, magnitude, and nature of the impact in California are not well known. More specifically, the effect of the Younger Dryas climate oscillation on temperatures in California needs to be more fully understood.

A paleolimnological approach is employed in an attempt to resolve this problem. Lake sediments from the Pleistocene-Holocene transition in five lakes in the Eastern Sierra Nevada were dated, and sediment was analyzed. Loss-on-ignition analysis was performed to help determine the extent of the Younger Dryas in each core. A high-resolution, quantitative reconstruction of July surface water temperatures was conducted by investigating the dynamics of chironomid (midge fly) assemblages in the lake sediments over time. A previously formulated transfer function for chironomids in the Eastern Sierra Nevada was applied to quantitatively relate changes in chironomid assemblage to surface water temperature changes throughout this time period. All five of the lakes exhibited a response to the Younger Dryas cold event. The lower elevation lakes showed the most dramatic response, with one of the lakes exhibiting a 4.5 °C drop in inferred July surface water temperature. The evidence displayed by these chironomid reconstructions implies that there was a widespread cooling in the Eastern Sierra Nevada during the Younger Dryas climate oscillation.

Fire and Vegetation Variations of the Last 4,000 Years in Northwestern Montana

Mitchell J. Power, Cathy Whitlock, and Patrick Bartlein
Department of Geography, University of Oregon, Eugene, OR

A laminated sediment core from Foy Lake, Montana, provides annual-to-decadal-scale resolution of landscape change over the last 3,800 years. Sedimentary charcoal and pollen analyses were used to document fire and vegetation changes of the last 120 years and compare them with those of the late Holocene. The 1910 fires burned over two millions acres in Idaho and Montana and charcoal from these extralocal fires is present at Foy Lake. No other fire event is recorded in the sediments of the 20th century. The pollen record indicates an increase in shrubs and grasses from 1895 to 1960 as a result of vegetation changes caused by timber harvesting and livestock grazing. During the last three decades, the effects of fire suppression and a shift towards parkland forests are also observed in the pollen and charcoal record. In comparison, the long-term record at Foy shows variability that likely reflects variations in vegetation and fire regime due to climate change. Fire activity (inferred from the frequency of charcoal peaks) was initially low (averaging 6 episodes/1,000 years) from 3,800 to 2,200 cal yr BP. It increased from 7 episodes/1,000 years at 2,200 cal yr BP and reached 14 episodes/ 1,000 years at 800 cal yr BP. Fire episodes were at a maximum of 21 episodes/1,000 years at ca. 500 cal yr BP and then decreased to present levels of 14 episodes/1,000 years. The level of charcoal for the 1910 fires is not anomalous when compared with charcoal peaks (fire episodes) from the prehistoric record. The pollen record suggests an open forested landscape prior to 2,200 cal yr BP. Between 2,200 cal yr BP and 800 cal yr BP the forest was more closed or widespread and after 800 cal yr BP the vegetation began to resemble the modern parkland. Changes in both the pollen and charcoal records for the Late Holocene are coincident in time, suggesting a temporal linkage of vegetation and fire that is ultimately controlled by climate change. A comparison of landscape changes during the last century with those of the late Holocene suggests that the recent changes in forest and fire regime during the period of Euro-American land-use exceed anything that occurred in the last 3,800 years. The forest parkland that exists at Foy Lake at present in the face of fire suppression is not unlike those that existed prior to the arrival of Euro-Americans about 150 years ago.

The Western Weather and Climate of PACLIM Year 2002-2003

Kelly T. Redmond
Western Regional Climate Center

After a four year recovery from its exhausting performance in 1997-1998, El Niño returned in summer 2002, in more or less average form. Despite expectations and moderate apprehension, the event has in western North America has thus far in its lifetime yielded only occasional gloom and not much doom. One feature of this event has been the relatively warmest water (in standardized terms) near the date line, as warm as ever recorded there. The major story of the "PACLIM Year" turned out to be widespread and severe drought as a dry spring and early summer in 2002 exacerbated in many places the effects of a dry and snow-deficient winter 2001-2002. This led to two fires of a half million acres each and overall a very active fire season. After a lackluster monsoon, autumn brought relief to parts of the Rockies, but a very slow start to the coastal precipitation season. Very wet conditions were experienced along parts of the coast in November and especially December, but they did not everywhere, or far inland, erase the deficits that had accumulated for the winter thus far. November finally ended a year and a half with cool coastal temperatures in California. January brought extremely warm conditions, far exceeding previous records, and the winter as a whole was warm in the West, cool in the East. In the Southwest, February, and to a lesser extent March, finally brought the heavy precipitation typically associated with El Niño. The overall precipitation departure pattern in the West bore only a modest resemblance to the "canonical" El Niño pattern. PDO values were quite positive during the winter of 2002-2003, a change from the past few years. Most snowpacks ended the winter below average, some well below, and the Columbia and Colorado are both forecast to deliver much reduced flows and volumes. This period of extended and extensive drought is the most severe in at least a half century, and perhaps could exceed past droughts. Because of this, the current drought will likely have lasting social and policy consequences. Late season storms in Colorado and in the northern Rockies did improve snowpacks in some basins to near average. In Alaska, the winter has been very far above average in temperature, and some coastal areas have been considerably wetter than usual. The Arctic Ocean coastline has been much warmer than average for the past six months. In Hawaii, for the winter Oahu, Kauai, and particularly the Big Island have been generally dry, with a few exceptions.

Out of Sight But Not Out of Mind: Observing the Mountains

Kelly T. Redmond
Western Regional Climate Center

Human and natural systems at low elevations depend for sustenance on water resources supplied at high elevations. Though small in spatial area, the alpine and subalpine zones are enormous in terms of importance. Numerous forms of evidence suggest that climate variability in the mountains does not necessarily mimic or parallel (and thus correlate well with) that in the nearby lowlands. Additional forms of evidence indicate that the relation between low and high elevations for precipitation can vary substantially on time scales from single winters to decades. These differences can only be illuminated by resorting to study of data sets from high altitudes, of sufficient quality. Unfortunately there are far fewer long-term reliable records from high than from low elevations. This reflects the severe atmospheric conditions, harsh environments for instruments, expense and difficulty of human access and maintenance, special problems of accurately measuring frozen precipitation (especially in large quantities), communications difficulties, and perhaps a failure to adequately recognize how important it is to have such information. No long-term baseline system exists expressly for the purpose of monitoring climate variability and detecting slow and subtle changes in this important water supply region. Recent studies show strong societal vulnerability to the water ramifications of even modest changes in temperature near the snow lines. Long felt to be a world unto themselves, technology, population pressures, and perhaps climate itself will place unprecedented stresses on mountain systems. Efforts are under way to install a national Climate Reference Network at low to mid elevations. An analogous mountain Climate Reference Network is needed at high elevations, utilizing existing and new sites, covering all major mountain ranges and regions, designed to work accurately and reliably in rugged conditions, and featuring attention to siting, maintenance and documentation. Such a network would be "Outta Sight" in both senses, but strongly in mind for managers and consumers of water and other resources.

Potential Predictability of Central Sierra Snowpack Related to Early Season Northern Pacific Ocean Swells

Temoc Rios[1], John A. Dracup[1], and Hugo G. Hidalgo[2]
[1] Department of Civil and Environmental Engineering, University of California Berkeley
[2] Scripps Institute of Oceanography, University of California, San Diego

Previous studies have shown that the potential energy—expressed by the height of the mid-troposphere, its amplitude, phases and position—in the Northern Pacific Ocean is related to snowpack variations in the Western United States. This investigation focuses on the possible correlation between winter snowpack accumulation in the Sierra Nevada and the early fall/winter arrival of long period swells from the Northern Pacific. The swell energy impinging upon the offshore waters of the western coast is an analogue to storm energy released by the Northern Pacific low pressure trough and may be a good indicator of the energy available for breakdown of the Western North American high pressure ridge. Using archived coastal and buoy data from the Army Corps of Engineers, the Coastal Data Information Program and from the National Data Buoy Center we focus on swells greater than 13 seconds in period coming from the WNW to NW directions and hitting the California offshore waters during the transition from fall to winter months (October to December). These data are related to California Department of Water Resources Sierra snowpack data from 1956 to 2001 Recently, coastal buoy data has evolved to collect frequency, spectral data and direction along with standard meteorological data, increasing the fine structure of the data available.

Water Year 2003: A Good Year in Northern California But a Non-traditional El Niño

Maurice Roos
California Department of Water Resources, Sacramento, California

This paper is a review of the 2003 water year in northern California and how precipitation, snowpack, runoff, and water storage have accumulated so far this season, with some comparisons to recent years. The water year started off with one big statewide storm in early November. December statewide precipitation was twice average, and the snowpack was over 150% of the seasonal average at the end of the month on January 1, or about 60% of the April 1 average, which is the usual date of maximum accumulation. January turned out to be less than half average except in the far north, which was wetter, especially on the Trinity River at about 80%. Many storms were unseasonably warm. By February 1, statewide seasonal snowpack percentages had dropped to average for the date and about 65% of the April 1 average. Precipitation in the southern half of the State was now less than normal. February storms were a disappointment, adding only 5% to 10% to the snowpack (about one-third of the average gain for the month) and forcing water supply forecasters to reduce the March 1 snowmelt runoff projections to about three-fourths of average. Water year runoff is expected to be about 10% better than snowmelt percentages because of the above normal winter season runoff. This is below average, but not drought levels, and somewhat better than conditions in much of the West. In-state major reservoir water storage on March 1 was near average, better in the north and less in the south and on the east side of the Sierra.

The early winter long lead seasonal forecasts for December through February had forecast a typical El Niño, that is, a wet Southwest and dry Pacific Northwest. In California, that would have meant a drier north and a wetter south, relative to normal. That did not happen; instead there was a pronounced wetter north, drier south gradient, with winter wetness extending into western Oregon. A southern storm track did develop to some extent in February. One storm on February 12 brought heavy, although not unusual, rains in the Transverse Ranges of southern California after a extended mid-winter dry spell. The moisture originated unusually far to the south at about 5 degrees north of the equator; that storm went on to produce a major snowstorm in the Northeast that Presidents' day weekend.

Temperature Monitoring at Upper Treeline Sites in the Western U.S.

Louis A. Scuderi
Dept. of Earth and Planetary Sciences, University of New Mexico, Albuquerque, NM

Alpine treeline, the transition zone between subalpine forest and alpine tundra, has long been recognized as a geographic location where tree growth is sensitively balanced between conditions too severe for growth (above treeline) and sufficient for growth (within the closed canopy of the forest). At treeline, annual growth has frequently been related to temperature during different portions of the year, and on longer time scales the position of alpine treeline has been used as a general indicator of temperature variability related to climate change. However, because of the high cost involved in continuously monitoring temperatures in this environment, most of the hypothesized mechanisms relating tree growth to climate had not been tested with appropriate temperature data from treeline or by extrapolations from distant sites. Since movement of the alpine treeline over time is commonly used as an indicator of temperature variability related to global scale climate change it is critical that we begin to document and understand the "true" relationship between climate and alpine treeline position.

Low cost temperature sensors that could be placed for extended periods of time were installed for monitoring at three sites in July 1998 and were in continuous operation until August 2001. At each site sensors were arrayed in a transect extending from approximately 50 m above treeline to 50 m below the upper forest boundary. The effort has resulted in extended records from three treeline sites in the western United States (the Sierra Nevada and White Mountains of California, and the Rocky Mountains of Colorado). Each site is also associated with established millennial length tree ring chronology from temperature sensitive species (foxtail pine- Cirque Peak, Sierra Nevada, CA; bristlecone pine- Sheep Mountain, White Mountains, CA; bristlecone pine- Mt. Evans, CO). Three to four years of data have now been collected from each site and a suitably large and representative data set now exists for analysis. A fourth site at treeline in the southern portion of the Sangre de Cristo Range of New Mexico provided one additional year of data, however the sensor array was destroyed early in the second summer by a lightning strike. A related project in Ecuador provided additional data for comparison purposes from an equatorial treeline site. Treeline elevations were at approximately 3,600 m in California and Colorado, 3,800 m in New Mexico, and 3,400 m in Ecuador.

The data set from the western United States now consists of nearly 17,000 individual temperature observations from each of three sites over a three to four year period (51,000 total plus another 5,000 observations from the New Mexico site). Data was collected four to six times a day with data collection times configured to capture minimum pre-dawn and maximum mid-afternoon air temperature. Initial analysis of this data along with analysis of existing meteorological records from surrounding weather stations suggests that some existing temperature based hypotheses about tree line formation and maintenance over time are flawed while others are supported by the collected data. The most important results to date appear to be;

1. A minimum winter temperature hypothesis which places treeline at an elevation where winter minimum temperatures fall below -40 °C (and where needles are damaged by freezing of cell water) appears to be unsupported by the collected data. Specifically, analysis of the collected data and regression analysis of this data to the records of distant weather stations suggest that during the past century tree line minimum temperatures never reached as low as -40 °C and in fact only on a few occasions reached as low as -25 °C. This temperature is well above the freezing point of water in the cells of needle leaf conifers found at tree line. However, it is possible that a minimum temperature limit treeline altitude control may be operating on a longer time scale than covered by the data analysis period (1928-2001) and may not be captured in the short historical temperature record. An alternative theory may be that the low temperature exotherm may correspond to the minimum temperature along the northern edge of the species' range. The position of treeline for all three sites appears to be the same, limited to a minimum temperature of about -25 °C and may reflect a physiological limit for the species.
2. The summer average temperature hypothesis which proposes that tree line forms at the elevation of the July 10°C mean temperature isotherm is supported by data from the western United States but is not supported by data from South American tree lines. This suggests that the hypothesis, which was originally developed for tree lines in temperate latitudes (30-50°N) may not be globally applicable and as such a summer temperature maximum threshold is probably not the "cause" of alpine tree line formation globally.

3. All sites (including Ecuador) show a significant difference between temperatures measured within the canopy (just below the tree limit) and those measured just above the tree limit. This suggests that a possible causal factor for tree lines worldwide may be the interaction between temperature decreases with rising elevation and the insolating effect (reduction of wind velocity, diurnal warming and maintenance of warmer temperatures at night, etc.) that the forest canopy produces. This aerodynamic/microclimatic view of treeline also appears to be supported by studies that suggest that isolated trees in topographic hollows above treeline can survive for extended periods of time and by the evolution of tree form from the upright trees of the closed forest stand to the aerodynamically flattened surfaces of krummholtz trees in the alpine zone.

The Way Forward from Uncertainty From Equilibrium Modeling

Gary D. Sharp[1] and Leonid Klyashtorin[2]
[1] Center for Climate/Ocean Resources Study, Monterey, CA.
[2] VNIROV, Moscow, Russia

The similarities between the arguments for and against using equilibrium modeling in climate projections or fisheries management provide a unique opportunity to argue for change in both. Methodologies that are completely or nearly completely driven by assumptions about representative sampling—rather than on understanding of complex interactions—are wrong far more often than they are correct, within acceptable error limits. Using the ever-changing observations from various of earth's surface or satellite remote sensing platforms, and extending these imperfect records backward in time, and extending their representativeness over space, has led to major quandaries about the value of global climate models in the projection of anthropogenic global warming. Similarly, the hindcast methods used to 'assess' population status, and create acceptable options for fisheries catches, have created a monster—crisis-based management—simply because of their focus on sampling landed catches, rather than on accounting for the many variables that would affect them. These uncertainties and resulting management failures usually are attributable to ignoring known indicators of either population stress, or climate-driven physical process changes that affect either distributions or early life history survival probabilities. The relatively recent acceptance that natural cycles do matter, in both fisheries and climate change, and that cycles occur on several time and space scales, has made projections more dependent upon accounting for cyclical and quasi-cyclical changes.

What is also evident is that living organisms respond to these climate-signals more directly than do those monitoring the consequences in catch/landings data. Turning the monitoring around, to face forward, indicates the need for a careful analysis of historical data sets, physical and biological, to determine the likely directions of recruitment survival, and population behavior measured by monitoring population status, i.e., fat content and growth rates, as well as distribution and abundance changes in real time. Leonid Klyashtorin's recent efforts to categorize temporal dynamics for the major fish species uncovered far more than biological implications. The Russian Arctic Institute Atmospheric Circulation Indices provide unique opportunity to track regional changes, and their peaks and bulls can be usefully forecast from direct geophysical observations, such as the Earth's rotation rate – several years in advance. Thus, they provide insights about when and how to focus sampling within and among the species, so as to best determine population states and trends. These activities, in turn, provide more adequate information about the state of the critical global environment, on more realistic time and space scales, so that Earth's climate trends can also be assessed. Examples will be provided.

Glacial and Interglacial Patterns in the Devils Hole, Nevada, Record: Are We Currently in Marine Isotope Stage 3?

Saxon E. Sharpe
Desert Research Institute, Reno, Nevada

Devils Hole, located about 130 km west of Las Vegas, Nevada, is an accurately dated calcite vein that records the isotopic signal of groundwater in the recharge area of the regional aquifer from

approximately 568,000 to 60,000 yr BP The high $\delta^{18}O$ values in the Devils Hole record interglacial climates and the low values record glacial or intermediate climates. These isotopic changes reflect a cyclic change of glacial and interglacial climates in southern Nevada.

Comparison of the Devils Hole $\delta^{18}O$ and age data with the orbital parameters eccentricity and precession and age data suggests a formal relation. This relation generates a series of precession sequences each lasting about 100,000 years. Each precession sequence contains either 4 or 5 summer precession radiation maxima and begins and ends with an interglacial period with a glacial period occurring mid-sequence. The pattern of interglacial to glacial periods in the Devils Hole record shows a remarkable consistency over the last 475,000 years.

The repetitive pattern of the Devils Hole isotope record suggests that Marine Isotope Stages (MIS) 4, 3, and 2 may, in fact, be one MIS stage. Thus, glacial MIS 4 and 2 could be considered one glacial stage with an MIS 3 interstade. If glacial MIS 4 and 2 are defined as separate MIS in the last precession sequence, this sequence would be the only sequence containing three interglacial (MIS 5, 3, and 1) and two glacial periods (MIS 4 and 2) over the last 475,000 years. If MIS 4, 3, and 2 are considered one MIS, the pattern of the previous 4 precession sequences is repeated.

Endogenous Versus Exogenous Origins of Crises

D. Sornette
UCLA and CNRS-Univ. Nice, France

Using the recently introduced multifractal random walk (MRW) model with application to turbulence and to finance, we show that systems with long-range persistence and memory exhibit different precursory as well as recovery patterns in response to shocks of exogeneous versus endogeneous origins. This offers the tantalizing possibility of distinguishing between an endogeneous versus exogeneous cause of a given shock, even when there is no “smoking gun”. This could help in investigating the exogeneous versus self-organized origins in problems such as the causes of major biological extinctions, of change of weather regimes and of the climate, in tracing the source of social upheaval and wars, and so on. Remarkable empirical tests show that this concept can be applied concretely to differentiate the effects on financial markets of the Sept. 11, 2001, attack or of the coup against Gorbachev on Aug. 19, 1991 (exogeneous) from financial crashes such as October 1987 (endogeneous). More generally, we propose that catastrophic events are “outliers” with statistically different properties than the rest of the population and result from mechanisms involving amplifying critical cascades. We describe a unifying approach for modeling and predicting these catastrophic events, or “ruptures,” that is, sudden transitions from a quiescent state to a crisis. Such ruptures involve interactions between structures at many different scales. Applications and the potential for prediction are discussed in relation to the rupture of composite materials, great earthquakes, turbulence and abrupt changes of weather regimes, financial crashes and human parturition (birth).

Mountain Climatic Gradients as Natural Ecological Experiments: Results from the Sierra Nevada Global Change Research Program

Nathan L. Stephenson
U.S. Geological Survey, Western Ecological Research Center, Sequoia–Kings Canyon Field Station, Three Rivers, CA

The current goal of the Sierra Nevada Global Change Research Program is to understand and predict the effects of global changes (particularly changing climate and fire regimes) on montane forests. Yet the task of gaining a mechanistic understanding of forest dynamics is beset with notoriously severe problems. Most of these problems result from the great spatial and temporal scales encompassed by forest dynamics, which preclude many forms of experimental manipulation. We have sought to overcome these problems through integrated studies organized around three themes: contemporary ecology, paleoecology, and modeling. Each of these themes takes advantage of the Sierra Nevada's substantial climatic gradients as "natural experiments." The Sierra Nevada's great elevational relief provides a steep temperature gradient which, in turn, is overlain by a gradient of decreasing precipitation from west to east. These climatic gradients combine with highly variable soils and topography to create a landscape that includes an extraordinary range of local site water balances, allowing us to evaluate climatic and other mechanisms controlling forest composition, structure, and dynamics.

Research to date has revealed strong climatic controls of fire regimes, forest distribution, and forest dynamics, with significant implications for forest carbon dynamics. Additionally, modeling efforts have revealed which portions of the landscape might be most sensitive to changes in temperature and precipitation. We hope to generalize our findings beyond the Sierra Nevada as part of the broader Western Mountain Initiative, which includes USGS-funded global change programs at Olympic, northern Rockies, and Colorado Rockies.

Speleothem Records of Glacial-Interglacial Transitions in the Sierra Nevada, California

Greg M. Stock and James C. Zachos
Earth Sciences, University of California, Santa Cruz

The degree of synchronicity between regional and global climate change in western North America remains an open question. For example, periods of desiccation in Basin and Range pluvial lakes have been linked to climate oscillations in the North Atlantic during deglaciation, while temperature records from the western Basin and Range and California coast suggest that warming in western North America preceded global deglaciation. We have acquired four speleothems from three caves in the Sierra Nevada foothills that date back 160 ka. Preliminary stable isotope ($\delta^{18}O$ and $\delta^{13}C$) and TIMS U-series investigation show that the speleothem isotopic compositions vary from glacial to interglacial in a systematic fashion. Specifically, $\delta^{18}O$ values are low (~-10‰) during the glacial stages, and high (~-6‰) during the interglacial stages. We interpret the large shift in $\delta^{18}O$ values from glacial to interglacial conditions as due to a combination of increased air temperature and reduced precipitation amounts during interglacials, a combination ultimately affecting the isotopic composition of cave dripwater. The inferred reduction in precipitation rates is supported by speleothem growth ratesthat slow during interglacial periods. This trend is broadly consistent with pluvial lake and other climate records from the western Basin and Range. Because similar isotope values and growth trends are preserved in speleothems separated by 150 km distance and 600 m elevation, we are confident that the signal reflects regional climate change. These high-resolution speleothem records should ultimately aid in resolving the timing and magnitude of climate events in western North America relative to those in the North Atlantic and elsewhere.

Spatial and Elevational Trends in Climate in the Pacific Northwest in the Last 150 Years

George H. Taylor
Oregon State University

The Pacific Northwest has seen a great deal of variation in climate over the last 150 years. Some of this variability appears to be due to well-known Pacific-wide factors such as ENSO and PDO, but other effects appear to be important as well. Many of these climate forcings have characteristic signals; ENSO warm events, for example, are likely to bring milder and drier winters than normal. However, there appear to be significant differences in spatial and elevational trends that manifest themselves over time.

Monthly climate maps for the period 1895-1999 were produced using the PRISM model. These formed the basis for an analysis of spatial and elevational variability. It was determined that spatial variations in climate response to large-scale forcings are quite significant. Elevational variations are significant as well, suggesting a vertical decoupling of climate trends.

Rapid Climate Change in the Earth System: Past, Present, Future

Lonnie G. Thompson
Distinguished University Professor, Department of Geological Sciences and Research Scientist, Byrd Polar Research Center

Unprecedented global changes of the 20th century have heightened awareness of human vulnerability to potential climate changes in the next millennium. Half of the Earth's surface area lies between 30 °N and 30 °S and supports 70% of the population. Thus, variations in the occurrence and intensity o the El Niño-Southern Oscillation and monsoons are of significance to humanity. Here meteorological records are available from selected high altitude, low- and mid-latitude ice caps. The studies described here were undertaken as part of a long-term program to acquire the global-scale, high resolution climatic and environmental history essential to better understand the linkages between the low and high latitudes.

This lecture explores the recent contributions of records from ice caps in Asia, South America and Africa to gain a better understanding of tropical climate and the global significance of the tropical hydrological cycle. These ice core records provide a long-term perspective essential to distinguish natural variation in the climate system from the anthropogenic influences superimposed during the last century. These new tropical records raise additional questions about our understanding of the role of the tropics in global climate change while documenting major disruptions in tropical climate such as a 5.2 ka cold wet event coincident with the formation of some of the first cities and the ~4 ka drought coincident with the "First Dark Age". Unfortunately, as a result of recent warming, all know tropical glaciers and ice caps are retreating and soon will no longer continue to preserve viable paleoclimatic records. The lecture will also touch some of my observations of how as human beings we bring about change!

Precipitation Reconstruction in the Southern Canadian Cordillera

Emma Watson and Brian Luckman
Dept. of Geography, University of Western Ontario, London, Canada

A network of 53 ring-width chronologies has been developed from valley floor stands of Douglas-fir and ponderosa pine in the southern Canadian Cordillera. Separate earlywood and latewood chronologies were developed for a 28 chronology subset of these data. All three ring-width parameters were used to develop a set of independent annual (prior July-current June) precipitation reconstructions for 13 meteorological stations dispersed across the region. The individual reconstruction models pass a number of verification tests conducted using independent data and calibrate between 35%-60% of the variance in the instrumental record. The reconstructions range from 165-688 years in length. Correlations with both instrumental and proxy precipitation/PDSI records from western Canada and the northwestern United States indicate that although the reconstructions are developed for stations within individual valleys, coherent precipitation anomalies are identified at a number of spatial scales. Coincident, prolonged intervals of dry conditions are estimated for the years: 1717-1732, 1839-1859, 1917-41 and 1968-1979. Shorter dry intervals are identified between 1701-1708, 1756-1761, 1768-1772, 1793-1800, 1868-1875, 1889-1897, 1985-1989, 1581-1586, 1626-1630, and 1641-1653. The long term context provided by these reconstructions indicates that the severity of the drought in the 1920-1930s is not unprecedented for individual sites. However, this event was the most widespread severe dry period to have affected the southern Cordillera over the past 300 years. Wet conditions occur in the majority of reconstructions for the years: 1689-1700, 1750-1755, 1778-1789, 1800-1830, 1880-90, 1898-1916 and 1942-1960. These precipitation reconstructions have recently been combined with proxy-temperature data available for the area to develop preliminary reconstructions of Fraser River streamflow and mass balance for the Peyto Glacier. These studies demonstrate the utility of a multi-species/multi-parameter approach to exploring historical environmental changes within this mountainous environment.

A Pollen Record of Late Pleistocene-Holocene Vegetation and Climate History, Lassen National Park, California

G. James West
U.S. Bureau of Reclamation, Sacramento, CA

A 6.3 meter sediment core from Little Willow Lake provides a 13,500-year pollen record of vegetation history for Lassen National Park. Located 1,829 m above sea level within a mixed red fir forest, Little Willow Lake covers approximately 2.5 hectares. The pollen profile provides a sequence of local and regional vegetation for the southern-most Cascades.

The vegetation succession covers the transition from the late glacial climates of the Pleistocene to the post-glacial climates of the Holocene- initially a sagebrush steppe prior to 12,500 yrs BP; then a pine dominated forest from 3,100-12,500 yrs BP, and finally the red fir forest of today. Abrupt transitions from sagebrush steppe to pine forest and the shift to the red fir forest took place in <500 years in response to millennial scale climate change. Between 12,500-13,500 yrs BP the climate was more seasonal, analogous to the climates of high elevations within the Great Basin today. Conditions were warmer than today between 3,100-9,000 yrs BP, with the warmest period between ca. 7,500-9,000 yrs. BP. The expansion of fir beginning ca. 3,100 yrs BP appears to be congruent with that observed in the central and southern Sierra and eastern Klamath Ranges, indicating that the climate cooled and moisture levels increased, particularly winter snow depths.

Climate Information and Wildfire Management

Anthony L. Westerling[1], Barbara J. Morehouse[2], and Thomas W. Corringham[3]
[1] Scripps Institution of Oceanography, La Jolla, CA
[2] CLIMAS, University of Arizona, Tucson, AZ
[3] Dept. of Economics, UCSD, La Jolla, CA

Understanding of large-scale climate patterns may improve the cost-effectiveness of wildfire management in the United States. Short-term weather forecasts have long been used by wildfire management agencies to assist with suppression efforts during the fire season. As the sophistication and skill of climate forecasting and climate information increases, so do opportunities for improved management of suppression and presuppression activities. We seek to understand and characterize the information networks and decision making processes within the federal, state, and local agencies charged with managing wildland fire. In particular, we seek to find points in the decision making processes at which climate information and climate forecasts could be used to improve cost-effectiveness. Possible applications of climate products include the strategic prepositioning of initial attack forces, and the strategic use of prescribed burns and other fuels management efforts. Further, long-term decadal climate outlooks could be integrated into Fire Management Plans to guide long-term budgeting, fuels, and land use decisions. To characterize the decision and information networks we are conducting a survey and interviews of Fire Managers and climate information users at various levels of the U.S. fire management agencies.

Statistical Reconstructions of Western U.S. Paleo Fire Regimes

Anthony Westerling[1] and Thomas Swetnam[2]
[1] Climate Research Division, Scripps Institution of Oceanography, La Jolla, CA
[2] Laboratory of Tree Ring Research, University of Arizona, Tucson, AZ

Wildfire is a natural and necessary element of many ecosystems. Nearly a century of wildfire suppression and land management policies in the western United States have resulted in heavy biomass accumulations in some ecosystems, fueling a growing incidence of catastrophic, stand-replacing fires in areas where they were rare under natural fire regimes. Current fire and ecosystem management policy contemplates ecosystem restoration on an enormous scale, involving prescribed fires and mechanical fuel reductions on millions of hectares and the subsequent reintroduction of presuppression fire regimes. Success in this venture depends critically on understanding how climate variability and change may constrain future fire regimes and ecosystems. Statistical models of annual area burned can successfully reconstruct interannual variability in paleo wildfire regimes using paleo proxies for soil moisture. We show how reconstructions for the western U.S. help to integrate modern observed fire histories with fire scar reconstructions of annual area burned. These reconstructions reveal similar ENSO- to decadal-scale climate signals in modern and paleo fire regimes, and help to discern the effects of changes in fire management from other long-term effects in observed wildfire histories.

Climate, Fire, and Vegetation in the Northwestern U.S.: Exploring the Linkages on Multiple Scales

Cathy Whitlock[1], Patrick Bartlein[1], Andrea Brunelle[1], Sarah Shafer[2], Jennifer Marlon[1], and Colin Long[1]
[1] Dept. of Geography, University of Oregon, Eugene, OR
[2] U.S. Geological Survey Earth Surface Processes (Central Region), Corvallis, OR

A network of paleoecological sites in the northwestern U.S. provides an opportunity to examine the linkages among fire, climate, and vegetation change on multiple temporal and spatial scales. Throughout the Holocene, regional differences in fire activity are apparent: the Coast Range has been characterized by relatively few fires, the Klamath Mountains have experienced continuous burning, and fire regimes in the northern Rockies have been strongly governed by submillennial-scale climate variability. Within the northern Rockies, high-elevation sites have had lower fire frequency than low-elevation sites. The amplification of the seasonal cycle of insolation in the early Holocene and its attenuation in the late Holocene have been important millennial-scale controls on both vegetation and fire regimes. The insolation maximum in the early Holocene led to enhanced monsoonal circulation and a stronger-than-present subtropical high, and the juxtaposition of these strengthened circulation features accentuated the spatial heterogeneity of precipitation, vegetation, and fire regimes at the subregional scale. The paleoecological record has important implications for understanding modern and future fire regimes. In some locations, the present fire regime was established in the last century, but other sites show near-modern conditions have existed for several millennia. Simulations of fire-related climate variables suggest heightened fire activity in most areas in the future, and point to the early Holocene as a possible "fire analogue." Thus, a long-term perspective needs to be incorporated into the concept of historical range of variability and considered in forest management.plans for the future.

Rainfall and Landsliding in Mountainous Areas—the Orographic Paradox

Raymond C. Wilson
U.S. Geological Survey, Menlo Park, CA

With their steep topography, mountain ranges are prime habitat for landslides. The high relief also produces strong orographic effects on passing storm systems, creating significant spatial variations in the distribution of precipitation. Orographic lifting of the air mass causes adiabatic cooling, increased condensation, and a proportional increase in the amount of rainfall on the windward slopes leading

up to the ridge crest. In the lee of the ridge, adiabatic warming of the descending air mass inhibits condensation and sharply decreases both the amount and frequency of precipitation. In the central California Coast Ranges, mean annual precipitation (MAP) values may vary by as much as a factor of five between the highest, wettest ridges, compared to the driest areas low on the lee slopes.

In light of these strong orographic rainfall gradients, one would expect similarly strong spatial variations in the frequency of debris flows and other landslides, with landsliding concentrated on the wetter windward slopes and relatively sparse on the dry lee slopes—yet such is not the case. Data on rainfall amounts and debris-flow occurrence in the San Francisco Bay area indicate that, while orographic effects produce strong variations in rainfall amount, a major storm system may simultaneously trigger debris flows over very wide areas, on both windward and leeward slopes. The absolute amount of rainfall appears to be less crucial than how this amount compares to the long-term rainfall distribution at that site, which is also influenced by orographic variations. In fact, the long-term frequency with which storms trigger landslides appears to be fairly constant. This self-canceling behavior allows us to estimate regional rainfall/debris-flow thresholds by normalizing out the local orographic effects.

Analysis of Reconstructed Streamflow in the Upper Colorado and Sacramento River Basins

Connie A. Woodhouse[1] and David M. Meko[2]
[1] NOAA Paleoclimatology Program, NCDC, Boulder, CO
[2] Laboratory of Tree-Ring Research, University of Arizona, Tucson, AZ

Tree-ring reconstructions of annual streamflow have been generated for the Sacramento River and the Upper Colorado River basins, two watersheds that contain critical water supplies for major metropolitan areas, as well as for rural and agricultural uses. Separately, the two reconstructions provide long-term perspectives on hydrologic drought, allowing recent regional droughts in the 20th and 21st centuries to be assessed in a broader temporal context. Together, the reconstructed streamflow records allow a comparison of concurrent or overlapping drought in the two basins. Extended periods of concurrent drought are of particular interest because California relies on water supplies from both the northern Sierra Nevada, which is drained by the Sacramento River, and the central Rocky Mountains, drained by the upper Colorado River. Periods of overlapping severe drought conditions in the 20th and 21st century have occurred, but only the mid-1970s drought conditions are closely matched in relative intensity and timing in both basins.

Smoothed time series of the pair of reconstructions show annual streamflow in the two basins is not well correlated, although there are notable periods of shared drought around 1850, the late 1770s, early 1710s, the 1580s, and an extended period in the second half of the 15th century. In this study, we selected two of these periods for further analysis, 1575-1600, and 1840-1860. A year-by-year examination of tree-growth anomalies across the western U.S. was used to assess the spatial pattern of drought and to ascertain whether drought in the two regions was coincidental or due to extensive drought conditions across the western U.S. Other aspects of drought in the Sacramento and Upper Colorado were explored using cross-spectral analysis of the streamflow reconstructions. Spectra show significant differences, particularly at the highest frequencies (less than 2.5 years) and 10-20 year frequencies, but in-phase coherence at four to seven years. This coherence suggests a possible relationship to ENSO, although the 20th century gage records show the two basins to be transitional with respect to ENSO influence.

Vegetation Responses to Climate Variability in the Last Interglacial

Wallace Woolfenden
USDA Forest Service, Lee Vining, CA

An 180,300-year pollen record from Owens Lake, California indicates that desert vegetation had tracked the last two glacial and interglacial cycles, which were driven by orbital changes. A relatively high-resolution pollen sequence, dating from 132,100 to 122,400 yr BP, spans the transition from the pleniglacial into most of the last interglacial. The average 220-yr sampling interval provides an opportunity to study vegetation change on both orbital and sub-orbital scales. The last interglacial is similar to the Holocene and the paleoecological data set can be used for a comparative study of vegetation and climate dynamics of the deserts of southeastern California. Such a study is important toward understanding climate/vegetation interactions for future projections of the consequences of human-induced global change. Owens Lake lies on an ecotone between the cold sagebrush desert and mixed shrub hot desert and so its sediments contain a historic vegetation archive sensitive to climatic change. According to the pollen sequence the juniper-pinyon pine and big sagebrush woodland had dominated the southern Owens Valley during the pleniglacial (Tahoe glaciation of the Sierra Nevada). As surface temperature increased juniper decreased over a thousand-year period until 130,000 yr BP when taxa representing warm desert vegetation surged within 200 years, as if a threshold was reached. These taxa differentially decreased about 4,000 years later as surface temperature declined. The early interglacial appears to have been warmer than the Holocene although wetter, possibly due to low-pressure anomalies over the eastern Pacific and more frequent summer and fall rainfall from humid air masses brought in by southerly flow.

Reconstructing Past Moisture Variability in the Rocky Mountain Region Using Testate Amoebae from *Sphagnum*-Dominated Peatlands

Jennifer R. Zygmunt, Robert K. Booth, and Stephen T. Jackson
Department of Botany, University of Wyoming, Laramie, WY

Records of past climate variability with multi-decadal to centennial-scale resolution have been successfully reconstructed using testate amoebae (Protozoa: Rhizopoda) as paleohydrological proxies. Testate amoebae are abundant and well preserved in *Sphagnum*-dominated peatlands, where assemblage composition is primarily controlled by substrate moisture. Recent efforts have been focused on the development of transfer functions to infer past surface-moisture conditions quantitatively from fossil testate amoeba assemblages. We investigated the potential of using testate amoebae to reconstruct high-resolution records of Holocene moisture variability in the Rocky Mountain region. Relationships between environmental variables (e.g. water-table depth, pH, conductivity, bulk density) and testate amoeba assemblages were investigated at 139 microsites within 15 *Sphagnum*-dominated peatlands in the central Rocky Mountains (WY, ID, CO). Our primary objectives were to identify controls on testate amoeba assemblage composition and to develop a calibration dataset that can be used to reconstruct peatland paleohydrology. Substrate moisture,

measured as depth to the water table, was identified as the dominant control on assemblage composition, with pH acting as a secondary control. We developed transfer functions to infer past changes in water-table depth from fossil testate amoeba assemblages using several models. Assuming good modern analogues, water-table depth can be reconstructed from fossil assemblages with a mean error of 7.0 cm. We used our calibration dataset to infer the water-table depth history of a *Sphagnum*-dominated peatland in Yellowstone National Park. Preliminary results suggest that testate amoebae have great potential for generating sensitive, high-resolution records of past moisture variability in the central Rocky Mountain region.

Appendix A: Agenda

Twentieth Annual PACLIM Workshop
Asilomar State Conference Grounds
Asilomar State Conference Grounds, Pacific Grove, California
April 6-9, 2003

PACLIM is a multidisciplinary workshop that broadly addresses the climatic phenomena occurring in the eastern Pacific and western America. Its purpose is to understand climate effects in this region by bringing together specialists from diverse fields including physical, social, and biological sciences. Time scales addressed range from weather to paleoclimate. This year marks our twentieth meeting and a time for celebration of the longevity of the original PACLIM vision of multidisciplinary collaboration centered around climate variability's vital role in all our fields. Our primary theme this year addresses climatic influences in mountain environments. Mountain environments are uniquely sensitive to climate changes with important effects that cascade through snowpack, streamflow, ecosystems, and society. Connie Millar (Pacific Southwest Research Station, Forest Service), Henry Diaz (Climate Diagnostics Center), Kelly Redmond (Western Regional Climate Center), and Scott Starratt (USGS) organized and attracted fine collections of talks and posters on this theme. As always, the remainder of PACLIM will be dedicated to a wide range of climate-related topics.

The atmosphere of the Workshop is intentionally informal, and room and board are provided for many of the participants. The Workshop is organized by representatives from several organizations, but historically has been spearheaded by U.S. Geological Survey scientists. Held annually, the Workshop has benefited from funding and other forms of support from several agencies (public and private). This year's PACLIM is sponsored by:

The CALFED Bay-Delta Science Program:	Sam Luoma
The Forest Service Pacific Southwest Research Station:	Hilda Diaz-Soltero
The U.S. Geological Survey Water Resources Discipline:	Bill Kirby
The U.S. Geological Survey Geologic Discipline:	Martha Garcia
The NOAA Office of Global Programs:	Harvey Hill
The State of California Department of Water Resources:	Zach Hymanson
The U.S. Naval Postgraduate School:	Tom Murphree

Agenda

Sunday Evening, April 6
Current Events and a Dose of Complex Systems Theory
Moderator: Mike Dettinger

3:00 pm+	Registration etc.
6:00-7:00 pm	Dinner
7:00-7:10 pm	Opening Comments Mike Dettinger (USGS) and Janice Tompson (LBCC)
7:10-7:40 pm	*The Western Weather and Climate of PACLIM Year 2002-2003* Kelly Redmond (WRCC)
7:40-8:10 pm	*Water Year 2003: A Good Year in Northern California But a Non-traditional El Niño* Maury Roos (California DWR)
8:15-9:00 pm	*Endogenous Versus Exogenous Origins of Crises* Didier Sornette (UCLA)
9:00+ pm:	Socializing

Monday Morning, April 7
Moderator: Connie Millar
Special Session: Integrated Climate Research in the Mountains
Part I: Paleo Perspectives

7:30-8:30 am	Breakfast
8:30-8:40 am	Introductory Remarks Connie Millar (PSW) and Henry Diaz (CDC)
8:40-9:10 am	*Unexpected Forest Responses to Climate Change in Mountain Regions: The Role of Landscape Heterogeneity* L.B. Brubaker (UW), D. Gavin (U of IL), J.S. McLachlan (Dartmouth), W.Y. Fujikawa (UW), and D.G. Sprugel (UW)
9:10-9:40 am	*Climate, Fire, and Vegetation in the Northwestern U.S.: Exploring the Linkages on Multiple Scales* Cathy Whitlock (U of OR), Patrick Bartlein (U of OR), Andrea Brunelle (U of OR), Sarah Shafer (USGS), Jennifer Marlon (U of OR), and Colin Long (U of OR)
9:40-10:10 am	*Statistical Reconstructions of Western U.S. Paleo Fire Regimes* Anthony Westerling (SIO) and Thomas Swetnam (U of AZ)
10:10-10:30 am	Break
10:30-11:00 am	*Regional Timing of Neoglaciation in the Western Cordillera: Constraints from Glacial and Lacustrine Records* Douglas H. Clark (Western Washington University)
11:00-11:30 am	*Analysis of Reconstructed Streamflow in the Upper Colorado and Sacramento River Basins* Connie A. Woodhouse (NOAA Paleoclimatology), and David M. Meko (U of AZ)
11:30-12:00 pm	*Regional Climate and Environmental Change Recorded in Ice Cores from the Upper Fremont Glacier, Wyoming: Implications for Long-Term Stewardship of Buried Waste at U.S. Department of Energy Facilities* L. Dewayne Cecil (USGS), Mitch Plummer (INEL), David L. Naftz (USGS), Lisa J. Graumlich (Montana State), Paul F. Schuster (USGS), Jaromy R. Green (USGS), and David D. Susong (USGS)
12:00-1:00 pm	Lunch

Monday Afternoon, April 7
Moderator: Scott Starratt
Special Session: Integrated Climate Research in the Mountains
Part II: Rather Recent

1:00-1:30 pm	*Out of Sight, But Not Out of Mind: Observing the Mountains* Kelly T. Redmond (WRCC)
1:30-2:00 pm	*Climate Linkages Between Uplands and Lowlands* Henry F. Diaz and Jon K. Eischeid (CDC)
2:00-2:30 pm	*Spatial and Elevational Trends in Climate in the Pacific Northwest in the Last 150 Years* George H. Taylor (OSU)
2:30-3:00 PM	*A Comparison of Free-Air and Surface Temperature Trends at High Elevations in the Mountainous West of the U.S.* Nicholas C. Pepin (U of Portsmouth), Mark Losleben (CU), and Mike Hartman (CIRES)
3:00-3:30 pm	Break
3:30-4:00 pm	*Sources of Hydrologic Predictability in the Columbia River Basin: A Comparison of the Role of Hydrologic State Variables and Winter Climate Forecasts* Alan F. Hamlet and Dennis P. Lettenmaier (UW)
4:00-4:30 pm	*Determining Long-Term Water Quality Change in the Presence of Climate Variability: Lake Tahoe (USA)* Alan D. Jassby (UC Davis)
4:30-5:00 pm	*Global Environmental Effects on Mountain Ecosystems: A Case Study from Glacier National Park* Daniel B. Fagre (USGS)
5:00-5:30 pm	*Mountain Climatic Gradients as Natural Ecological Experiments: Results from the Sierra Nevada Global Change Research Program* Nathan L. Stephenson (USGS)
5:30-6:00 pm	*Climate Mapping Challenges in the Western United States* Chris Daly (OSU)
7:00-8:00 pm	Dinner at the Monterey Bay Aquarium

Monday Evening, April 7
Moderator: Dan Cayan
Abrupt Climate Changes

8:00-9:00 pm	*Rapid Climate Changes: Past, Present, and Future* Lonnie Thompson (Ohio State University)
9:00+ pm	Socializing at the Monterey Bay Aquarium

Tuesday Morning, April 8
Moderator: Henry Diaz
Special Session: Integrated Climate Research in the Mountains
Part III: Looking Ahead

7:30-8:30 am	Breakfast
8:30-9:00 am	*A High Elevation Tropical Climate Reference Network* Douglas R. Hardy and Raymond S. Bradley (U of Mass, Amherst)
9:00-9:30 am	*A Mesoscale Modeling and Assimilation Study of the Role of Snowpack on Climate Variability in the Sierra Nevada Region* Jiming Jin and Norman L. Miller (LBL)
9:30-10:00 am	*Elevational Dependence of Hydrologic Response to Projected Sierra-Nevada Warming* Noah Knowles (USGS)
10:00-10:30 am	Break
10:30-11:00 am	*Predicting Climate Change in a Green World: A Daunting Challenge* John Harte (UCB)
11:00-11:30 am	*WestMap: The Western Climate Mapping Initiative* Andrew C. Comrie (U of AZ), Kelly Redmond (WRCC) and Christopher Daly (OR State)
11:30-12:00 am	*Panel Discussion of Options for Expanding Mountain Climate Research* Henry Diaz, moderating
12:00-1:00 pm	Lunch

Tuesday Afternoon, April 8
Moderator: Jim West
Past Climates

1:00-1:30 pm	*Speleothem Records of Glacial-Interglacial Transitions in the Sierra Nevada, California* Greg M. Stock and James C. Zachos (UCSC)
1:30-2:00 pm	*Columbia River Flow Since AD 1750 Reconstructed from Tree Rings* Ze'ev Gedalof (UW), David L. Peterson (USDA FS), and Nathan J. Mantua (UW)
2:00-2:30 pm	*Tree-Ring Based Reconstructions of Precipitation Variability in Northeastern Utah* Stephen T. Gray (U of WY), Stephen T. Jackson (U of WY), and Julio L. Betancourt (USGS)
2:30-3:00 pm	Break
3:00-3:30 pm	*Proxy Reconstruction of the Entire Pacific Sea Surface Temperature Field* Alexander Gershunov (SIO), Michael Evans (U of AZ), and Malcolm Hughes (U of AZ)
3:30-4:00 pm	*Development and Limitations of Transfer Functions Used to Reconstruct Air Temperatures from Ice Cores, Wind River Range, Wyoming* David L. Naftz, David D. Susong, Paul F. Schuster, L. Dewayne Cecil, and Michael D. Dettinger (USGS)
4:00-4:30 pm	*Precipitation Reconstruction in the Southern Canadian Cordillera* Emma Watson and Brian Luckman (U of West Ontario)
4:30-5:00 pm	*Vegetation Responses to Climate Variability in the Last Interglacial* Wallace Woolfenden (USDA FS)
5:00-5:30 pm	*Assessment of Environmental Influences on California Commercial Fish and Invertebrate Landings* Jerrold G. Norton and Janet E. Mason (PFEL NMFS)
6:00-7:30 pm	Dinner

Tuesday Evening, April 8
Evening Talk and Posters

7:30-8:15 pm	*Late Quaternary History of the Atacama Desert and Pacific Slope of the Central Andes* Julio L. Betancourt (USGS), Jay Quade, Claudio Latorre, Jason Rech, Christa Placzek, Camille Holmgren, Mathias Vuille and Kate Rylander
8:15-10:00 pm	Posters and Discussion (over refreshments)

Wednesday Morning, April 9
Moderator: John Dracup
Modern Climate Applications

7:30-8:30 am	Breakfast
8:30-9:00 am	*Rainfall and Landsliding in Mountainous Areas—The Orographic Paradox* Raymond C. Wilson (USGS)
9:00-9:30 am	*Central Sierra Air Temperature, Snowmelt Discharge, and River Chemistry—Monitoring, Modeling, and Prediction* David H. Peterson, Richard Smith, Stephen Hager, Daniel Cayan, and Michael Dettinger (USGS)
9:30-10:00 am	*Spatial and Temporal Variability in Snowpack Controls: Two Decades of SnoTel Data from the Western United States* Mark Losleben (CU) and Nicholas Pepin (U of Portsmouth)
10:00-10:30 am	Break
10:30-11:00 am	*Is Sierra Nevada Snowmelt Independent of Elevation?* Jessica D. Lundquist (SIO), Michael D. Dettinger (USGS), and Daniel R. Cayan (SIO/USGS)
11:00-11:30 am	*Climatic Teleconnections for Influencing California Reservoir Operations* Levi D. Brekke and John A. Dracup (UCLA)
11:30-12:00 am	*Onset of Spring in the 21st Century—Updates from 2000-2003* Dan Cayan (SIO)
12:00-1:00 pm	Lunch and Exit

Appendix B: Poster Presentations

Directional Positive Feedback and Pattern at an Alpine Treeline
Kathryn J. Alftine (CSU Monterey Bay)

Fractional Snow Cover in the Colorado River and Rio Grande Basins, 1995-2002
Roger C. Bales (U of AZ)

Tidal Cycles in Santa Barbara Basin Sediment
Wolfgang H. Berger (SIO), Arndt Schimmelmann (Indiana U), and Carina B. Lange (U Concepcion)

PDO Selectively Removes Winter Season ENSO-Precipitation Signal in the Western United States
David P. Brown and Andrew C. Comrie (U AZ)

Cytometric Sorting of Pinaceae Pollen and Its Implications for Radiocarbon Dating and Stable Isotope Analyses
Roger Byrne (UC Berkeley), Jungjae Park (UCB), Lynn Ingram (UCB), and Tak Hung (Union Biometrica)

Integration of Fire-Climate Information into a Decision Support System: The Walter Project
Michael A. Crimmin, Susan M. Taunton, Stephen R. Yool, Andrew C. Comrie, and Barbara J. Morehouse (U AZ)

What Happens When Pacific Climate Goes East over the Mountains?
Walter E. Dean and Joseph G. Rosenbaum (USGS)

The Thermal Evolution of Snowpack at Gin Flat, Yosemite National Park, Winter and Spring 2002
Michael Dettinger (USGS) and Frank Gehrke (Cal DWR)

Subregional Climatology Affects Area Burned By Wildfire in the U.S. Pacific Northwest
Ze'ev Gedalof (U of WA), David L. Peterson (PSW), and Nathan J. Mantua (U of WA)

Hourly Measurements of Concentrations of Nitrate Plus Nitrite and Dissolved Silica in the Merced River
Stephen W. Hager, Richard E. Smith, and David H. Peterson (USGS)

Effects of Climate Change on the Pacific Northwest Ski Industry
Alan F. Hamlet, Philip Mote, Amy K. Snover, and Dennis P. Lettenmaier (UW)

Low-Frequency Climatic Variations in the 20th Century in the Upper Colorado River Basin: Teleconnections with the North Pacific?
Hugo Hidalgo (UCB/SIO)

Paleoclimate in San Francisco Bay and Its Watershed: What Do We Know and What Do We Need to Know?
Lynn Ingram (UCB), Frances Malamud-Roam (UCB), Joan Florsheim (UCD), and Malcolm Hughes (U of AZ)

Hydrologic Changes of Salton Sea During the Late Holocene: Evidence from Radiocarbon Dated Isotopic Records
Hong-Chun Li (USC), Teh-Lung Ku (USC), H. Paul Buchheim (Loma Linda U) and Xiaomei Xu (UCI)

Pacific Teleconnections and Fire in the Western United States: 1700-1900
Jeremy S. Littell (U of WA) and David L. Peterson (USDA FS, PSW)

Soil Moisture in the Alpine and Sub-Alpine, Niwot Ridge, Colorado
Mark Losleben (U of CO), Kurt Chowanski (U of CO), and Timothy Bardsley (NRCS)

Meteorology and Hydrology in Yosemite National Park: A Sensor Network
Jessica Lundquist, Dan Cayan, and Mike Dettinger (SIO)

700-Hectopascal Atmospheric Circulation Patterns Associated with Winter Precipitation in the Yellowstone Region
David L. McGinnis (Idaho State), Gregory J. McCabe (USGS), and Heather K. Conley (U of IA)

Extracting Seasonal Precipitation Signal from Tree-Ring Width
David M. Meko and Christopher H. Baisan (U AZ)

A 7,000-Yr Record of Climate Change Reconstructed from Pyramid Lake, Nevada
Scott A. Mensing (UNR)

Responses of High-Elevation Pines in the E. Sierra Nevada and W. Great Basin to Late Holocene Decadal- and Century-Scale Climate Variability
Constance I. Millar (USDA Forest Service, PSW Research Station), Robert D.Westfall (PSW), Diane L. Delany (PSW), John C. King (Lone Pine Research), and Harry Alden (Smithsonian Inst)

High Resolution Analysis of Subfossil Midges: Indicators of Fish Introduction and Climate Change in the Sierra Nevada of California
David F. Porinchu, Glen M. Macdonald and Aaron P. Potito (UCLA)

High Resolution Time-Series of the Younger Dryas Cold Event in the Eastern Sierra Nevada, California
Aaron P. Potito, Glen M. Macdonald, and David F. Porinchu (UCLA)

Fire and Vegetation Variations of the Last 4,000 Years in Northwestern Montana
Mitchell J. Power, Cathy Whitlock, and Patrick Bartlein (U of OR)

A Wireless, Near-Real-Time Hydrometeorological Sensor Array in the Santa Margarita Ecological Reserve
Aleksandr Revchuk (UCSD), Daniel Cayan (SIO), Michael Dettinger (USGS), Todd Hanson (UCSD), Hans-Werner Braun (UCSD), Pablo Bryant (SDSU), Mark van Scoy (SDSU), Larry Riddle (SIO), Douglas Alden (SIO)

Potential Predictability of Central Sierra Snowpack Related to Early Season Northern Pacific Ocean Swells
Temoc Rios (UC Berkeley), John A. Dracup (UCB), and Hugo G. Hidalgo (SIO)

Temperature Monitoring at Upper Treeline Sites in the Western US
Louis A. Scuderi (UNM)

The Way Forward from Uncertainty from Equilibrium Modeling
Gary D. Sharp (CCORS) and Leonid Klyashtorin (VNIROV)

Glacial and Interglacial Patterns in Devils Hole, Nevada, Record: Are We Currently in Marine Isotope Stage 3?
Saxon E. Sharpe (DRI)

A Pollen Record of Late Pleistocene-Holocene Vegetation and Climate History, Lassen National Park, California
G. James West (USBR)

Climate Information and Wildfire Management
Tony Westerling (SIO), Barbara Morehouse (U of AZ), and Thomas Corringham (UCSD)

Reconstructing Past Moisture Variability in the Rocky Mountain Region Using Testate Amoebae from *Sphagnum*-Dominated Peatlands
Jennifer R. Zygmunt, Robert K. Booth, and Stephen T. Jackson (U of WY)

Appendix C: Participants

Kathryn Alftine
CSU Monterey Bay
904 Provincetown Dr
Salinas, CA 93906

Lorenzo Alvarez
Division of Oceanology, Dept. of Ecology
CICESE
KM 107 CARR. TIJ - ENS
Ensenada, Baja California, Mexico

Diana Anderson
Center for Environmental Sciences and Education
Northern Arizona University
PO Box 5694
Flagstaff, AZ 86011

R. Scott Anderson
Center for Environmental Sciences and Education
Northern Arizona University
PO Box 5694
Flagstaff, AZ 86011

Allison Bair
Northern Arizona University
309 W. Eim Ave.
Flagstaff, AZ 86001

Barry Baker
The Nature Conservancy
2060 Broadway Suite 230
Boulder, CO 80302

Roger Bales
University of Arizona
Dept. of Hydrology and Water Resources
Tucson, AZ 85718

John Barron
U.S. Geological Survey
345 Middlefield Road MS910
Menlo Park, CA 94025

Rodrigo Beas
Division of Oceanology, Dept. of Ecology
CICESE
KM 107 CARR. TIJ - ENS
Ensenada, Baja California, Mexico

Julio L. Betancourt
Desert Laboratory
U.S. Geological Survey
1675 W. Anklam Road
Tucson, AZ 85745

Richard R. Brandt
Dept. of Geography and Regional Development
University of Arizona
Harvill Building #2, PO Box 210076
Tucson, AZ 85721

Levi Brekke
Civil and Environ. Engineering Dept.
UC Berkeley
602 Davis Hall, Tac 1710
Berkeley, CA 94720

Canie Brooks
Long Beach City College
4901 East Carson Street
Long Beach, CA 90808

David Brown
University of Arizona
Harvill Building, Box #2
Tuscon, AZ 85719

Linda Brubaker
College of Forest Resources
University of Washington
Box 352100
Seattle, WA 98195-2100

Roger Byrne
Geography Dept., UC Berkeley
501 McCone Hall
Berkeley, CA 94720

Richard Casey
Ocean Research Intl
650 Loring Street
San Diego, CA 92109

Dan Cayan
Scripps Institution of Oceanography
UC San Diego
9500 Gilman Drive - 0224
La Jolla, CA 92037

L. Dewayne Cecil
U.S. Geological Survey
900 N. Skyline Drive, Suite C
Idaho Falls, ID 83402

Doug Clark
Dept. of Geology
Western Washington University
516 High Street
Bellingham, WA 98225-9080

Andrew Comrie
Dept. of Geography
University of Arizona
409 Harvill
Tucson, AZ 85721-0076

Thomas Corringham
Scripps Institution of Oceanography
UC San Diego
C/O Anthony Westerling,
9500 Gilman Dr
La Jolla, CA 92093

Mike Crimmins
Dept. of Geography And Regional Dev.
University of Arizona
Harvill Building, Box #2
Tucson, AZ 85721

Chris Daly
Oregon State University
316 Strand Agriculture Hall
Corvallis, OR 97331-2209

Walter Dean
U.S. Geological Survey
MS 980 Federal Center, Box 25046
Denver, CO 80225

Mike Dettinger
U.S. Geological Survey
Scripps Institution of Oceanography
9232 Lapeer Ct
Santee, CA 92071

Henry Diaz
NOAA/OAR/CDC
325 Broadway
Boulder, CO 80305

Hilda Diaz-Soltero
USDA Forest Service
Pacific Southwest Research Station
PO Box 245
Berkeley, CA 94701

John Dracup
Civil and Environ. Engineering Dept.
UC Berkeley
533 Davis Hall M.C. 1710
Berkeley, CA 94720-1710

Duane Dykema
National Weather Service
21 Grace Hopper Ave., Stop 5
Monterey, CA 93943

Daniel Fagre
U.S. Geological Survey
USGS Science Center, Glacial National Park
West Glacier, MT 59936

Joan Florsheim
UC Davis
One Shields Ave
Davis, CA 95616

Ze'ev Gedalof
Climate Impacts Group, Joint Institute for the Study of the Atmosphere and Oceans
University of Washington
University of Victoria, Tree-Ring Laboratory, Box 3050 Stn. CSC
Victoria, British Columbia, Canada V8W 3P5

Alexander Gershunov
Scripps Institution of Oceanography
UC San Diego
9500 Gilman Dr
La Jolla, CA 92093-0224

Stephen T. Gray
Dept. of Botany
Univ. of Wyoming
PO Box 3165
Laramie, WY 82071

Alan Hamlet
University of Washington
Box 352700
Seattle, WA 98195

Douglas Hardy
Dept. of Geosciences and Climate System Research Center
Univ. of Massachusetts
Amherst, MA 01003

John Harte
UC Berkeley
Bldg. T 4, Rm. 100
Berkeley, CA 94720

Hugo Hidalgo
UC Berkeley
Scripps Institution of Oceanography
9500 Gilman Dr., Dept. 224
La Jolla, CA 92093

B. Lynn Ingram
EPS Dept. and Dept. of Geography
UC Berkeley
113 McCone Bldg
Berkeley, CA 94720-4767

Alan Jassby
Dept. of Environmental Science and Policy
UC Davis
Davis, CA 95616

Jiming Jin
Lawrence Berkeley National Lab
One Cylotron Road; MS 90-1116
Berkeley, CA 94720

Greg Johnson
USDA-NRCS
National Water and Climate Center
101 SW Main St., Suite 1600
Portland, OR 97204

Taylor Joyal
Northern Arizona University
920 W. Grand Canyon#2
Flagstaff, AZ 86001

Olga Katsuk
Long Beach City College
4901 East Carson Street
Long Beach, CA 90808

John Keyantash
Dept. of Earth Science
CSU Dominguez Hills
1000 E. Victoria St.
Carson, CA 90245

Noah Knowles
U.S. Geological Survey
Menlo Park
345 Middlefield Rd., MS 496
Menlo Park, CA 94025

Kate Koczot
Climate Research Division
U.S. Geological Survey
9232 Lapeer Ct
Santee, CA 92071

Lydia B. Ladah
Division of Oceanology, Dept. of Ecology
CICESE
KM 107 CARR. TIJ - ENS
Ensenada, Baja California, Mexico

Hong-Chun Li
Dept. of Earth Sciences
Univ. of Southern Caifornia
3651 Trousdale Parkway
Los Angeles, CA 90089-0740

Jeremy Littell
Fire and Mountain Ecology Lab
University of Washington
PO Box 352100
Seattle, WA 98195-2100

Mark Losleben
Mountain Research Station
Univ. of Colorado
818 Country Road, 116
Nederland, CO 80466

Deborah Luchsinger
National Renewable Energy Laboratory
1617 Cole Blvd. MS 1621
Golden, CO 80401

Jessica Lundguist
Scripps Institution of Oceanography
9500 Gilman Dr.
La Jolla, CA 92093-0213

Frankie Malamud-Roam
Dept. of Geography
UC Berkeley
189 McCone
Berkeley, CA 94720-4767

Sharon Masek-Lopez
Northern Arizona University
461 E. Kiowa
Flagstaff, AZ 86001

James Mason
Pacific Fisheries Environmental Group
NOAA
1352 Lighthouse Ave
Pacific Grove, CA 93950

Caitilin McCracken
Northern Arizona University
923 W. Coconino Ave., #3
Flagstaff, AZ 86001

David L. McGinnis
Idaho State University
Campus Box 8072
Pocatello, ID 83209-8027

Cara Meeker
Northern Arizona University
OSP Box 5694 NAU
Flagstaff, AZ 86011

David Meko
Laboratory of Tree Ring Research
University of Arizona
105 W. Stadium
Tuscon, AZ 85721

Scott Mensing
Dept. of Geography
University of Nevada
201 Mackay Science Hall, MS 154
Reno, NV 89557

Constance I. Millar
USFS-PSW Research Station
800 Bucharan St.-WAB
Albany, CA 94710

Tom Minckley
Dept. of Geography
University of Oregon
107 Candon Hall
Eugene, OR 97403

Keith Mootsey
Long Beach City College
4901 East Carson Street
Long Beach, CA 90808

Eduardo Morteo
Division of Oceanology, Dept. of Ecology
CICESE
Km 107 Carr. Tij - Ens
Ensenada, Baja California, Mexico

Christopher Moy
Dept. of Geological and Environmental Sciences
Stanford University
Braun Hall
Stanford, CA 94305

David Naftz
U.S. Geological Survey
2329 Orton Cir.
Salt Lake City, UT 84119

Yanina Narvaez
Division of Oceanology, Dept. of Ecology
CICESE
Km 107 Carr. Tij - Ens
Ensenada, Baja California, Mexico

J. Madeleine Nash
Freelance Science Writer
Time Magazine Contributor
4014 21st St.
San Francisco, CA 94114

Jerrold G. Norton
Pacific Fisheries Environmental Lab
1352 Lighthouse Ave
Pacific Grove, CA 93950

Nick Pepin
Dept. of Geography
University of Portsmouth
Buckingham Building, Lion Terrace
Portsmouth, PO1 3HE UK

David Peterson
Water Resources Division
U.S. Geological Survey
345 Middlefield Road
Menlo Park, CA 94025

David Porinchu
Dept. of Geography
UC Los Angeles
1255 Bunche Hall
Los Angeles, CA 90095-1524

Aaron Potito
Dept. of Geography
UC Los Angeles
1255 Bunche Hall
Los Angeles, CA 90095-1524

Kelly Redmond
Western Regional Climate Center
Desert Research Institute
2215 Raggio Parkway
Reno, NV 89512-1095

David Rhode
Desert Research Institute
2215 Raggio Parkway
Reno, NV 89512

Rob Richardson
Northern Arizona University
Enviro. Sci. Box 5614
Flagstaff, AZ 86001

Larry Riddle
Scripps Institute of Oceanography
UC San Diego
Climate Research Division 0224
La Jolla, CA 92093-0224

Temoc Rios
Dept. of Civil and Environmental Engineering
UC Berkeley
218 Wilson St.
Albany, CA 94710

Maury Roos
CA Dept. of Water Resources
1305 Lynette Way
Sacramento, CA 95831

Jonathan Sandoval
Division of Oceanology, Dept. of Ecology
CICESE
Km 107 Carr. Tij - Ens
Ensenada, Baja California, Mexico

Arndt Schimmelmann
Indiana University
Dept. of Geological Sciences
Bloomington, IN 47405-1403

Louis Scuderi
Dept. of Earth and Planetary Sciences
University of New Mexico
224C Northrop Hall
Albuquerque, NM 87131-1116

Gary Sharp
Center for Climate
Ocean Resources Study
780 Harrison Road
Salinas, CA 93907

Saxon Sharpe
Desert Research Institute
2215 Raggio Parkway
Reno, NV 89509

Janelle Sikorski
Northern Arizona University
1464 University Heights
Flagstaff, AZ 86001

Larry Smith
U.S. Geological Survey
6000 J Street
Sacramento, CA 95819

Didier Sornette
Dept. of Earth and Space Sciences
UC Los Angeles
595 Charles Young Drive East, Box 951567
Los Angeles, CA 90095-1567

Scott Starratt
U.S. Geological Survey
345 Middlefield Road
Menlo Park, CA 94025

Anne Steinemann
Georgia Institute of Technology
Scripps Institution of Oceanography
Atlanta, GA 30332-6491

Nate Stephenson
U.S. Geological Survey
Sequoia-Kings Canyon Field Station
HCR Box 4
Three Rivers, CA 93271

Lora Stevens
University of Nebraska
214 Bessey Hall
Lincoln, NE 68588-0340

Greg Stock
Earth Science Department
UC Santa Cruz
Santa Cruz, CA 95064

Renee Takesue
Mendenhall Postdoc
U.S. Geological Survey
345 Middlefield Rd
Menlo Park, CA 94025

George Taylor
Oregon Climate Service
Oregon State University
316 Strand Hall
Corvallis, OR 97331-2209

Lucenia Thomas
U.S. Geological Survey
345 Middlefield Rd. MS 496
Menlo Park, CA 94025

Lonnie G. Thompson
Byrd Polar Research Center, Ohio State Univ
108 Scott Hall 1090
1090 Camack Road
Columbus, OHIO 43210-1002

Janice Tomson
Long Beach City College
4901 East Carson Street
Long Beach, CA 90808

Jaime Toney
Northern Arizona University
3708 N. Thomas Dr.
Fiagstaff, AZ 86001

Elmira Wan
U.S. Geological Survey
345 Middlefield Rd., MS 975
Menlo Park, CA 94025

Steve Wathen
ENH Department, UC Davis
One Shields Ave.
Davis, CA 95616

Emma Watson
Dept. of Geography
University of Western Ontario
London, Ontario, Canada N6A 5O2

G. James West
U.S. Bureau of Reclamation
3429 Oyster Bay
Davis, CA 95616

Anthony Westerling
Scripps Institution of Oceanography
9500 Gilman Dr
La Jolla, CA 92093-0224

Robert Westfall
Sierra Nevada Research Center
USDA Forest Service
PO Box 245
Berkeley, CA 94701

Cathy Whitlock
Dept. of Geography
University of Oregon
Eugene, OR 97403-1251

Ray Wilson
U.S. Geological Survey
345 Middlefield Rd., MS 977
Menlo Park, CA 94025

Connie Woodhouse
NOAA Paleoclimatology
325 Broadway E/Cc23
Boulder, CO 80305

Wally Woolfenden
USDA Forest Service
120 Wilson Rd.
Swall Meadows, CA 93514

Xiaomei Xu
Dept. of Earth System Science
UC Irvine
220 Rowlad Hall
Irvine, CA 92697-3100

Jennifer Zygmunt
University of Wyoming
716 Gibbon
Laramie, WY 82072